

INSTITUTO POLITÉCNICO NACIONAL

**CENTRO DE BIOTECNOLOGÍA GENÓMICA**



**“Design, Synthesis and Biological Evaluation of New Carboxylic Acid  
Derivatives as Trans-sialidase Inhibitors of *Trypanosoma cruzi*”**

**THESIS SUBMITTED**

**TO OBTAIN THE DEGREE OF DOCTOR OF PHILOSOPHY (Ph.D.) IN BIOTECHNOLOGY**

**BY**

**MUHAMMAD KASHIF**

*M.Sc. (BZU), M. Phil. (IUB), Chemistry, Pakistan*

**Reynosa, Tamaulipas, México**

**July, 2018**

**INSTITUTO POLITÉCNICO NACIONAL  
CENTRO DE BIOTECNOLOGÍA GENÓMICA**



**“Design, Synthesis and Biological Evaluation of New Carboxylic Acid  
Derivatives as Trans-sialidase Inhibitors of *Trypanosoma cruzi*”**

**THESIS SUBMITTED**

**TO OBTAIN THE DEGREE OF DOCTOR OF PHILOSOPHY (Ph.D.) IN BIOTECHNOLOGY**

**BY**

**MUHAMMAD KASHIF**

*M.Sc. (BZU), M. Phil. (IUB), Chemistry, Pakistan*

**Reynosa, Tamaulipas, México**

**July, 2018**



## ABSTRACT

Chagas is a lethal chronic disease that currently affects 8–10 million people worldwide, primarily in South and Central America. *Trypanosoma cruzi trans*-sialidase (TcTS) is an enzyme that is of vital importance for the survival of the parasite due to its key role in the transfer of sialic acid from the host to the parasite surface. Based on molecular docking, molecular dynamics and structure-activity relationship studies, it has been discovered that the *trans*-sialidase amino acid residues Arg35, Arg245, Arg314, Tyr119, Trp312, Tyr342, Glu230 and Asp59 have the vital importance for the transfer mechanism. The molecules with –NH,–OH and –COOH groups on an aromatic ring could be used as a scaffold for the development of new and potent *trans*-sialidase inhibitors due to their key interaction with active enzyme sites. In particular, carboxylic acid derivatives have importance over the sugar moiety due to their ease of synthesis and unique structure-activity relationship.

In this work we designed one hundred seventy five (175) benzoic acid/carboxylic acid derivatives, *para*-aminobenzoic acid derivatives (10), 3-amino-3-arylpropionic acids (series A) (15), phthaloyl derivatives of 3-amino-3-arylpropionic acids (series B) (15), 4-carboxyl phthaloyl derivatives of 3-amino-3-aryl propionic acids ( series C) (15), 4-methyl phthaloyl derivatives of 3-amino-3-arylpropionic acids (series D) (15), 3-Nitrophenylcarbamoyl benzoic acid (series E) (25), 4-carboxyphenylcarbamoyl benzoic acid (series F) (25), 4-methylphenylcarbamoyl benzoic acid (series G) (30) and 4-methylcyclohexanecarbamoyl benzoic acid (series H) (30) and their molecular docking studies were performed by AutoDock Vina 5.6 . The 2,3-dehydro-3-deoxy-*N*-acetylneuraminic acid (DANA), the natural ligand of TcTS was used as a reference with predicted binding affinity -7.8 kcal/mol. Highest predicted binding affinity was shown by compounds C-11 and D-11 (-11.0 kcal/mol). The two dimensional (2D) and three dimensional (3D) interaction of these compounds in catalytic pocket of TcTS showed these compounds have the best orientation in the catalytic pocket and

showed the hydrogen bond,  $\pi$ - $\pi$  stacking,  $\pi$ -cation,  $\pi$ -alkyl and hydrophobic interaction with active amino acid residues of TcTS. The most prominent interaction was found between Tyr119 and Trp312 amino acid mounted at the mouth of catalytic pocket and responsible for the control of substrate into the pocket.

All designed, novel compound was synthesised by reported procedures. The FTIR,  $^1\text{H}$  NMR and  $^{13}\text{C}$  NMR spectroscopy were used to confirm the synthesis of compounds. The  $-\text{NH}$ , ( $3400\text{-}3600\text{ cm}^{-1}$ ),  $-\text{OH}$  broad ( $3300\text{-}2800\text{ cm}^{-1}$ ),  $-\text{C}_2\text{O}_2\text{N}$  (phthalimido) ( $1770_{\text{asymmetric}}$ ,  $1690_{\text{symmetric}}\text{ cm}^{-1}$ ) and carbonyl ( $\text{C}=\text{O}$ ) peak in the range of ( $1700\text{-}1610\text{ cm}^{-1}$ ) in FTIR confirmed the presence of the functional group in all series. In the  $^1\text{H}$  NMR  $-\text{OH}$  proton shift ( $10\text{-}13$  ppm), the  $-\text{NH}$  proton ( $7\text{-}9$  ppm) and proton  $\text{CH-N}$  of phthalimide in range of  $5.80\text{-}5.30$  ppm also strengthen the synthesis.

*In vitro* biological activity was evaluated at  $10\text{ }\mu\text{g/mL}$  to obtain lysis percentage %-lysis on trypomastigotes of NINOA and INC-5 strains and  $\text{LC}_{50}$  (es correcto  $\text{LC}_{50}$  o es  $\text{IC}_{50}$ ??) value of selected compounds were also determined, ~~and commercially available drugs nifurtimox and benznidazole were used as reference drugs.~~ In *para*-aminobenzoic acid series ~~the compound~~, three compounds (**5**, **9**, and **10**) sharing a *para*-aminobenzoic acid moiety showed more potent trypanocidal activity than the commercially available drugs nifurtimox and benznidazole in both strains: the lysis concentration of 50% of the population ( $\text{LC}_{50}$ ) was  $< 0.15\text{ }\mu\text{M}$  on the NINOA strain, and  $\text{LC}_{50} < 0.22\text{ }\mu\text{M}$  on the INC-5 strain. In the phthaloyl derivatives of 3-amino-3-aryl propionic acids (A-D), most of the compounds showed greater the 80% trypanocidal activity ~~but for the individual strain~~. The compound (D-11) showed an equal % lysis ( $63 \pm 8$  and  $65 \pm 6$ ) and  $\text{LC}_{50}$  value ( $18.94 \pm 2.70\text{ }\mu\text{g/mL}$  and  $16.60 \pm 2.36\text{ }\mu\text{g/mL}$ ) in NINOA and INC-5 strains, respectively, which is better than reference drugs. In series (E-H), no one compound showed the most prominent trypanocidal activity for NINOA and INC-5 strain.

TcTS enzyme inhibition of selected compounds was determined by High-Performance Ion Exchange Chromatography with Pulse Amperometric detector (HPAEC-PAD). The compound F-7, ((2-(2-(4-carboxyphenyl) hydrazine-1-carbonyl) terephthalic acid) showed the 97%, TcTS enzyme inhibition and compounds D-11, (3-(5-methyl-1,3-dioxoisindolin-2-yl)-3-(naphthalene-2-yl)propanoic acid) and D-4 (3-(4-hydroxyphenyl)-3-(5-methyl-1,3-dioxoisindolin-2-yl)propanoic acid) of series D showed the highest 86.9% and 82.5 % TcTS enzyme inhibition, respectively. ~~Further compounds~~ showed the moderate TcTS inhibition value. The other compounds showed.....

## CHAPTER ONE

### 1.1. INTRODUCTION

*Trypanosoma cruzi* (*T. cruzi*), a protozoan parasite is a causative agent of Chagas disease (CD), which is also known as American trypanosomiasis. It was first described in humans by the Brazilian physician Carlos J.R Chagas in 1909 [1]. The three main vector species studied in the transmission of *T. cruzi* to humans are *Triatoma infestans* (a), *Rhodnius prolixus* (b) and *Triatoma dimidiata* (c) (**Fig. 1**) [2]. These infected insects feed on the blood of humans and their domesticated animals and in the process, they store parasite-laden excrement. The parasites are transmitted through contact with a skin lesion, mucosal surfaces or the conjunctiva. Transmission may also happen congenitally, by blood transfusion, during organ transplantation, and eventually by ingestion of contaminated food or drink [3-7].

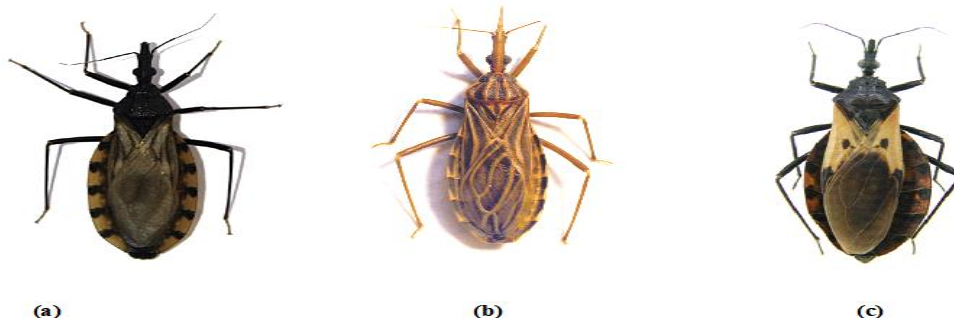


**Fig. 1.** Three main vector species involved in the transmission of *T. cruzi* to humans are *Triatoma infestans* (a), *Rhodnius prolixus* (b) and *Triatoma dimidiata* (c).

According to the Pan-American Health Organization (PAHO) 2014, the CD is a zoonosis endemic to 21 countries of America. It is estimated that around 8 to 10 million people are infected in North, Central, and South America and around ~~about to~~ 90 to 100 million people need protection because they are at risk of infection. CD was first reported in 1940 in Mexico and in 1955 in Texas, in the United States [8, 9]. A seroprevalence between one to six million

cases of CD has been reported in Mexico and 0.1 million people in Canada [10]. In the United States, there are approximately 300,000, individuals infected with *T. cruzi*, although one report estimated 250,000 in Texas alone [11]. CD has also been reported in non-endemic countries due to migration. Globally, CD in different nations ranges from 140 in Australia to 12,000 in England, and in Europe, it has been determined that there are between 68,000 and 123,000 individuals contaminated with *T. cruzi* (**Fig. 2**) [12-15]. Moreover, around 12,500 deaths per year are attributed to CD according to the World Health Organization [16].

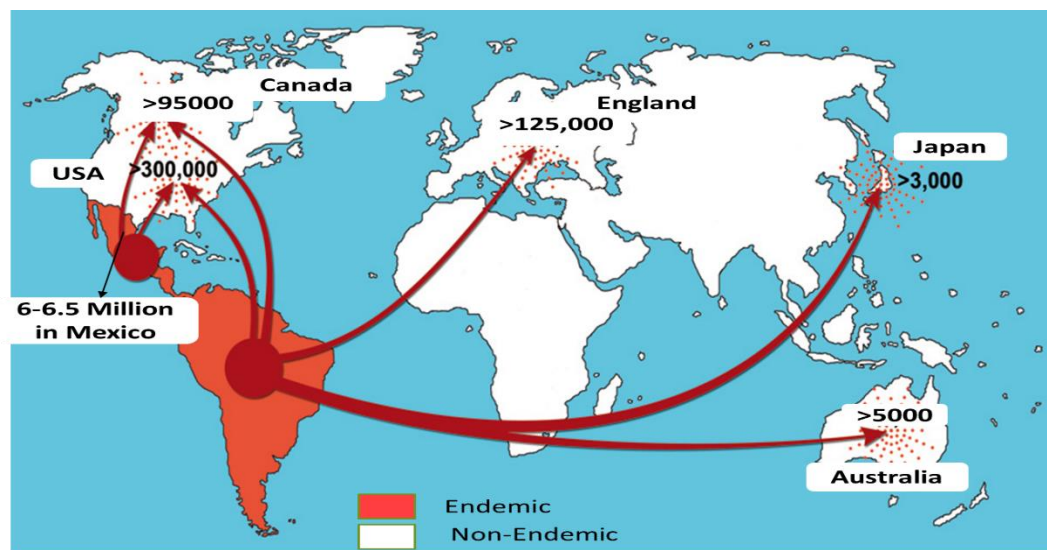


**Fig.2.** The prevalence of Chagas to worldwide, from endemic to no-endemic countries.

According to World Health Organization (WHO), CD is considered it one of 17 neglected tropical diseases and its budgetary burden estimated to be \$7.19 billion yearly worldwide [16] and according to one estimate the overall economic losses from CD only in Mexico may exceed \$3 billion annually [11], comparable to more well-known severe illnesses such as that produced by rotavirus or cervical cancer [17].

Chagas disease has two clinical stages, acute phase, and chronic phase. The acute phase is frequently symptom-free or exhibits only mild symptoms and signs that are not unique to



Chagas disease. The most considered marker of acute Chagas disease is called Romana's sign (**Fig. 3**), another symptom may include swelling and/or redness at the skin infection site (termed chagoma), fever, headaches and body aches, fatigue, nausea, vomiting, abdominal discomfort or pain and liver and/or spleen enlargement. Following acute phase, symptoms are common to another diseases which made it difficult to diagnose. The chronic phase symptoms of CD vary varies according to the most affected organs by the persistent presence of the parasites ~~within the tissues of these organs~~, in most cases, symptoms may include the following: irregular heartbeats, palpitations (abnormal heartbeat sensations), fainting (syncope), cardiomyopathy (chronic disease of the heart muscle), congestive heart failure (dilated heart), shortness of breath (dyspnea), emphysema and Sudden death [18-20].



**Fig. 3.** Romana's sign, a typical sign of Chagas' disease, this image is downloaded from the CDC website ([www.cdc.gov](http://www.cdc.gov)).

Current chemotherapy treatment involved, the nitroheterocyclic compounds benznidazole (*N*-benzyl-2-(2-nitro-1*H*-imidazole-1-yl) acetamide, Bnz) (a) and nifurtimox (3-methyl-*N*-[(5-nitrofuran-2-yl)methylidene]thiomorpholin-4-amine-1,1-dioxide, Nfx) (b) (**Fig. 4**), launched by Bayer in 1967 and Roche in 1972, respectively, are the only two drugs currently used for the treatment of Chagas disease, although they are not effective against its chronic form [21], diminish in efficacy the longer a person has been infected [22], and the treatment is associated with severe toxic side-effects as, skin bluster, reduction in bone marrow, nausea, vomiting,

allergic dermatitis, peripheral neuropathy, insomnia, anorexia, rapid weight loss and most important is these drugs are also recognized as mutagenic and genotoxic [23-28]. Some strains of *T. cruzi* are also reported to be resistant to Nfx and Bnz [29]. ~~The mode of action of Bboth Nfx and Bnz are antifungal agents and combat the parasite directly,~~ the mode of action of both drugs involved the production of free radicals and/or electrophilic metabolites. The nitroreductase reduced the nitro group of both drugs with the formation of various free radical intermediates and electrophilic metabolites. In Nfx the radicals undergo the redox cycling with molecular oxygen and production of  $O^{2-}$  and  $H_2O_2$  ~~reported and is the main mechanism of action of Nfx~~ but in Bnz the trypanocidal effect does not depend on oxygen radical [30]. Posaconazole and ketoconazole, which are involved inhibition of ergosterol biosynthesis and antifungal drugs, are also being in clinical trial for CD [31]. A wide range of attempts was made for the formulation of vaccine and several strategies has been evaluated including the use of the ~~over the year ranging from the~~ whole parasite to recombinant protein, viral vectors and DNA in mice models but currently no vaccine has been approved for treatment of CD [32].



**Fig. 4. Chemical S**tructures of drugs ~~are~~ currently used for the treatment of CD, (a) benznidazole and (b) nifurtimox.

#### 1.1.1. Life cycle of *T. cruzi*

*Trypanosoma cruzi* (*T. cruzi*) is a parasitic species that belongs *Euglenoid* protozoan, having Domain: *Eukarya* Kingdom: *Excavata*, Phylum: *Euglenozo* Class: *Kinetoplastida*, Order: *Trypanosomatida* Genus: *Trypanosoma* having a special section called *Stercoraria*. It is mainly found in Latin America, Central and South Africa, and some other non-endemic countries [33-35]. Protozoa of the *Trypanosomatidae* family show, during their life cycle, several forms which can be easily identified by light microscopy and can be classified as (a) Amastigotes, also known as spheromastigotes, micromastigotes having kinetoplastidia anterior to the nucleus and without free flagellum with the spheroid shape. (b) Epimastigotes, which are spindle-shaped organisms, 20-40 mm long. The kinetoplast is located anterior to the nucleus and no undulating membrane. (c) *Trypomastigotes*. These forms have a length of about 25 mm and a diameter of about 2 mm. The kinetoplast is located posterior to the nucleus and undulating membrane runs length of the organism [33]. The life cycle of *T. cruzi* can be divided into two parts depending on host vertebrates and invertebrates. When *triatomine* feeds on vertebrates host by sucking bloodstream from infected vertebrates. These trypomastigotes change into epimastigotes in the midgut of bug. In the bug intestine of bug, the epimastigotes divided repeatedly by binary fission and move into the rectum of bug where and again change into metacyclic trypomastigotes which are released with feces and are capable to infect the vertebrate host. After entering to vertebrate host from mucous membrane or wound from feces of bugs they change into amastigotes, these amastigotes which multiply themselves into cell plasma by binary fission and change into trypomastigotes, which is a non dividable form of *T. cruzi*; and when cell membrane burst these trypomastigotes enters bloodstream and first clinical stage of CD benigns, started from here (Fig. 5), and this process of host cell invasion and induced cell death by *T. cruzi* continues for years inside the mammalian host as the infected individual progresses into the chronic stage of Chagas' disease [35].

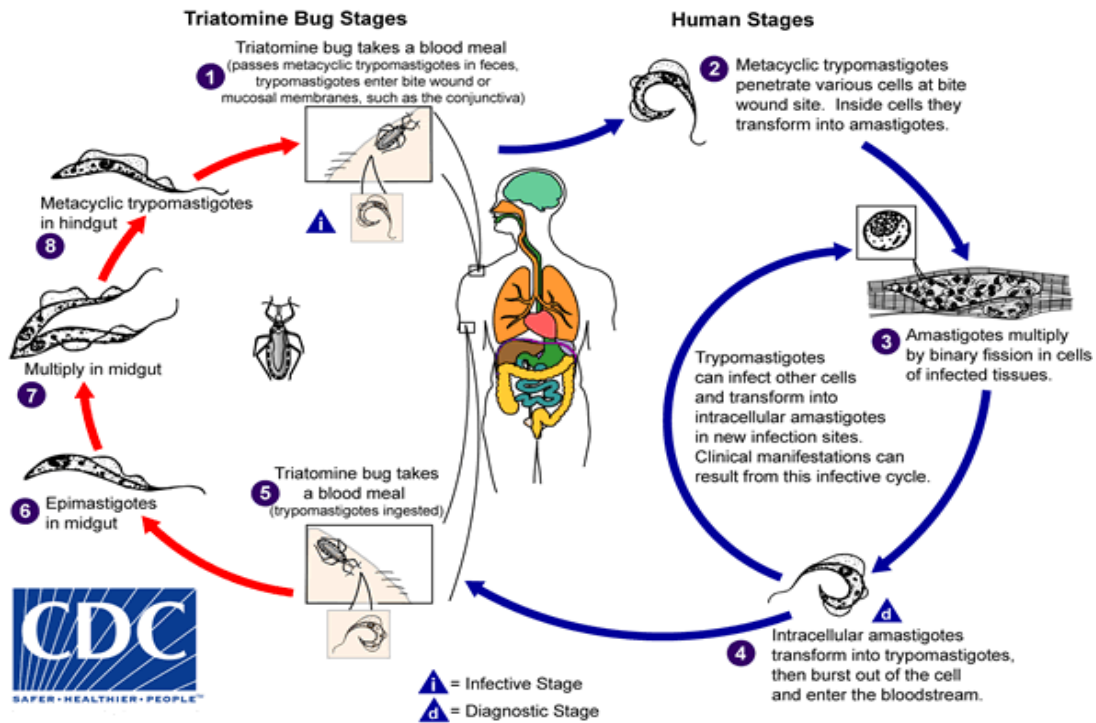


**Fig.5.** The life cycle of *T. cruzi* showing the various forms of the protozoan in the invertebrate (triatomines) and vertebrate (mammals) hosts. Figure reproduced from the Center of Control Diseases homepage ([www.cdc.gov](http://www.cdc.gov)).

### 1.1.2. Drug targets in *T. cruzi*

Advances in proteomics and knowledge of the parasite's biochemistry have identified different key enzymes in the *T. cruzi* life cycle, which are crucial for the survival and development of the parasite. Some of these are homologous to the host and some are different. Efforts have been made to explore *T. cruzi* enzymes as potential therapeutic targets for the design of new drug leads including inhibitors [36]. These enzymes are: topoisomerases [37, 38], *trans*-sialidase [39], proline racemase [40], cysteine proteinase (cruzipain) [41], trypanothione reductase [42], hypoxanthine-guanine phosphoribosyl-transferase [43], glyceraldehyde-3-phosphate dehydrogenase [44], dihydrofolate reductase [45], proteasome (esto no es enzima) [46], and galactose in the furanose configuration, which is a component of parasite glycoconjugates that does not exist in mammals [47].

Some structural parts of *T. cruzi* such as kinetoplast DNA (kDNA) [48] sites and its sterol metabolism [49] can also be used as chemotherapeutic targets. Particularly, in this review, we analyzed *trans*-sialidase and inhibitors that could be helpful for the development of new anti-Chagas drugs.

### 1.1.3. *Trans*-sialidase

After *T. cruzi* enters the mammalian bloodstream, it must combat the host immune system. Surface sialylation plays an important role in this event, with the parasite needing sialic acid for survival in the host. This occurs because *T. cruzi* is unable to synthesise sialic acid *de novo*. Sialic acid (sugar with a nine-carbon backbone) plays an important role in normal and pathological processes in mammals due to its negative charge and hydrophilicity. Sialic acids regulate the immune system and also serve as components of binding sites for various pathogens and toxins [50]. *T. cruzi* uses *trans*-sialidase (TcTS) to disguise itself from the host immune system [51]. TcTS is a glycosylphosphatidylinositol (GPI) protein (**Fig. 6**) that is associated with the parasite membrane.

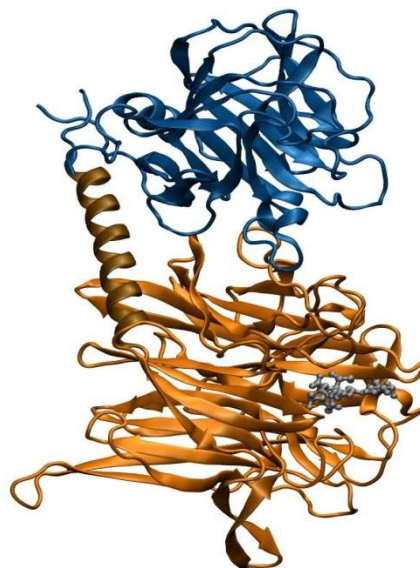


**Fig. 6.** Structure of TcTS. The orange ribbons, catalytic domain, the blue ribbons, lectin-like domain, and the alpha-helix linker region. Sialic acid is shown in silver balls and sticks within the active site of the catalytic domain. Coordinates are from PDB code 1MS8.

TcTS has a molecular mass estimated at 160-200 kDa (monomeric form) [52] and it is considered a key enzyme for the transfer of sialic acid molecules from the host cell-surface glycoconjugates to its own surface mucin as glycoproteins [53]. The transfer is specific and involves sialic acid  $\alpha$ -(2--3)-linked to the donor and the formation of the same linkage with  $\beta$ -galactopyranosyl groups in acceptor (parasite) (**Fig. 7**) [54]. TcTS also transfers  $\alpha$ -(2--3), linked N-glycolyl neuraminic acid to terminal  $\beta$ -galactopyranosyl groups [55]. The genomic study of *T. cruzi* revealed that it contains more than 1400 genes. These members of the TcTS gene family protein are classified into eight groups. TS group I proteins have catalytic activity related to *T. cruzi* and *T. brucei* phylogenetic clade and other TS groups that belong to other trypanosomatids have inactive copies [56-58].

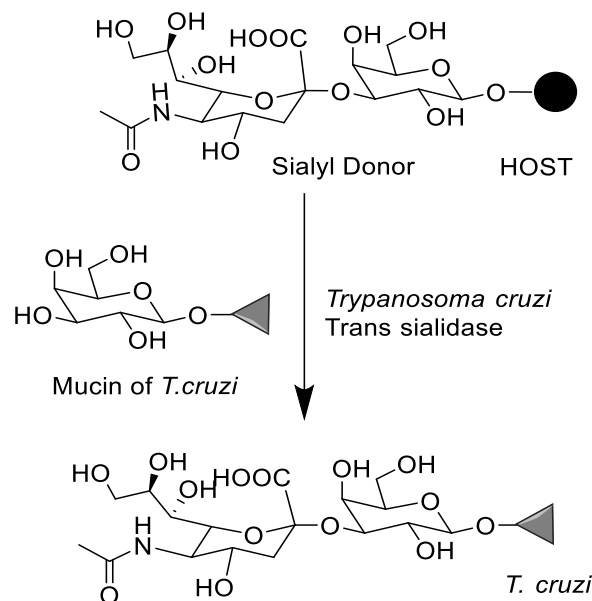


**Figure (7).** Transfer of sialic acid from host glycoconjugates to the  $\beta$ -galactopyranosyl unit of mucin. The transfer is specific to the 3-position of a terminal  $\beta$ -Galp unit. ● Oligosaccharide linked in mammal glycoconjugates. ▲ Oligosaccharide in a mucin of *T. cruzi*

Expression of TcTS enzyme also depends on the trypanosome strain; therefore, the pathogenicity of *T. cruzi* is influenced by the variation in expression of the TcTS level [59]. The specific activity of the TcTS in epimastigotes is 17% of that found in trypomastigotes [60]. Both infective trypomastigotes and epimastigotes (development stages of *T. cruzi*) express the active TcTS enzyme as shed acute-phase antigen (SAPA). These stages have identical activities but differ in the SAPA domain [61-63]. In epimastigotes, SAPA is a trans-membrane protein, while in trypomastigotes TcTS is associated with the membrane via a GPI anchor [64]. The TcTS structure contains three domains: N terminal, a catalytic domain that folds into a six-bladed  $\beta$  propeller structure [65], a C-terminal lectin-like domain that is catalytically inactive, and an unfolded domain which contains the 12-amino acid-long repeat known as SAPA [66].

On the other hand, TcTS preferentially catalyses the transfer of sialic acid residues from  $\text{Sia}\alpha 2-3\text{Gal}\beta 1\text{-R}$  containing donors and attaches them to an  $\alpha 2-3$  linkages to terminal  $\beta$ -Galp containing acceptors (transfer reaction). In the absence of a carbohydrate acceptor, TcTS irreversibly transfers sialic acid to a water molecule, thus functioning as a sialidase (hydrolysis reaction) as in Figure 8 [67].

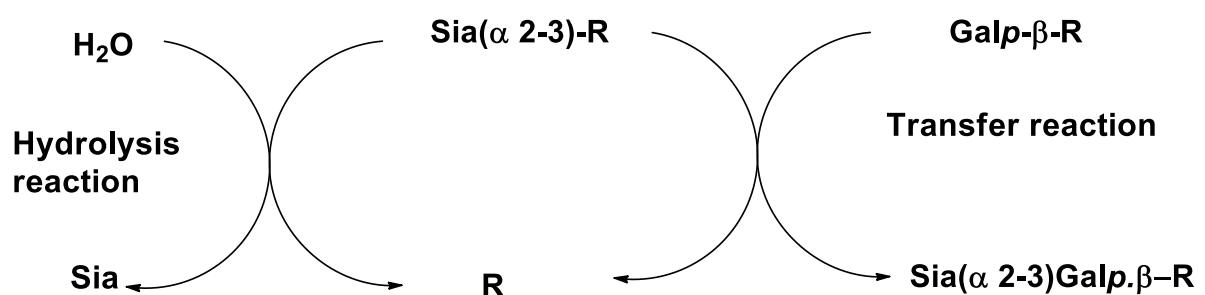


**Figure (8).** Representation of transfer and hydrolysis activities of TcTS.

#### 1.1.4. Catalytic mechanism of *trans*-sialidase

The crystal structure and molecular layout of TcTS have shown that it contains conserved features of sialidase, such as an arginine triad (Arg35, Arg245 and Arg314), which contributes to the binding of a carboxylic group of sialic acid derivatives, while the acetamido group is stabilized by Asp96 (**Fig. 9**).

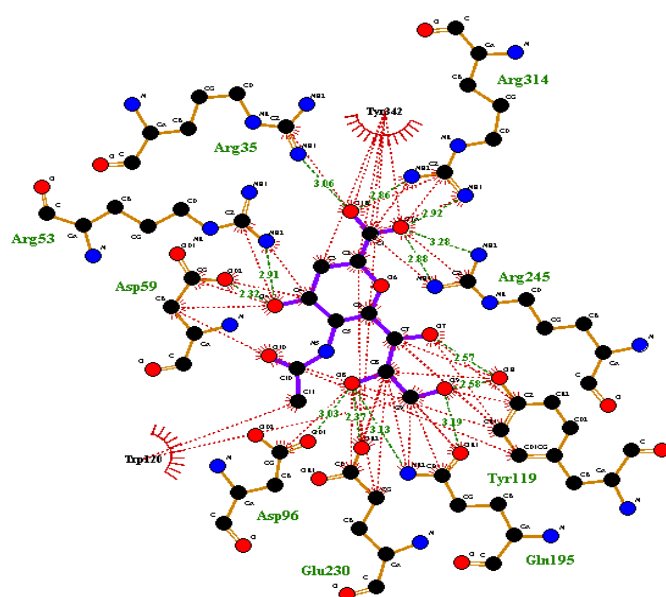


**Figure 9.** Sialic acid analog 2,3-dehydro-3-deoxy-*N*-acetylneuraminic acid (DANA) interaction on active sites of *Trypanosoma cruzi trans*-sialidase (TcTS) enzyme (green line showing a conventional hydrogen bonding interaction and red lines showing a hydrophobic interaction). The image was produced with LigPlot+ software (v.1.4, European Bioinformatics Institute (EMBL-EBI), Hinxton, Cambridge, UK).

A transition state has been reported, which is stabilized by Tyr342, Glu230; on the other hand, glutamic acid Glu357 helps stabilize Arg35 and aspartic acid, Asp59 is essential for catalysis. Furthermore, the side chain residues Val95, Leu176 and Trp120 show high *trans*



glycosylase activity in TcTS [68]. Two aromatic amino acid residues Tyr119 and Tyr248 in TcTS are reported. These tyrosine residues combine with Trp120, Val203 and Trp312 which contribute to the exclusion of water from the cleft and are hydrophobic in nature [65]. The transfer mechanism of TcTS over hydrolysis is facilitated by the aromatic amino acids Tyr119 and Trp312 and is also involved in the formation of acceptor binding sites [69, 70]. The crystal structure shows the change in position of Tyr119 in the presence and absence of sialoside [65]. Energetically, ligand binding in TcTS involves the transfer of a proton and computational-analyses have shown that in the catalytic mechanism a stable covalent intermediate is formed with a sialic acid ring, and the pair Tyr342/Glu230 acts as an unusual catalyst in which the hydroxyl group of Tyr342 acts as a nucleophile which is facilitated by Glu230 (Fig. 10) [71]. X-ray structures and experiments trapping the intermediate with fluoro sugars followed by peptide mapping and crystallography also provide evidence for this reaction mechanism [65]. Comparison of TcTS with other trypanosomatids such as *T. rangeli* (70% amino acid identity) indicated that an alteration in the active site cleft is responsible for different types of enzymatic action in *T. cruzi*.

From the molecular dynamic simulation, it is known that Tyr119 and Trp312 are key hydrophobic residues that confer flexibility to the catalytic cleft mouth and play a vital role in TcTS catalytic activity because both residues allow substrate access in the catalytic pocket in a controlled manner and also help to orient. Two regions for the substrate bindings were observed in the catalytic cleft. The first comprised of Tyr 119 and Trp312, where substrate/acceptor lactose resides, and the second where sialic acid resides in the active site. The loop carrying Trp312 is reported opposite to the catalytic cleft and helps to stabilize the galactoside moiety in the enzyme pocket. The bond between sialic acid (Neu5Ac2en) and the substrate has been observed to undergo major conformational changes with Tyr sterically

displaced about 2 Å and a shortening of the distance between the Tyr hydroxyl group and the sialic acid C2 atom has also been reported [72-75].

Saturation transfer difference (STD) NMR experiments for studying the binding of *p*-nitrophenyl glycosides of sialic acid and its analogs to TcTS, reported that the shortening of the glycerol side chain significantly favours the transfer reaction over hydrolysis but this effect is opposite with 9-O-acetylation of Neu5Ac [76].

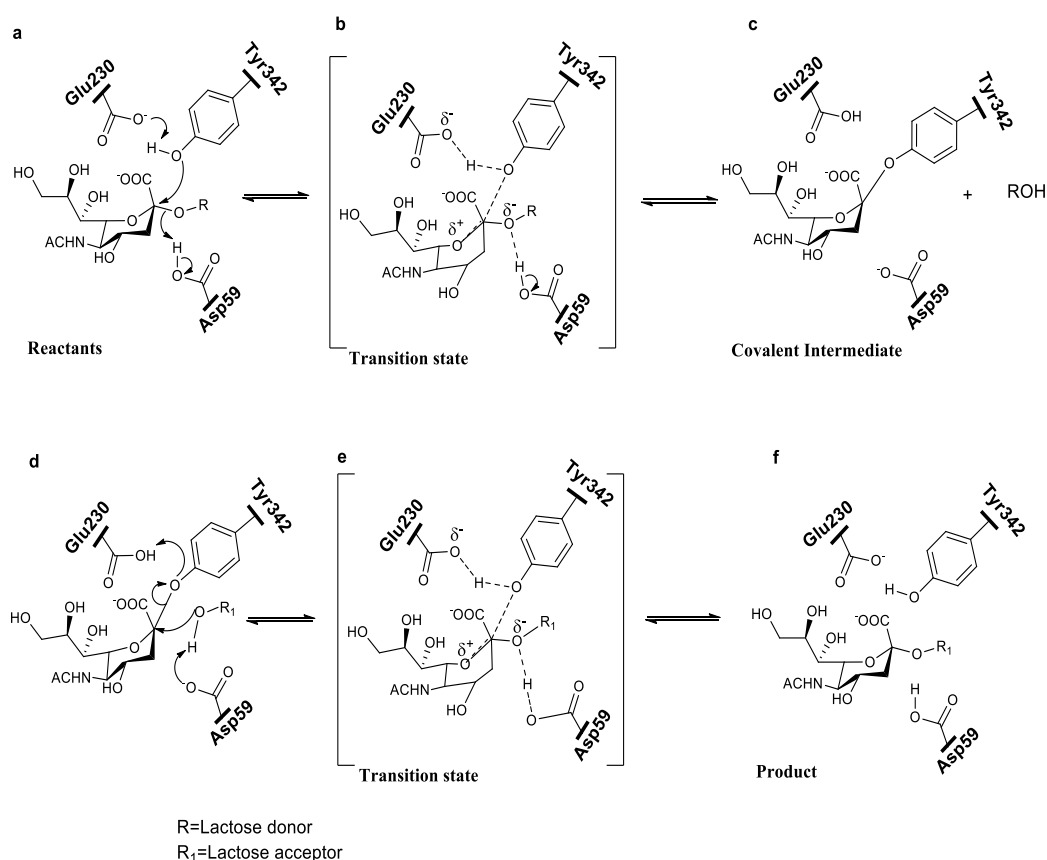


**Figure (10).** Reaction mechanism of trans-sialidase enzyme showing Tyr342 acting as nucleophile and Glu230/Asp59 stabilizing the intermediate.

The *trans*-sialidase enzyme has unique features compared to influenza neuraminidase and there is no apparent correlation between these two. TcTS has two binding sites: one is the sialic acid acceptor and the other for glycosylation. Moreover, the arginine triad and Asp/Glu are located in the same region in both cases, but in contrast, the presence of Glu119, Glu227,

Glu276, Glu 277, Asp151 and an extra Arg53 residue, are more negatively charged residues compared to neuraminidase versus TcTS [70, 77, 78].

### 1.1.5. Development of trans-sialidase inhibitors

A literature survey has shown that TcTS enhances the virulence factor of *T. cruzi* by altering the host immune response; also, it is nonhomologous to host mammalian sialidase. This has made it more unique as a drug target in *T. cruzi* for the development of inhibitors. However, no effective TcTS inhibitor, which reduces the catalytic activity of the enzyme, has been reported yet. By using rational drug design and a computational method, some interesting lead compounds have been obtained, but it is reported that these compounds can inhibit trans-sialidase 50% at millimolar concentrations.

The molecules that have been tested as TcTS inhibitors are listed below, they are as molecules that are analogous to acceptor or donor substrate and molecules unrelated to TcTS substrate.

### 1.1.6. Sialic acid donor-based substrate analog inhibitors

The donor-based inhibitors are structurally similar to sialic acid and could be classified as donor substrate analogous compounds. The 2,3-Dehydro-2-deoxy-N-acetylneuraminic acid (DANA) compound (**1**) (Fig. **11**) was found to be a good inhibitor against the influenza neuraminidase ( $K_i = 4 \mu\text{M}$ ), but very weak against TcTS ( $K_i = 12.3 \text{ mM}$ ) [77]. Zanamivir, 4-Guanidino-2,4-dideoxy-2,3-dehydro-N-acetylneuraminic acid (**2**) (Fig. **11**) ( $\text{IC}_{50} = 5 \text{ nM}$ ), obtained by replacement of a hydroxyl group in DANA with a guanidine group, and oseltamivir (Tamiflu) ethyl (3R,4R,5S)-4-acetamido-5-amino-3-pentan-3-yloxy-cyclohexene-1-carboxylate (**3**) (Fig. **11**) ( $\text{IC}_{50} = 1 \text{ nM}$ ) in which a hydroxyl group of DANA was replaced by an amino group are approved drugs with a potent inhibitor effect for influenza A and B but weak inhibitors of TcTS ( $K_i = 12.29 \text{ mM}$ ) [68]. 4-amino-2-deoxy-2,3-didehydro-N-acetylneuraminic acid (**4**) (Fig. **11**) and N-(4-nitrophenyl) oxamic acid (**5**) (Fig. **11**) were also

the best inhibitors against influenza enzymes ( $IC_{50} = 10 \mu M$ ) but were weaker against TcTS. Furthermore, the most frequently used inhibitor with its derivate is Neu2en5Ac, 5-N-acetyl-2,3-didehydro-2-dideoxy neuraminic acid, compared to another free Neu2en5Ac had a weak inhibitory effect for classical sialidase, but no effect on *trans*-sialidase [78-80].

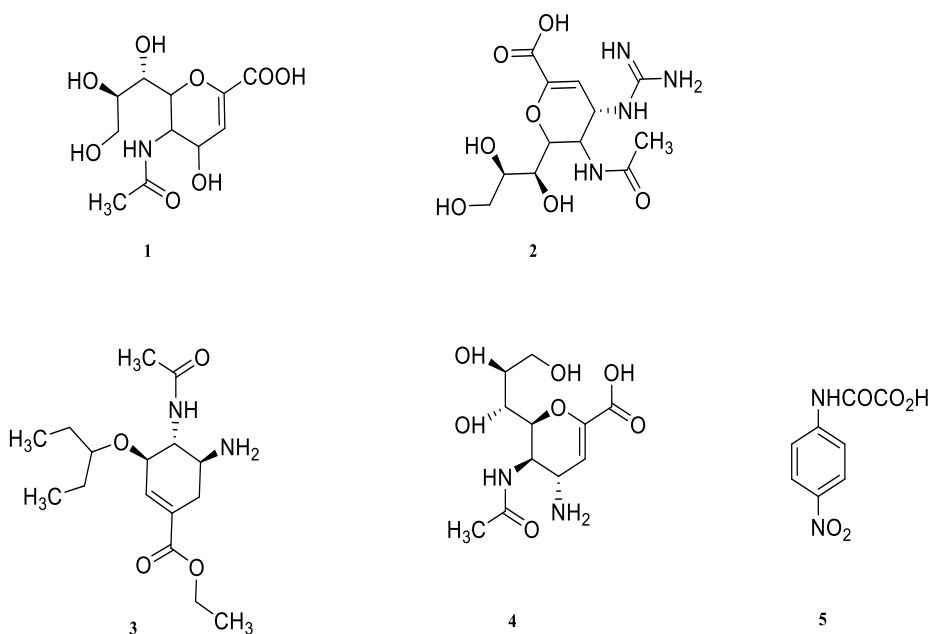


**Fig. (11).** Structure of compounds *trans*-sialidase donor-based inhibitors. 1....., 2.....3.....4.... and 5.....

#### 1.1.7. Sialic acid irreversible donor based substrate analogous inhibitors

Another group of TcTS inhibitors which are known as irreversible donor substrate analogous is 2,3-difluorosialic acid (**6**) (Fig. **12**) and 2-[2-(difluoromethyl)-4-nitrophenyl]-3,5-dideoxy-D-glycero- $\alpha$ -D-galacto-2-nonulopyranosid acid (Neu5AcFNP) (**7**) (Fig. **12**). These have shown an inhibitory concentration of 20 mM and 10 mM for TcTS, respectively. Furthermore, it was reported that 2,3-difluorosialic acid forms a covalent bond with the Tyr 342 hydroxyl group, and temporarily inhibits the enzyme; however, when the excess of the inhibitor is removed, the enzyme again becomes active. In contrast to this, Neu5AcFNP also lies in the same category and forms a covalent bond with Arg245 and Asp247 residues, and it

was confirmed by mass spectroscopy, but it is noteworthy that Neu5AcFNP inhibited infection by *T. cruzi* trypomastigotes in mammalian cells [68, 81].

The dansyl-Neu5AcFP derivative (**8**) (**Fig. 12**) was also considered a time-dependent irreversible inhibitor of TcTS. The aromatic rings in this derivative form a covalent bond with Asp247 and Arg245, which inactivates the enzyme; this was proven by MALDI-TOF/TOF-MS [82]. 2,3-difluorosialic acid derivatives (also known as irreversible inhibitors), in which 9 carbon was substituted by different compounds such as umbelliferyl (**9**), 4-(phenyl carbamide) butyramide (**10**) and benzamide (**11**), (**Fig. 12**). These were reported as good inhibitors decreasing the activity of TcTS 1000-fold [83]. Neu5Aca2-3-Gal $\beta$ -O-octyl, a thio disaccharide (**12**) (**Fig. 12**), was also a poor inhibitor of TcTS at millimolar concentration [84].

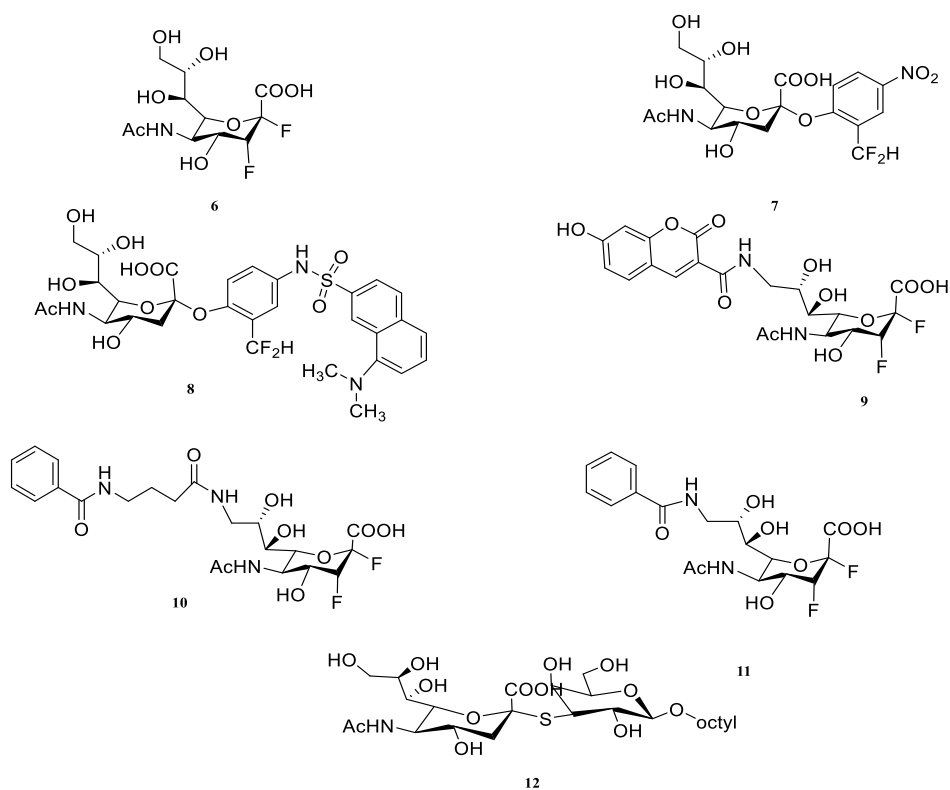


**Fig. (12).** Structure of irreversible donor substrate analogs of sialic acid?. numbers

### 1.1.8. Sialic acid acceptor-based substrate analogue inhibitors

A natural substrate of....., the GM3 ganglioside (**13**) (**Fig. 13**) with IC<sub>50</sub> values in the range of 10-100 μM, was found to be a more potent transialidase..... inhibitor compared to others since this fills both sialic acid acceptor and donor sites. However, in sialic acid, when C4, C7, and C8 are modified with deoxy or methoxy groups, respectively, the inhibitory activity of the ganglioside GM3 decreases for *trans*-sialidase, and it is not considered a good inhibitor [85].

Lactitol (**14**) (**Fig. 13**), an acceptor analogous molecule which has the ability to bind both active sites of *trans*-sialidase with an apparent Km value of 0.26 mM and IC<sub>50</sub> value of 0.57 mM, was found to weakly inhibit cell infection by ~~inhibition~~ (20-27%) inhibition. Furthermore, making modifications to lactitol by adding Gal<sub>p</sub>, Gal<sub>f</sub>, or benzyl, led to a penta saccharide called Penta 5ol (**15**) (**Fig. 13**) with an IC<sub>50</sub> value of 0.61 mM [86, 87].

Most of these types of inhibitors have shown good inhibitory effects against neuraminidase but weak inhibitory activity against TcTS; for example, ganglioside is an excellent inhibitor against neuraminidase, but a weak one against TcTS, even if it binds both active sites of *trans*-sialidase [88].

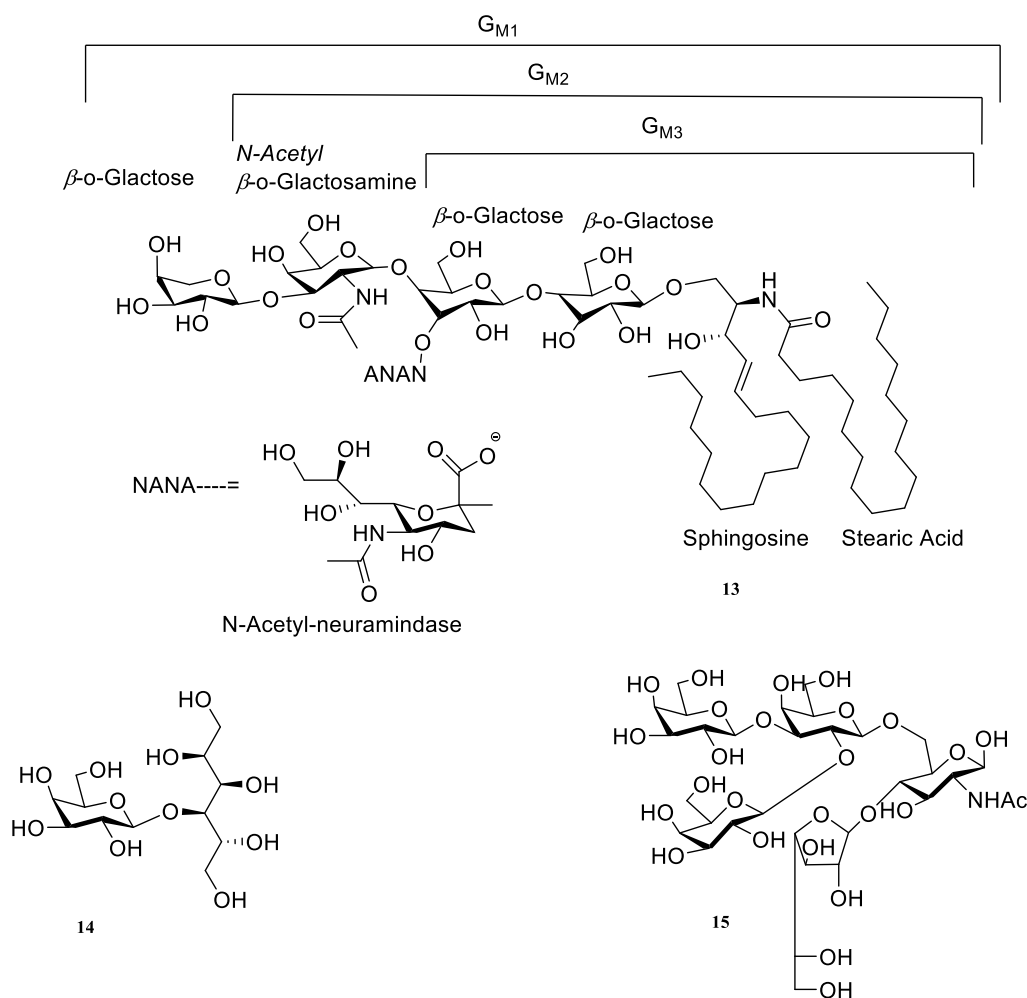


**Fig. (13).** Structure of *trans*-sialidase acceptor-based inhibitor compounds. numbers

In 2010, triazole substituted galactosides (**16a** and **16b**) (**Fig. 14**) with 17% and 37% inhibition values at 1 mM, respectively, and 50% trypanocidal activity at 200  $\mu$ M (16 a) were obtained by click chemistry but were found to be poor inhibitors of TcTS, even though these molecules bind both active sites of *trans*-sialidase [89]. In 2015, the same research group obtained mixed cyclic and linear triazole-linked oligomers using CuAAC click chemistry. The triazole-linked oligomers—pseudo-galacto-oligomers—were shown to be acceptor



substrate for multi-copy cell surface TcTS. Furthermore, these multivalent TcTS ligands blocked macrophage invasion by *T. cruzi* [90].

In 2011, octyl *N*-acetyllactosamine (**17**) (**Fig. 14**) were found to be good inhibitors against TcTS compared to other compounds but failed to inhibit TcTS activity completely. It was observed that when a modification was made at the 3 or 6 position of the *N*-acetyl glucosamine residue or at the 6 position of the galactose residue of *N*-acetyllactosamine, these residues showed strong TcTS inhibition in a radiochemical *trans*-sialylation assay, but if the modification was made at 4 position in *N*-acetyllactosamine or 2 and 3 positions in galactose, then TcTS inhibition was abolished. An octyl galactoside series (**18**) (**Fig. 14**) was tested against *trans*-sialidase and it was found that these molecules have good inhibition activity with varied inhibition values with the presence of substituents such as OH to H/OMe/F/NH<sub>2</sub> in the octyl galactosides. The OMe substitution at the 6 carbon of galactoside showed the highest inhibition compared to the parent alcohol galactoside. When the OMe substitution was made at the 3 and 4 carbon of galactoside, the carbon 3 substitution yielded no activity, while less inhibition was observed with the substitution of 4 carbon. Both the octyl *N*-acetyllactosamine and the octyl galactoside series have shown 80% to 84% of TcTS inhibition at a concentration of 1 mM.

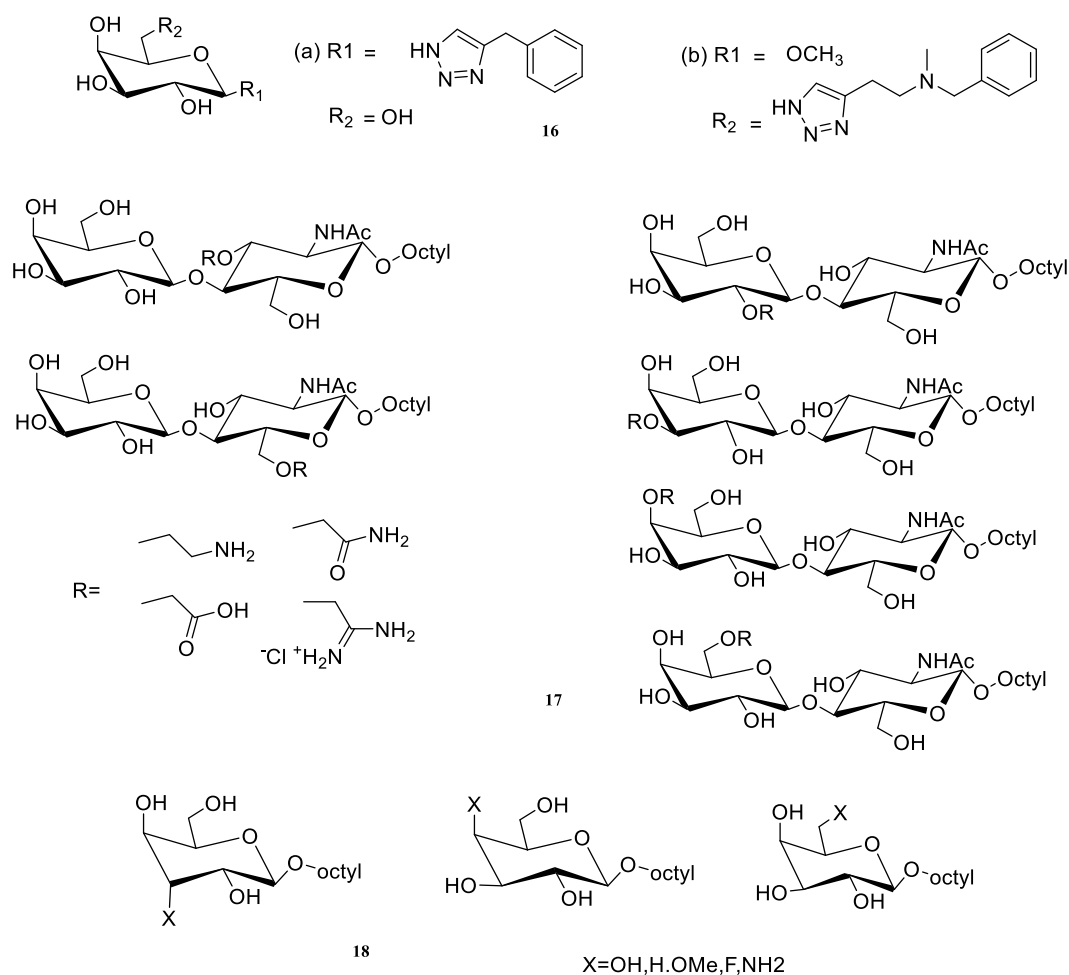


**Fig. (14).** Structure of galactoside derivatives as *trans*-sialidase acceptor-based inhibitors.

$\beta$ -thiogalactopyranosides derivatives (**19**), (**20**), (**21**), (**22**) and (**23**) (**Fig. 15**) with thio ether compounds showed some inhibition against TcTS with an IC<sub>50</sub> at the millimolar range. The structure-activity relationship (SAR) study revealed that the carboxylic group, cycloketone group, and weakly basic substituents interact with active sites of enzymes. Overall these studies suggested that the TcTS active sites are remarkably tolerant for both functional groups and the physical shape of inhibitors for the acceptor binding sites in the enzyme [91].

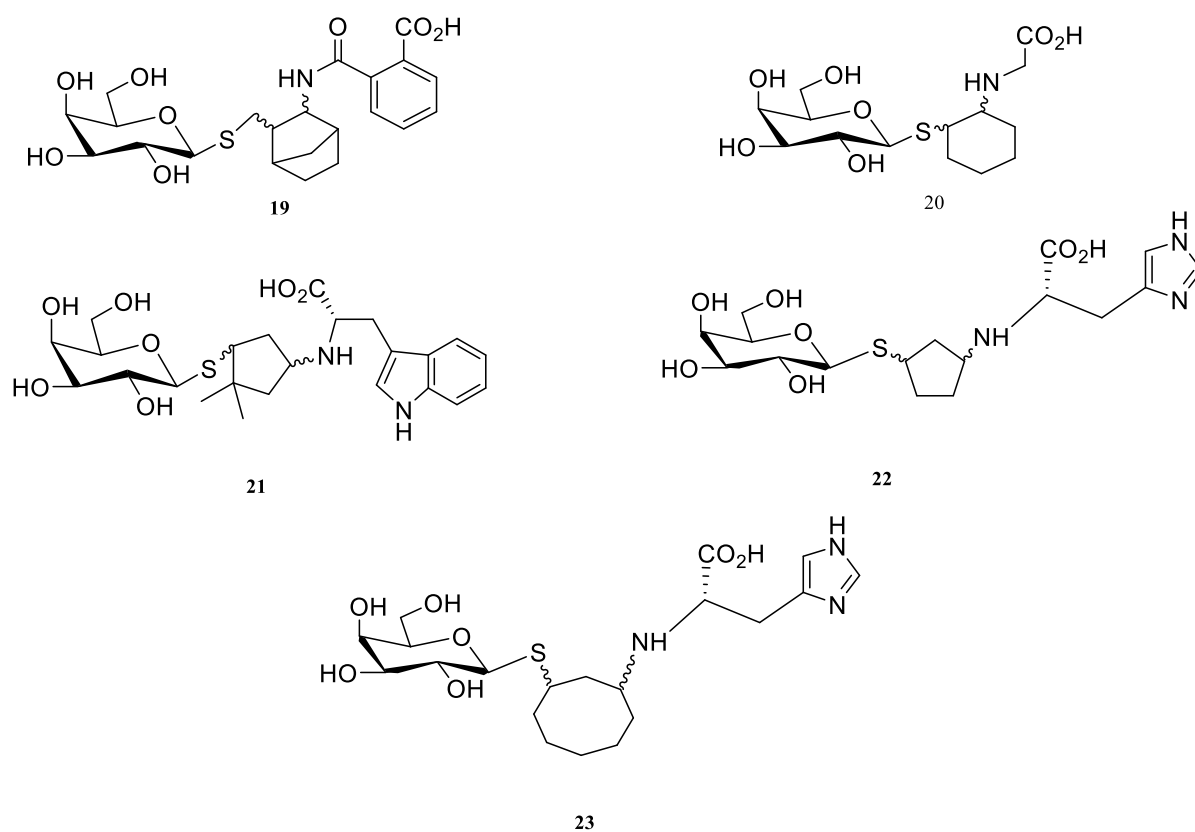


**Fig. (15).** Structure of  $\beta$ -thiogalactopyranosides *trans*-sialidase acceptor-based inhibitors

In 2014, mono- and divalent  $\beta$ -N- and  $\beta$ -S-galacto-pyranosides were synthesized and evaluated as sialic acid acceptor and inhibitors of TcTS by using high-performance anion exchange chromatography with pulsed amperometric detection (HPAE-PAD). In the case of mono-valent compounds, N-lactoside (**24**) (Fig. 16) and S-lactoside (**25**) (Fig. 16), were analyzed as acceptor substrates for TcTS and these showed inhibition values of 32% and 41%, respectively. A divalent N-lactoside (**26**) (Fig. 16), was the strongest competitive inhibitor with 70% TcTS inhibition among all tested compounds, while divalent S-lactoside (**27**) (Fig. 16) showed 53% TcTS inhibition [92].

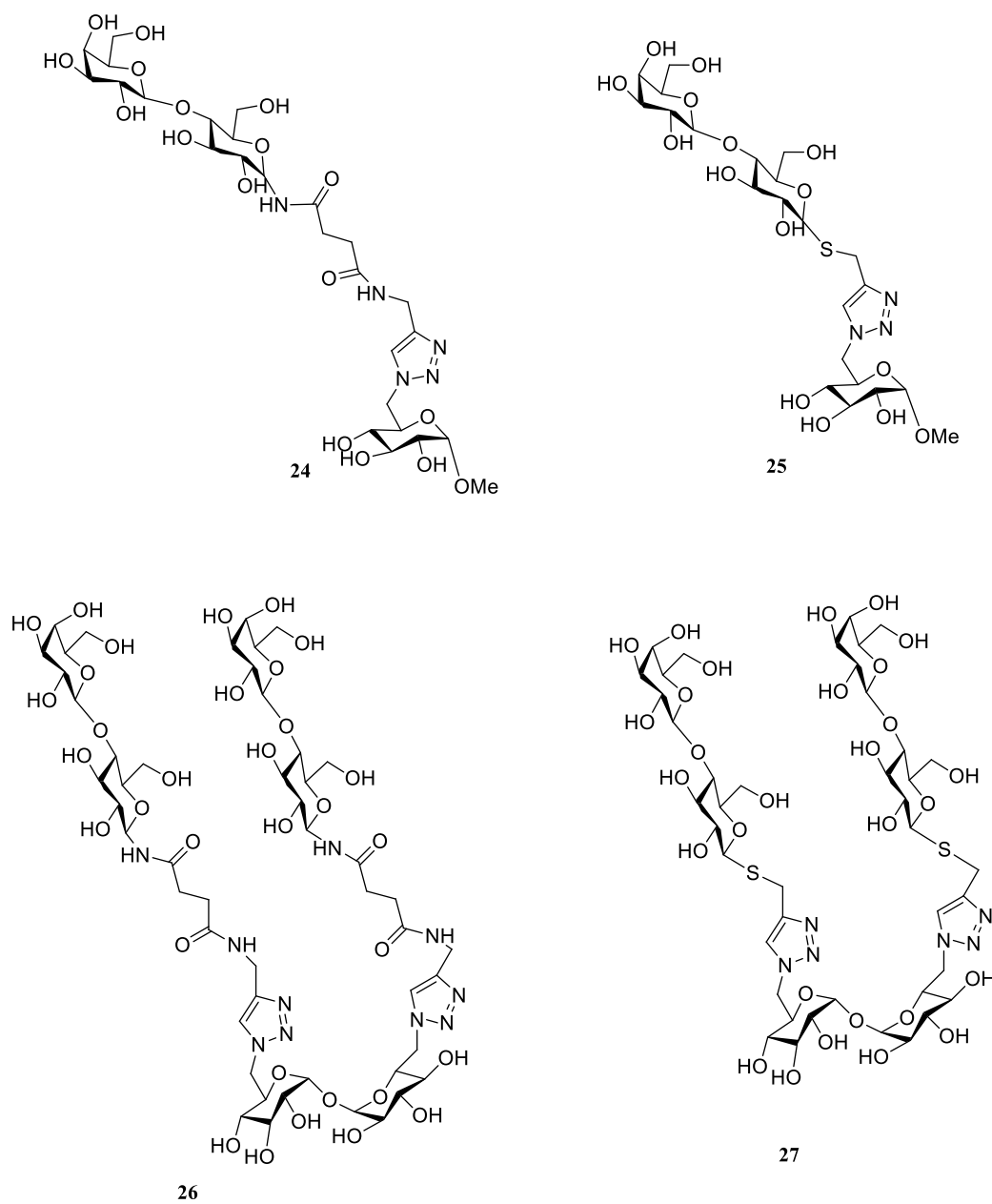


**Fig. (16).** Structure of mono- and divalent  $\beta$ -N- and  $\beta$ -S-galacto-pyranosides *trans*-sialidase acceptor-based inhibitors.

PEGylation of lactose analogues with multi-arm polyethylene glycol in which covalent conjugates of 8-arm PEG were synthesized and reported in 2012. TcTS radioactive inhibition assay was carried out and these compounds showed an inhibition value in the range of 0.08 mM to 0.70 mM [93].

Most recently in 2016, multivalent  $\beta$ -thiogalactopyranosides and thiolactosides were synthesized and evaluated as acceptor substrate and inhibitors of TcTS using HPAE-PAD and MALDI-TOF MS. In this study, monovalent, divalent, and multivalent thio-galactopyranosides were analyzed and the following results were obtained. In monovalent glycocluster, compound **(28)** (**Fig. 17**) showed 68% TcTS inhibition compared to other monovalent members of the series and in the case of divalent thioglycocluster, compound **(29)** (**Fig. 17**) showed 57% TcTS inhibition values. The octalactoside **(30)** (**Fig. 17**), in multivalent glycocluster series, was found to be a better inhibitor for competitive sialylation with a significant TcTS inhibition value of 82% when an equimolar concentration of substrate and inhibitor were used [94].

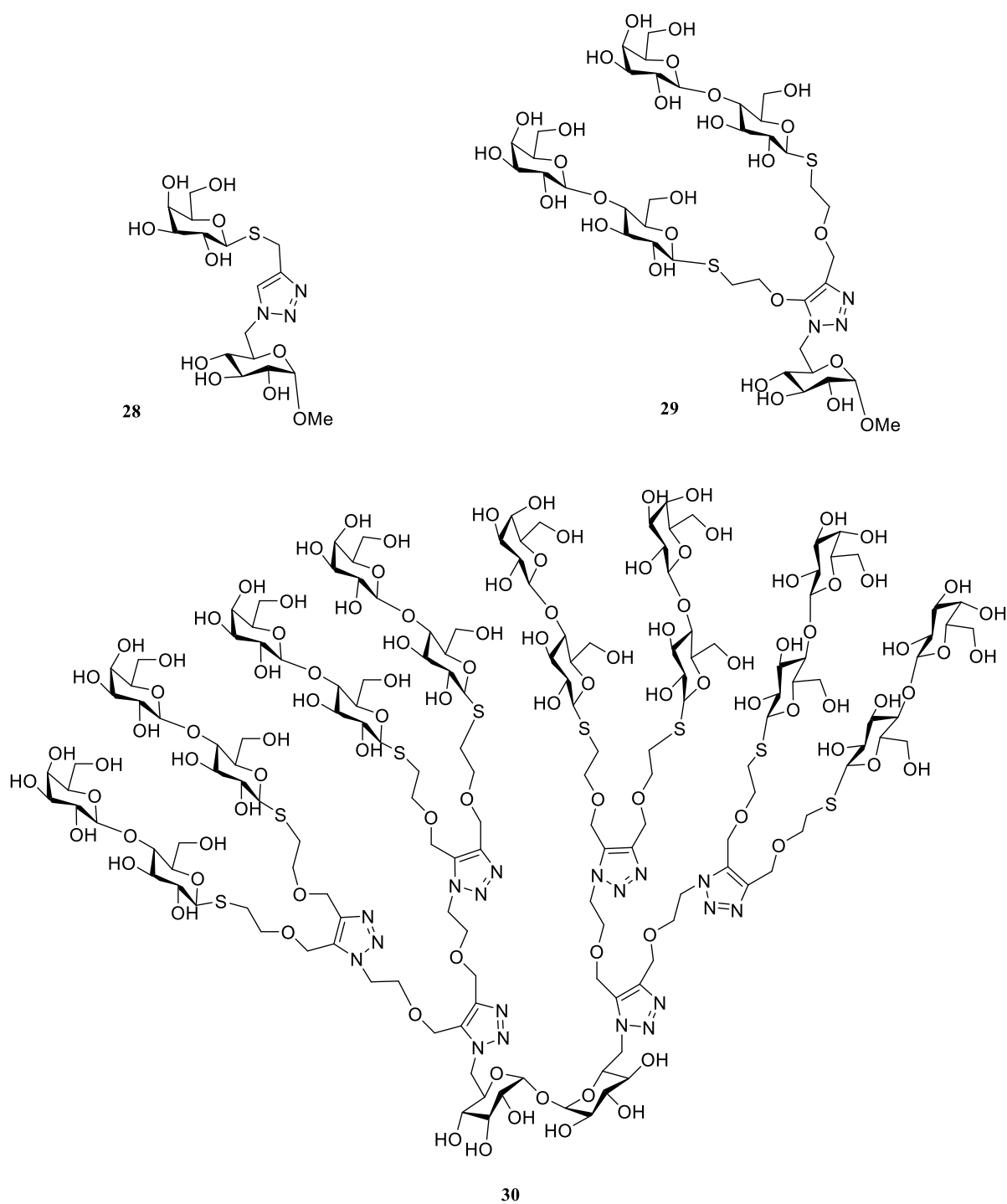


**Fig. (17).** Structure of multivalent  $\beta$ -thiogalactopyranosides and thiolactosides cluster *trans*-sialidase acceptor-based inhibitors.

In 2013, a series of deoxygenated 2, 3-difluoro-N-acetylneuraminic acid derivatives such as 5-N-acetyl-1,2,3,4,5-tetra-deoxy-2,3-difluoro-D-erythro- $\beta$ -L-manno-non-2-ulopyranosonic acid

(**31**) (**Fig. 18**) were also tested as sialidase and *trans*-sialidase inhibitors [95]. Most recently, in 2014, 3-O-substituted aryl  $\beta$ -D-galactopyranosides such as 4-methoxycarbonyl-2-nitrophenyl-3-O-carboxymethyl- $\beta$ -D-galactopyranoside (**32**) and 3 4-methoxycarbonyl-2-nitrophenyl 3-O-(5-tetrazolylmethyl)- $\beta$ -D-galactopyranoside (**33**) (**Fig. 18**) were obtained by modification of the galactoside compounds. The strategy used for the design of the proposed aryl galactosides was based on a molecular simplification of the well-known TcTS donor substrate 3'-sialyllactose, bioisosterism, and virtual screenings. These modified compounds showed 18% to 21% inhibition values, respectively, against *trans*-sialidase at 1 mM. Docking studies of compound **32** showed that the carboxylate group electrostatically interacts with arginine triade on the TcTS active site, while the carbohydrate group and a glycon moiety form hydrogen bonds with the enzyme. The bioisosteric substitution of the carboxylic acid group with the tetrazole ring had not shown a valuable effect in inhibition activity; this could be explained on the basis of the docking mode of these molecules because the docked mode of both **32** and **33** is quite different; the galactoside **33** penetrates more in the donor subsite and its glycol moiety made the staking interaction with Trp312 and Tyr119 in the acceptor subsite, and the pocket of TcTS which accommodates the N-acetyl group of sialic acid is occupied by the tetrazole group. In addition, hydrogen bonding was observed between the nitro group and the enzymatic arginine triad, instead of tetrazole [96].

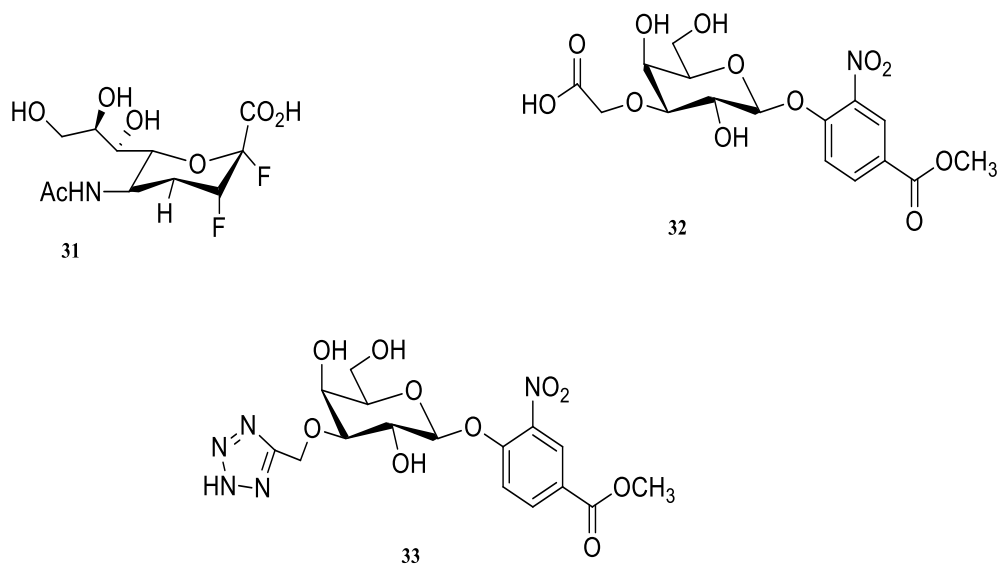


**Fig. (18).** Structure of *trans*-sialidase acceptor-based inhibitors.

### 1.1.9. Molecular Docking and discovery of Non-sugar based inhibitors (unrelated to sialic acid)

#### 1.1.9.1. Structure-based design and Macromolecules

The availability of three-dimensional biological macromolecules (proteins or nucleic acid), possessing the sequence of amino acid and bases provide the vast platform for the interaction of small molecules in the active cleft of macromolecules for the development and design of new drugs. The 3D structure of these molecules facilitates the chemist and biologist to understand the different types of interaction: as electrostatic, covalent, Van der Waals and hydrophobic between ligand and macromolecules which leads to the development of new drugs and pharmacophores.

Starting from known target enzyme, *in the silico* study are conducted to find the potential ligand and save the time and budget. Furthermore, ligand binding conformations, characterization of key intermolecular interaction, characterization of known and unknown binding sites and ligand and enzyme mechanism of binding can be studied. Next, biological



evaluations as potency, affinity, and efficacy, are carried out using diverse experimental platforms. Once a ligand and receptor have been determined, biological activity data correlate, then structure-based drugs design starts over new steps to include the functional group modification to increase the more interaction with binding sites.

A lot of computational techniques or methodologies are reported which facilitate the medicinal chemist to design the novel inhibitors or drugs, such as molecular docking, molecular modeling, molecular dynamics, pharmacophore design and fragmentation and free binding energy calculation [97-103].

#### ***1.1.9.2.Molecular Docking***

The molecular docking based on the “Lock and Key ‘model for the enzyme, which was put forwarded by the Nobel laureates Dr Emil Fischer [104]. The molecular docking can be defined as ‘A computational method in which the small molecules fits in the catalytic pocket of enzyme and complex formation occurs due to the intermolecular force of attraction, which results in liberation of free energy or predicted binding affinity (-kcal/mol) values in different scoring functions. These predicted binding affinity values are supposed to suggest the stability of molecule and enzyme complex.

There are different types of molecular docking

- i. Induced fit docking* based on ligand and receptors are flexibility [105]
- ii. Lock and key Docking* based on a lock and key theory, in which both ligand and receptors are rigid and show tight binding [106]
- iii. Ensemble docking* based on an approach which explains the flexibility and complexity of protein conformation, multiple proteins are used as an ensemble for ligand docking [107]

- iv. *Covalent docking* based upon the high level of potency and selectivity due to the formation of a strong linkage between the ligand and proteins [108]

The molecular docking can be performed in two ways: (a) manual docking and (b) automated docking. In manual docking, the active sites of the targets are defined and the ligand is paired in the complementary group and binding distance of each interaction is defined. The ligand is moved in binding sites by the installed program and as directed by the operator to search the best binding score. In automated docking, the software or program itself decide how to dock the ligand and palace the ligand inactive sites in a different orientation and different scoring functions are used to get the best ones [109]. The general flowsheet diagram (**Fig. 19**), showing the general procedure of molecular docking.

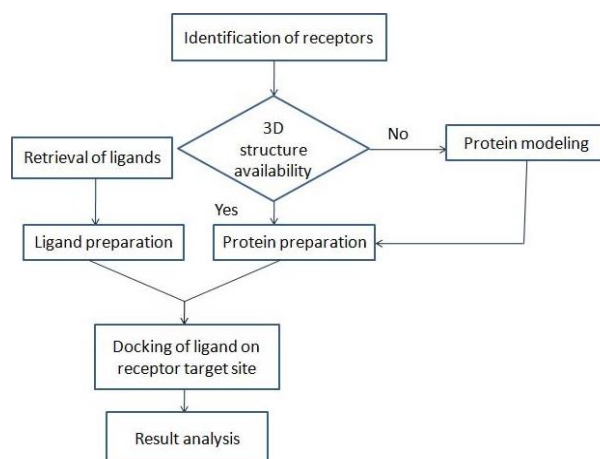


**Fig. (19).** Flowsheet diagram describing the basic steps of molecular dockings [105]

#### 1.1.9.3. *Docking software's*

There is much software available for docking, some of them are available free to use and some require a license. Each docking tools has its own unique algorithm and scoring terms to define the ligand and protein binding. Some most popular docking tools with their algorithm are summarized in **Table 1**.

**Table 1.** List of docking tools, their algorithm, scoring, and advantages

<i>S.No.</i>	<i>Software</i>	<i>Algorithm</i>	<i>Scoring</i>	<i>Advantages</i>
1	Glide (Grid-based Ligand Docking with Energetics)	Monte Carlo	Glide score	Lead discovery and lead optimization
2	Auto Dock	Lamarckian genetic algorithm	The empirical free energy function	Adaptability to user-defined input
3	GOLD (Genetic Optimization for Ligand Docking)	Genetic algorithm	GoldScore, ChemScore, ASP (Astex Statistical Potential), CHEMPLP (Piecewise Linear Potential), User defined	Allows atomic overlapping between protein and ligand
4	Surflex	Surflex-Dock search algorithm	Bohm's scoring function	High accuracy level by extending force-fields
5	FlexX	Incremental reconstruction	Modified Bohm scoring function	Provides a large number of conformations
6	ICM (Internal Coordinate Modeling)	Monte Carlo minimization	Virtual library screening scoring function	Allows side chain flexibility to find a parallel arrangement of two rigid helices
7	MVD (Molegro VirtualDocker)	Evolutionary algorithm	MolDock score	The high accuracy level of predicting binding mode
8	Fred (Fast Rigid Exhaustive Docking)	Exhaustive search algorithm	Gaussian scoring function	Nonstochastic approach to examine all possible poses within protein active site
9	Ligand Fit	Monte Carlo method	LigScore, Piecewise Linear Potential (PLP), Potential of Mean Force (PMF)	Generates good hit rates based on Lig Score
10	FITTED (Flexibility Induced Through Targeted Evolutionary Description)	Genetic algorithm	Potential of Mean Force (PMF), Drug Score	Analyzes the effect of water molecules on protein-ligand complexes
11	GlamDock	Monte Carlo method	ChillScore	Provides provision of two-dimensional analysis to screen ligands by targeting protein
12	vLifeDock	Genetic algorithm	PLP score, XCScore	Facilitates batch docking
13	iGEMDOCK	Genetic algorithm	Empirical scoring function	Highly significant in post-screening analysis

Various web servers are also available for molecular docking, UCSF-DOCK, Swiss Dock, 3D-garden, Clus pro, Patch Dock and Hex [105, 109].

With the help of *in silico* screening and SAR studies, a lot of compounds were obtained and tested against *trans*-sialidase which has been found to be structurally unrelated to the donor substrate-like structure, such as sialic acid and acceptor substrate-like structures, such as *trans*-sialidase. These compounds are mainly characterized by a cyclic molecule framework with some polar substituents, including pyridine, cyclohexene, anthraquinone, quinolone, chalcone, flavonoids, benzothiazole and derivatives with carboxylic acid substituents. However, *N*-acetyl-cyclohexenephosphonates monoalkyl esters (**34**) (**Fig. 20**) were found to be weak inhibitors with an IC<sub>50</sub> value of 4.7 mM. Furthermore, pyridoxal phosphate (**35**) (**Fig. 20**) was found with similar properties like cyclohexenephosphonates with a K<sub>i</sub> value of 7.3 mM and it was considered a non-competitive inhibitor. A non-radioactive fluorometric assay was employed to determine TcTS inhibition, in which sialyllactoside and 4-methylumbelliferyl-beta-D-galactoside were used as donor and acceptor substrate, respectively? [110, 81].

On the other hand, Neres *et al.*, found new benzoic acid derivatives as TcTS inhibitors by molecular docking and a virtual screening approach; the authors described that the 4-acetylamino-3-hydroxymethylbenzoic acid (**36**) (**Fig. 20**) was the best inhibitor against TcTS with a K<sub>i</sub> value around 300 μM and an IC<sub>50</sub> of 0.54 mM. Enzyme inhibition IC<sub>50</sub> and K<sub>i</sub> was assessed by using continuous and discontinuous fluorometric assay, respectively, and MuNANA (2'-(4-methylumbelliferyl)-β-D-N-acetylneuraminic) was used as a substrate. The presence of a carboxyl group or a hydroxyl group at the *para* position of the N-acetyl group plays an important role in the inhibition of *trans*-sialidase. Molecular docking has helped to design new derivatives in which the sugar ring of sialic acid is replaced by the benzene ring with the carboxylic group and substituents at *meta* and *para* positions. This showed the

carboxylate probe interaction with arginine triad (at  $-19$  kcal/mol); a favourable interaction with the cationic side chain of Arg93 was also detected. This was demonstrated by inspection of the DANA superimposed on the crystallographic conformation in complex with TcTS. This analysis showed that Trp120, Try113, and Val 95 formed the hydrophobic pocket and it was further confirmed by methyl and aromatic probes. This hydrophobic pocket has enough free space and can accommodate the phenyl ring and the N-acetyl group of DANA or sialic acid. The interaction with residue Glu230 and Asp196 with a positively charged amide probe and another protonated nitrogen probe was found at  $-13$  kcal/mole near the Asp51. The neutral  $-NH$  and  $-NH_2$  shows the interaction at  $-10$  kcal/mol with several active sites, namely close to the residues Glu230, Asp96 and Gln195, which was considered the most favourable binding position for DANA. All these results demonstrated that the positively charged groups, and the acylamino group, such as glycyllamino, fit into the hydrophobic pockets. The replacement of the phenyl ring of benzoic acid with heterocyclic compounds such as a pyridine ring has shown an excellent inhibitory effect. 5-acetylamino-6-aminopyridine-2-carboxylic acid became a new leader of this series with an  $IC_{50}$  of  $0.44$  mM (**37**) (**Fig. 20**) against TcTS. Furosemide (Lasix, a clinically used diuretic compound containing a furan ring) (**38**) (**Fig. 20**), was also tested as a TcTS inhibitor with an  $IC_{50}$  value of  $0.67$  mM, but these inhibition values are unacceptable for human therapy. To enhance the inhibition ability of the benzoic derivative, the phenyl ring was coordinated or substituted with heterocyclic molecules but these compounds showed poor TcTS inhibition and excellent influenza neuraminidase inhibition in phase III clinical trial. Docking analysis of compound (**38**) (**Fig. 20**) showed that the furan ring is interacting with TcTS at acceptor substrate sites which provide extra interaction compared to other aromatic derivatives [111].

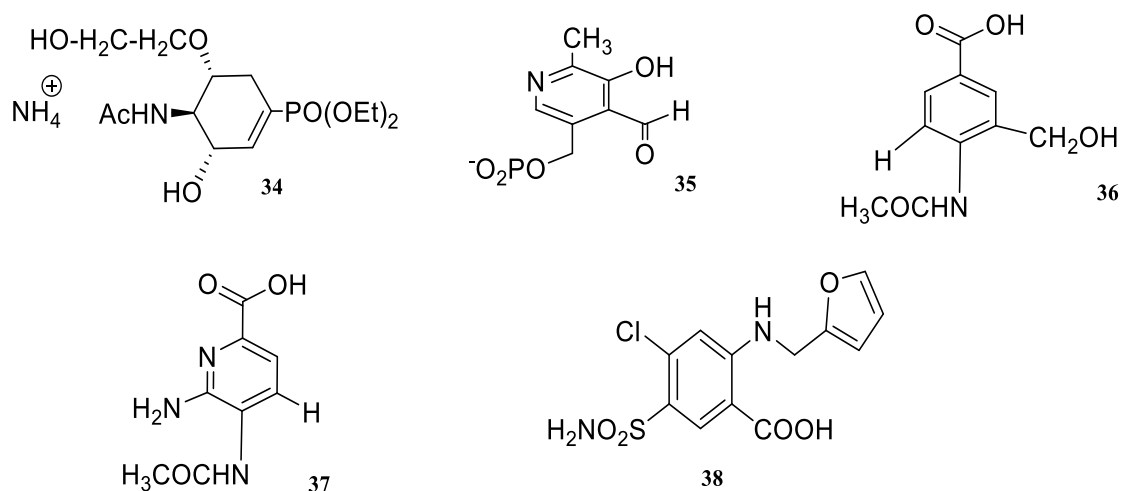


**Fig. (20).** Structure of trans-sialidase (Non sugar-based) inhibitor compounds.

After *in silico* screening for the discovery of novel TcTS inhibitors, targeting both sialic acid and sialic acid acceptor sites, *Neres et al.*, discovered novel non-sugar based inhibitor scaffolds such as 3-benzothiazole-2-yl-4-phenyl-but-3-enoic acid. 3-benzothiazole-2-yl-4-(2-isopropoxy) phenyl-but-3-enoic acid (**39**) (**Fig. 21**) showed an IC<sub>50</sub> value of 0.15 mM and 92% inhibition against the enzyme at 1 mM. Sulfonamide compounds (**40**) (**Fig. 21**) were found to be good inhibitors with an IC<sub>50</sub> value of 0.21 mM and 87% *trans*-sialidase inhibition at 1 mM as compared to chalcone and anthraquinone derivatives. MuNANA fluorometric assay in discontinuous mode was employed to assess enzyme inhibition and kinetic [112].

Comparison between the phenyl ring of a benzoic acid derivative with a benzothiazole ring (**39**) (**Fig. 21**) in docked confirmation showed good results. The carboxylate group showed interaction with the arginine triads when stacked between Tyr119 and Trp312 and it was reported that the phenyl ring of the compound displayed interaction with sialic acid binding sites. The benzoic acid derivatives with an -OH group also showed hydrogen bonding with Asp96 [113].

After the screening of a library of 2283 purified natural organic products, anthraquinones and flavonoid compounds were selected as promising inhibitors. Considering structural

availability for further investigation, two compounds were selected for further characterization. Screening for a TcTS inhibitor was conducted by the discontinuous fluorometric method using MuNANA as a substrate. Compound (41) anthraquinone, 6-chloro-9,10-dihydro-4,5,7-trihydroxy-9,10-dioxo-2-anthracene carboxylic acid (**Fig. 21**) with a  $K_i$  value of 0.58  $\mu\text{M}$ , and flavonoid apigenin (42) (**Fig. 21**) consisting of three rings A, B, and C, were obtained by virtual screening studies and were found to be specific but not good inhibitors of *trans*-sialidase, having an  $\text{IC}_{50}$  = 0.78 mM. The presence of several hydroxyl groups may have an important role in TcTS inhibition. Several compounds of the flavonoid family such as flavone, flavonol, isoflavone, flavanone and flavan-3-ol were also tested and found to have  $\text{IC}_{50}$  values in the range of 17  $\mu\text{M}$  and >1000  $\mu\text{M}$ . SAR studies for these compounds have shown that the presence of a hydroxyl group at 4-, 5- and 7- position is considered very important for their inhibitory activity compared to those flavonoids that have a hydroxyl group substitution at different positions and lacking a carbonyl group. The anthraquinone derivatives were also studied and  $\text{IC}_{50}$  values in the range of 0.58  $\mu\text{M}$  -1000  $\mu\text{M}$  were found. The SAR study of these anthraquinone derivatives showed that elimination of the carboxylic, chloro and hydroxyl group leads to the reduction of inhibition values against TcTS. Enzyme kinetics has shown that the inhibitory action of these compounds is reversible and not due to mechanism-based inhibition. The  $K_i$  values for both flavonoids and anthraquinone was found in the range of 0.6  $\mu\text{M}$  and 0.89  $\mu\text{M}$ , respectively. From the SAR study, it was concluded that compound (41) has good trypanocidal activity and its structure is good for TcTS inhibition, and compound (42) has excellent and specific inhibitor activity against TcTS, but does not inhibit human neuraminidase Neu2 [114].

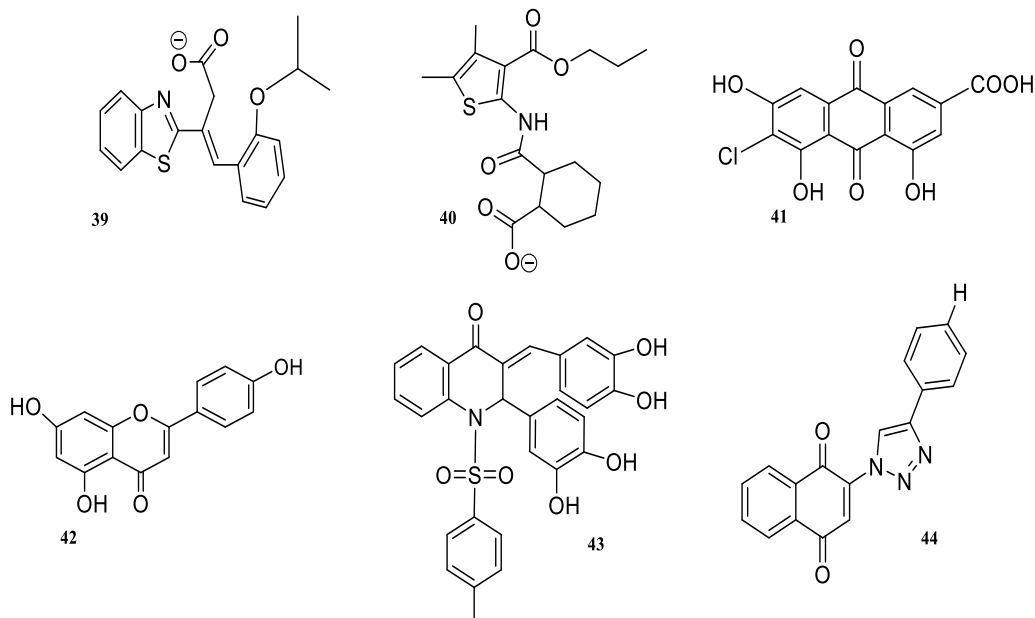


**Fig. (21).** Structure of *trans*-sialidase unrelated structure (non-sugar based) inhibitors.

Chalcone derivatives carrying a sulfonamide group and tetrahydroxy groups (**43**) (**Fig. 21**) have been used against *T. cruzi trans*-sialidase as potential inhibitors with inhibition values 0.6  $\mu\text{M}$  against *trans*-sialidase hydrolysis and 0.2  $\mu\text{M}$  against *trans*-sialylation. Trifluoromethylumbelliferyl  $\alpha$ -sialoside ( $\text{CF}_3\text{MuSA}$ ) was used as a substrate for the TcTS assay, and the released 4-trifluoro-methylumbelliferone was detected at 385 nm. These compounds have shown the best inhibition values against the human sialidase Neu2 and can be used as therapeutic agents in the future [115].

A set of 1,2,3-triazolic *para*-naphthoquinones (**44**) (**Fig. 21**) were obtained by click chemistry by modification of  $\beta$ -lapachones and were tested against *T. cruzi*. These compounds have shown an  $\text{IC}_{50}/24\text{ h}$  value of 10.9  $\mu\text{M}$  and a selectivity index (SI) of 18.9, indicating that they could be used as a treatment for CD; however, these showed low inhibitory effects against *trans*-sialidase [116].



## 1.2. Justification

The justification of this study are highlighted below

1. Chagas has infected 9-11 million people in Central, South and North America and about 6 to 6.5 million cases have been reported only in Mexico.
2. Only two drugs nifurtimox and benznidazole are being in use for treatment from last four decades, which are effective in acute stage but not chronic stage, that's why new drugs option to combat the Chagas are indispensable.
3. *Trans-sialidase* is a valid drug target for the development of chemotherapeutic drugs to combat Chagas disease because it is non-homologous to any mammalian enzyme and helps the *T. cruzi* to enhance the virulence factor by suppressing the host immune system to ensure the life-long survival of parasite in the infected host.
4. Literature reveals that carboxylic derivatives with substituents possessing different chemistry have the capability to bind the amino acid residues in catalytic pocket of TcTS enzyme which are involved in the sialic acid transfer from host to parasite surface. In particular, the carboxylic acid derivatives have importance over the sugar moiety rings due to ease of synthesis and unique structure-activity relationship, therefore these kinds of compounds could help to develop new anti-*Trypanosoma cruzi* agents.

### 1.3. Hypothesis

Novel carboxylic acid derivatives designed by molecular docking can inhibit the catalytic process of TcTS enzyme with a better trypanocidal activities

### 1.4. General Objective

The goals of this study were to design and discover new potential carboxylic acid/benzoic acid derivatives as TcTS inhibitors of *T. cruzi* that could be used to develop new treatments for Chagas<sup>2</sup> disease.

### 1.5. Specific Objectives (los verbos en infinitivo)

1. Design new carboxylic acid derivatives by molecular docking on *trans*-sialidase protein.
2. Synthesize and characterize ~~ation~~ of new carboxylic acid derivatives by spectroscopic techniques.
3. Determine ~~ation~~ of biological activity *in vitro* on *T. cruzi* strains and Structure-Activity Relationship (SAR) study
4. Determine ~~ation~~ of inhibition of *trans*-sialidase.

## CHAPTER TWO

### *2.1. Material and Methods*

#### *2.1.1. Bioinformatics analysis tools*

The software (a) AutoDock *version* 4.2, MGL Tools *version* 4.5.4 [117], (b) UCSF Chimera *version* 1.12 [118], (c) Auto Dock vina *version* 1.1.2 [119], (d) Discovery studio 2017 client R2 [120] (e) Ligplot ++ [121], and Edu PyMOL *version* 1.74 [122], were downloaded from web server and used for molecular docking study as well as to visualize the ligand and protein intermolecular interaction to design the new carboxylic acid derivatives.

#### *2.1.2. Trans-sialidase enzyme structure...*

*Trypanosoma cruzi* trans-sialidase with PDB ID (1MS8) was downloaded [123], in complex with 3-deoxy-2,3-dehydro-N-acetylneuraminic acid (DANA) by accessing the Research Collaboratory for Structural Bioinformatics (RCSB) Protein Data Bank (PDB).

#### *2.1.3. Validation of TcTS pocket (Receptors)*

A brief study of the catalytic pocket of TcTS enzyme was performed by using software Discovery studio client R2 2017 (A free available software online for protein-ligand interaction visualization) [120]. The catalytic pocket of TcTS was divided into three parts: (a), Entrance of pocket contains the two aromatic amino acid residues Tyr119 and Trp312 which are present opposite to each other, called gatekeeper and control the entrance of substrate in catalytic pocket (b) catalytic amino acid residues Asp59, Glu230 and Tyr342 next to gatekeepers involved in the stabilization of transition of state and found that Glu230, donate proton for the stabilization of transition state (c) An arginine triad (Arg35, Arg245 and

Arg314), which contributes to the binding of a carboxylic group of sialic acid derivatives and Asp96 which accommodate the acetamide group Fig (22) [124].

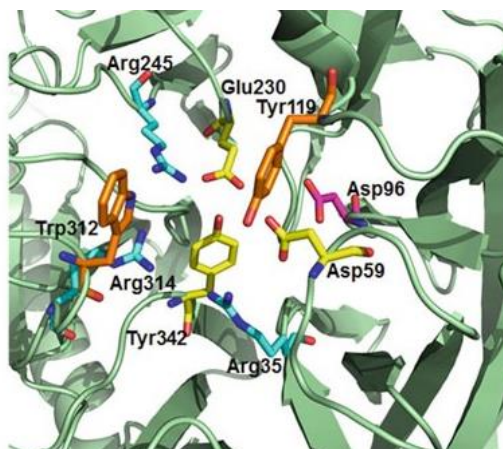


**Fig. 22.** Catalytic pocket of TcTS, enzyme (a) Golden amino acid showing gatekeepers, (b) yellow amino acid showing catalytic residues and (c) blue amino acid Arginine triad and (d) Pink amino acid Asp96 residue. The image was reproduced by Discovery studio 2017 client R2 using TcTS enzyme PDB ID 1MS8.

#### ***2.1.4. Receptor preparation***

The TcTS structure was prepared as receptor removing the ligand (DANA) and water molecules, for docking process. Vina [119] configuration file was generated by using the AutoDock [117] Tools software, and polar hydrogen and Gasteiger charges were added to finally get the file in PDBQT format. Then the location of the natural ligand was inspected to obtain the best grid box by using auto dock graphical interface. The first docking process was started with DANA (natural ligand) to obtain the most compromising size and space for active site of TcTS and several rounds of docking was carried out to obtain the following final size space dimension, X= 16Å, Y= 16Å & Z= 16Å, and centre 40.881, 63.047 and -

37.451 for X, Y and Z coordinates respectively. The binding energy of DANA obtained was used as a reference.

All compounds were drawn and energy minimized by using MarvinSketch software ([www.chemaxon.com](http://www.chemaxon.com)) [125] and was saved as the mol2 file format. The hydrogens and Gasteiger charges were added by AutoDock tools, and change the file format mol2 to PDBQT format [117]. Then each compound was docked with Vina and best predicted binding affinity was determined and ranked according to reference DANA. The compounds with higher values than reference were considered as weak binding ligand and vice versa. Ligand interaction with amino acid and 2D and 3D interaction were produced by using Discovery Studio Client 2017 R and UCSF chimera 1.12 [120].

## 2.2. Synthesis of new carboxylic acid derivatives

### 2.2.1. Synthesis

#### 2.2.1.1. Chemicals

Ammonium acetate, Malonic acid, 4-methoxybenzaldehyde, 4-methylbenzaldehyde, 4-ethylbenzaldehyde, 4-hydroxybenzaldehyde, 4-nitrobenzaldehyde, 4-fluorobenzaldehyde, 4-chlorobenzaldehyde, 4-bromobenzaldehyde, 1,4-Benzodioxan-6-carboxaldehyde, 7-nitro 1,4-Benzodioxan-6-carboxaldehyde, 2-naphthaldehyde, [1,1'-biphenyl]-4-carbaldehyde, 2-nitrobenzaldehyde, 2-furaldehyde, thiophene-2-carbaldehyde, 4-amino-2-hydroxybenzoic acid, 4-amino-3-hydroxybenzoic acid, 4-amino-2-chlorobenzoic acid, 4-amino-2,6-dichlorobenzoic acid, 4-amino benzoic acid, 4-amino-3-chlorobenzoic, 4-(aminomethyl)benzoic acid, 3,4-diaminobenzoic acid, 4-amino,3-bromobenzoic acid, ethyl 4-aminobenzoate, methyl 3,4-diaminobenzoate, aniline, benzene-1,4-diamine, pyridin-4-amine, 4-methylaniline, 4-chloroaniline, 4-nitroaniline, pyridin-2-ylmethanamine,

nicotinohydrazide, 4-(aminomethyl)cyclohexane-1-carboxylic acid, benzohydrazide, piperidine-4-carboxamide, 4-methoxyaniline, benzamide, 3,4-dimethoxyaniline, 3,4,5-trimethoxyaniline, 2-Methyl-4-quinolinamine, 2-hydroxybenzamide, 1H-benzo[d]imidazol-2-amine, benzo[d]thiazol-2-amine, 2-methylquinolin-4-amine, phthalic anhydride, 5-methyl phthalic anhydride, 3 nitro phthalic anhydride, methylhexahydro phthalic anhydride, trimellitic anhydride, acetone, methanol, ethanol, 1-butanol, n-hexane, cyclohexane, ethyl acetate, carbon tetrachloride, chloroform, dichloromethane, DMSO were purchased from Sigma Aldrich and were used as without any further purification.

## **2.3. Instruments and apparatus**

### **2.3.1. Glass Apparatus**

During the laboratory work, Pyrex glassware was used. The apparatus washed with detergents, sodium carbonate, and chromic acid. Glass ware dried at 65-70 °C in the oven and also with help of hot air-glass drying equipment.

### **2.3.2. Hotplate plus magnetic stirrer**

Thermo scientific model # mesh-20A hot plate cum magnetic stir was utilized.

### **2.3.3. Rotary evaporator**

Rotary Vacuum Evaporator Buchi Rotavapor R-100 made in Switzerland was employed.

### **2.3.4. TLC plates**

The purity and reactions were monitored by thin-layer chromatography (TLC) performed on silica gel plates prepared with silica gel 60 (PF-245 with gypsum, Merck, Tokyo, Japan), of

the thickness of 0.25 nm, particle size..... The developed chromatograms were visualized under ultraviolet light at 254–265 nm.

### 2.3.5. Melting Point Apparatus

Mel-Temp capillary apparatus (Electrothermal, Staffordshire, UK) was used for determination of the Melting point of synthesized compounds

### 2.3.6. Analytical balance

The electrical balance of Shimadzu, Japan model # AY220 was used for weighing.

## 2.4. General procedure for the synthesis

### 2.4.1. *Para-amino benzoic acid (PABA) derivatives*

The fifteen derivatives of para-amino benzoic derivatives were synthesized with the following general structure by a condensation reaction (**Fig. 23**).

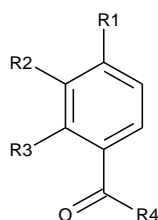


**Figure 23.** The general structure of *para*-amino benzoic acid derivatives

### 2.4.2. *Synthesis of novel Phthaloyl derivative of 3-amino-3-aryl propionic acids*

Compounds from series A, B, C, and D were synthesized, with the general structure (**Fig. 24**), which are described as 3-amino-3-aryl propionic acids derivatives (series **A**) and were synthesized by following the general procedure as described in the literature [126]. A mixture of appropriate aldehyde (1-15), malonic acid and ammonium acetate in (1:1.1:2.3), in 200 mL

of the 1-butanol was refluxed for 2-3 hours until the evolution of CO<sub>2</sub> ceased. The precipitate formed was filtered and washed with boiling 1-butanol (2 x 50 mL), boiling ethanol (2 x 50 mL) and 100 mL of water. Precipitates were dried at 80-100 °C for 8-10 h. The purity of the product was checked by TLC, and yield obtained about 65-80% in each reaction.

Compounds in three series (**B-D**) were synthesized by the fused reaction [127]. Equimolar (1:1) amount of appropriate 3-amino-3-aryl propionic acid and phthalic anhydride (series **B**), trimellitic anhydride (series **C**) and 4-methylphthalic anhydride (series **D**) were ground to form a homogenized mixture. The mixture was taken in 50 mL reaction flask and placed in an oil bath at 250 °C until the mixture fused. The reaction flask was kept at room temperature for 30 min and the product was obtained. The product was recrystallized in methanol and washed with acetone and chloroform. The purity of the product was checked by TLC and yield obtained about 85-90% in each reaction.

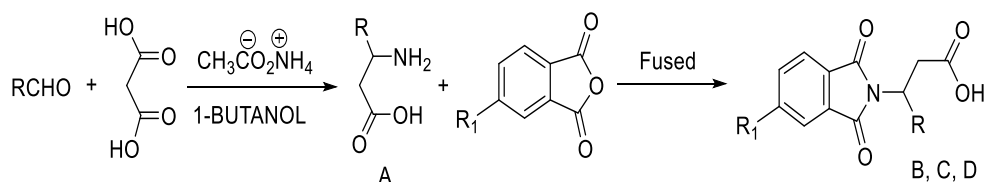


**Figure 24. Chemical reaction during the** ~~The general structure of~~ synthesis of 3-amino-3-arylpropionic (series A) and Phthaloyl derivative of 3-amino-3-aryl propionic acids (series B-D)

2.4.3. *Synthesis of the novel phenylcarbamoyl derivatives of, 3-nitrophthalic anhydride, Benzene-1,2,4-tricarboxylic anhydride, 5-methylphthalic anhydride and methylhexahydrophthalic anhydride*



Compounds from series E, F, G (**Fig. 25**) and H (**Fig. 26**) were synthesised by facile one-pot synthesis procedure using the acetic acid/ethyl acetate as solvent at room temperature, by following the procedure as described in the literature [128]. A solution of appropriate equimolar substituted aminobenzoic acid or substituted aniline in ethyl acetate (10 ml) was gradually added under vigorous stirring to a suspension of substituted phthalic anhydride in ethyl acetate (10 ml). Stirring was continued for 3-4 h at room temperature. The precipitate was formed which was filtered under vacuum rotary. ~~The precipitate was~~ and washed with ethyl acetate (2x15 ml), and chloroform and dichloromethane. TLC single spot showed the purification of product, yield was obtained in the range of 85% - 90%

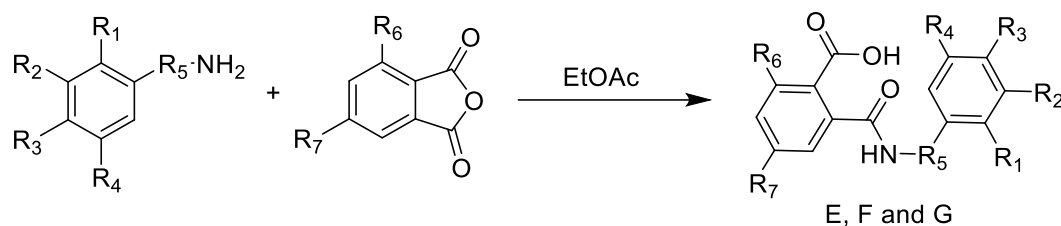


**Figure 25.** Chemical reaction and The general structure of phenyl carbamoyl derivatives 3-nitrophthalic anhydride (series E), Benzene-1,2,4-tricarboxylic anhydride (series F) and 5-methylphthalic anhydride (series G)

For, synthesis of series H, the methylhexahydrophthalic anhydride was used.

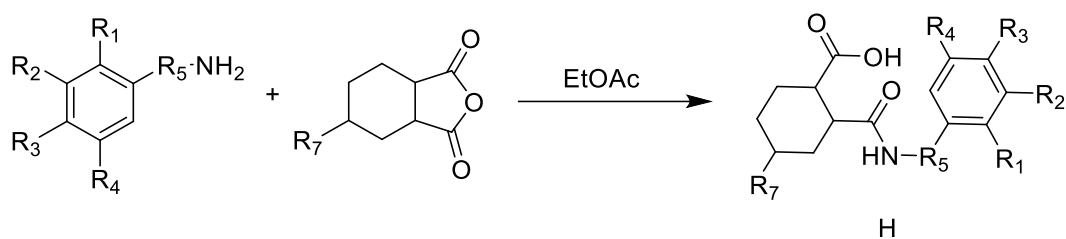


**Figure 26.** The general structure of phenylcarbamoyl derivatives of methylhexahydrophthalic anhydride. (the same suggestion)

## **2.5. Spectroscopic Analysis**

### **2.5.1. Infrared Spectrometer**

Infrared spectra were recorded using a Bruker Alpha FT-IR spectrometer (AXS Inc., Madison, WI, USA) spectrometer of compounds with platinum ATR assembly and OPUS software.

### **2.5.2. Nuclear Magnetic Resonance Spectrometer (NMR)**

NMR data were collected with Bruker Avance 500 spectrometer operating at 500 MHz ( $^1\text{H}$ ), and 126 MHz ( $^{13}\text{C}$ ).  $^1\text{H}$  proton NMR spectra were obtained in DMSO- $d_6$ , with TMS as an internal standard. Chemical shifts are given on the  $\delta$  scale (ppm)

## **2.6. Determination of biological activity in vitro on *T. cruzi* strains**

All synthesized compounds were evaluated ~~used to~~ *in vitro* evaluation, according to the reported procedure as in elsewhere with slight modification [129-135]. CD-1 mice (18-20 g) were infected by triatomine bugs carrying the metacyclic trypomastigotes of *T. cruzi* strains NINOA and INC-5. Blood was obtained by cardiac puncture of mice after 14 days, after the completion of parasite morphological cycle, at the peak of parasitemia  $1 \times 10^6/\text{mL}$ , using heparin as an anticoagulant. A stock solution of 10mg/mL of each synthesized compound and reference drugs (nifurtimox & benznidazole) were prepared in 1mL of DMSO, and further diluted with sterile water to make concentration 10  $\mu\text{g}/\text{mL}$ . A solution of DMSO and water (1:99), and blood contained the trypomastigotes were used as negative control. The test was carried out on 96-well microplates (Biofil JET) containing 5  $\mu\text{L}$  of the synthesized compound and 195  $\mu\text{L}$  of infected blood per well and each test was performed in triplicate.

LC<sub>50</sub> (LC meaning was determined before?) values were determined using Probit statistical analysis of the dose-response, and the results were expressed as the mean  $\pm$  standard deviation (SD). untreated blood trypomastigotes were used, As a negative control of lysis, wells with and as a positive control blood trypomastigotes treated with reference drug were used. After homogenization of ~~synthesized compound and infected blood~~, plates were incubated at 4 °C for 24 h [130]. After that ~~the incubation~~, the plates were kept at room temperature for 30 min and ~~take 5  $\mu$ L of blood were spread on slides, covered with a coverslip,~~ and trypomastigotes were examined with optical microscope 40x magnification. Anti-trypomastigote activity was determined as lysis percentage by comparing the remaining trypomastigotes in each concentration with respect to a negative control as described by method Berner and supplemented with Pizzi [136].

### ***2.7. Determination of inhibition of trans-sialidase.***

*Trans-sialidase* inhibition was determined by two methods

#### *a. A continuous fluorometric assay*

Inhibition was assessed using the continuous fluorometric assay described by Douglas and co-workers [137]. The assay was performed in triplicate (and on three different days) in 96-well plates containing phosphate buffer solution at pH 7.4 (25  $\mu$ L), a recombinant enzyme solution (amount of protein?25  $\mu$ L), and an inhibitor solution (25  $\mu$ L of a 4.0 mM solution). This mixture was incubated for 10 min at 26 °C followed by the addition of MuNANA (K<sub>m</sub> = 0.68 mM; 25  $\mu$ L of a 0.4 mM solution giving an assay concentration of 0.1 mM). The final concentration of the tested compounds was 1.0 mM, and the positive control was pyridoxal phosphate. The fluorescence of the released product (Mu) was measured after 10 min, with excitation and emission wavelengths of 360 and 460 nm, respectively, and ~~the~~ data were analyzed with GraphPad Prism software version 5.0 (San Diego, CA, USA). Inhibition

percentages were calculated by the equation:  $\% I = 100 \times [1 - (V_i/V_0)]$ , where  $V_i$  is the velocity in the presence of the inhibitor, and  $V_0$  is the velocity in the absence of the inhibitor.

b. High-performance Anion-exchange Chromatography with Pulsed Amperometric Detection (HPAEC-PAD).

i. *Inhibition of sialylation of N-acetylactosamine (LN)*

Reaction mixtures of 20  $\mu$ L, containing 1 mM ~~the~~ of the compounds from series A-D (novel Phthaloyl derivative of 3-amino-3-aryl propionic acids) and series E-H ( **Phenyl carbamoyl derivatives of phthalic anhydride**) were mixed with 20 mM Tris-HCl pH 7 buffer, 30 mM NaCl, 1mM 3-sialyl-lactose as donor, 1 mM N-acetylactosamine and were incubated with purified 300 ng trans-sialidase enzyme of *T. cruzi* [130] or 15 min at room temperature. Samples were diluted about 12 times with deionized water and analyzed by high-performance anion-exchange chromatography with pulsed amperometric detection (HPAEC-PAD). The percentage inhibition of TcTS enzyme was calculated from the amount of 3'-sialyl-N-acetylactosamine as compared to total amount of sialylated compounds in the presence or absence of tested compounds. All compounds were dissolved in DMSO (10 mM), and 2  $\mu$ L of these was used in incubation. The control assay mixture was prepared in absence of tested compounds, was performed accordingly by adding the 2  $\mu$ L of DMSO to incubated mixture [137, 138]

ii. *Analysis by HPAEC-PAD*

The Dionex ICS 5000 HPLC system was used, which was equipped with the pulsed amperometric detector, carboPac PA-100 ion exchange analytical column (4 x 250 mm) and PA-100 guard column (4 x 50 mm). The 80 mM NaOH with a linear gradient from 0 to 500 mM NaAcO was used for elution, at a flow rate of 0.9 mL/min within 60 min.

## CHAPTER THREE

### 3.1. Results and discussion

#### *3.1.1. Design of new carboxylic acid derivatives by molecular docking on trans-sialidase protein*

One hundred eighty (180) compounds derivatives of benzoic/carboxylic acid were designed and their molecular docking analysis was performed on the catalytic pocket of TcTS enzyme to determine their predicted binding free energy and interaction pattern with active amino acid residues which have a vital role in transfer mechanism of sialic acid from host to parasite surface.

#### *3.1.2. Design and molecular docking study of para-amino benzoic acid (PABA) derivatives*

Docking studies were conducted for compounds **1-15** in order to obtain potential putative interaction of these compounds on the active site of TcTS. The docking analysis was validated using the crystal structure of TcTS against the reference inhibitor DANA. The good superposition between the DANA structures oriented with AutoDock Vina 5.6 as compared with the orientation in the crystal structure (Protein Data Bank (PDB) accession number 1MS8) suggested that the chosen method is appropriate (**Figure 27**). The potential DANA binding site was also predicted as a deep cavity including a restricted space with two delimited regions, where the blue shift indicates a positive electrostatic potential (carboxylate interaction) and the red shift a negative electrostatic potential (amide interaction) (**Figure 27**).

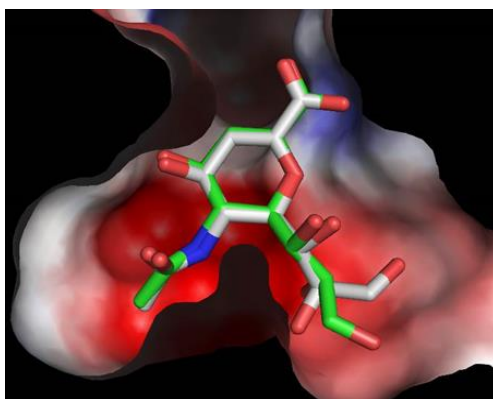


**Figure 27.** Best scored binding mode for DANA obtained with AutoDock Vina (gray) and binding mode for DANA in the original crystal structure (green). The TcTS surface is color-coded by the electrostatic potential (blue shift showing positive electrostatic potential & red shift showing negative electrostatic potential).

In this study, the proposed interaction modes of the benzoic and benzoate derivatives into the active site of TcTS were determined as the highest-scored conformations (best-fit ligands), which correspond to the structure with the most favorable free energy for binding in TcTS.

According to the results (**Table 2**), two major binding patterns were found, A and B (**Figure 28 A, B**). Moreover, some conformations that did not have a particular binding mode were grouped as C (**Figure 28C**). The first mode (A) is similar to that reported for DANA in the crystal structure (**Figure 28A**). Although this binding mode was found to be the best result for compounds **6**, and **15**, it does not correspond to the lowest energy conformation in most cases. It is noteworthy that, binding mode A was found to be among the best nine conformations for most of the ligands, having a good calculated affinity (Table 1). Similarly, molecules **3** and **7-10** showed their best-scored binding in an alternative way, designated A2 (**Table 2**), which is a slight variation of the binding mode A.

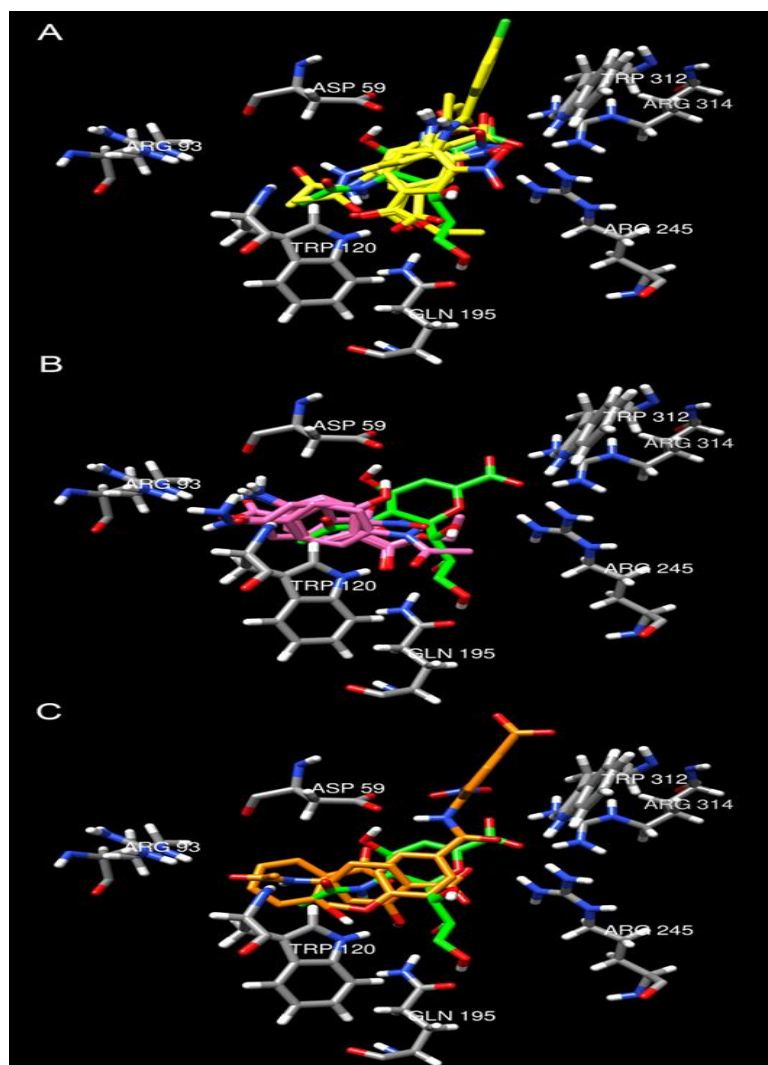


**Figure 28.** Best-scored conformations obtained for compounds **1-15** and their comparison with the ligand DANA in the crystal structure of TcTS (green). Compounds with binding modes classified as **(A)** are shown in panel **(A)** as yellow structures; those classified as **(B)** are shown in pannel **(B)** as pink structures; and those classified as **(C)** are shown in panel **(C)** as orange structures.

Figure 29A shows the best conformation for compound **15**, which corresponds to binding mode A, where the carboxylate group forms hydrogen bound interactions with Arg314 and Arg245 (donor site); these interactions can be slightly different for each ligand in binding mode A. For the molecules in binding mode A2, the nitro group adopts a similar orientation to the carboxylate group in DANA



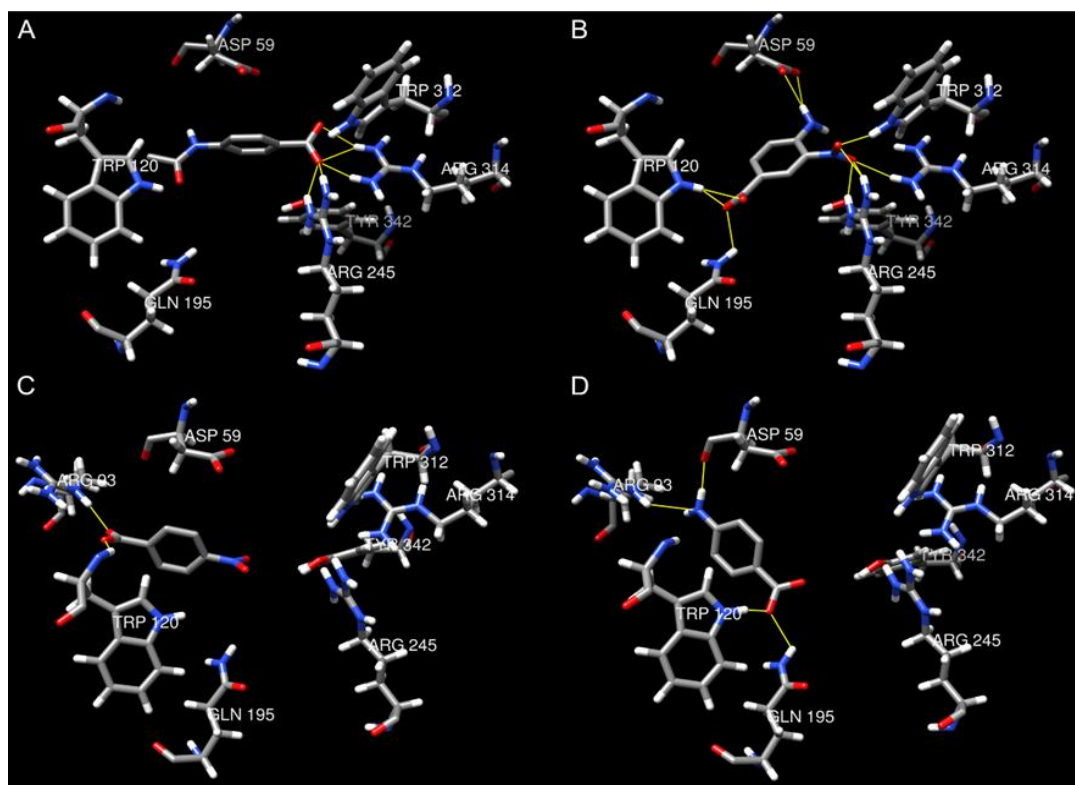


**Figure 29.** Best-scored conformations and interactions of selected compounds with TcTS. (A) compound **15** in binding mode A; (B) compound **7** in binding mode A2; (C,D) compounds **4** and **1** in binding mode B, respectively.

Figure 29B shows compound **7** in binding mode A2. It is noteworthy that, whereas the nitro group shows interactions with Arg314, Arg245, and Trp314, the carboxylate and amino groups have additional interactions with Gln195, Trp120, and Asp59, respectively. It is worth noting that all nitro benzoic acids and nitro benzoates are classified among the most active compounds in this series. Moreover, compound **7** has a higher score value.

The binding mode B observed in this study differs from the DANA crystal structure (opposite binding conformation), and has not been previously described (Figure 5B). Binding mode B is associated with compounds **1**, **2**, **4**, **5**, **12**, and **15** in their best-scored conformation; other compounds that exhibit binding mode B also have good scores, but not the best. Arg93 and Trp120 act as hydrogen donors to bind the carboxylate group at the position 1. These

interactions can also be found involving a nitro group as a hydrogen acceptor. A variation of binding mode B was found where the amine group or derivatives at the position 4 form an interaction with Arg93 and Asp59. Figure 6C,D shows examples of compounds in binding mode B.

The third binding mode (C) did not show a specific binding conformation, and it was different from modes A and B. It is associated with compounds **11**, **13**, and **14**; other compounds that exhibit binding mode C have good scores, but not the best. These compounds do not involve the characteristic interactions observed in the A and B modes or are binding on the exterior of the cavity (**Figure 28C**).

### ***3.1.3. Design and molecular docking study of novel phthaloyl derivative of 3-amino-3-aryl propionic acids***

The 3-amino-3-arylpropionic acids derivatives with different substituents were used, as starting point to design the TcTS inhibitors due to the presence of  $-\text{NH}_2$  and  $-\text{COO}^-$  groups. The substituents (**1-15**) were categorised according to their chemistry as electron donating substituents ( $-\text{OCH}_3$ ,  $-\text{CH}_3$ , and  $-\text{C}_2\text{H}_5$ ), electron withdrawing substituents ( $\text{OH}$ ,  $\text{NO}_2$ ,  $-\text{F}$ ,  $-\text{Cl}$ ,  $\text{Br}$ , and  $\text{C}_2\text{H}_2\text{O}_2\text{-mNO}_2$ ), aromatic substituents (naphthyl and bi-phenyl) and heterocyclic moieties (furanyl and thienyl) to understand the effects of these modifications on TcTS binding sites, trypanocidal activity, and enzyme inhibition.

To increase more the interaction of 3-amino-3-arylpropionic acids derivatives (series **A**) on TcTS active site, their novel Phthaloyl derivatives were designed by coupling them with phthalic anhydride (series **B**), trimellitic anhydride (benzene-1,2, 4-tricarboxylic anhydride) (series **C**) and 4-methylphthalic anhydride (series **D**). When these phthaloyl derivatives were

sketched in 3D and their energy was minimized, these compounds showed a chair shaped geometry, and when they were fitted in TcTS catalytic cavity, it was found the 3-aryl propionic acid skeleton deep inside the catalytic cavity with the carboxylic group flipped near to the active amino acid residues Arg35, Arg245, Arg314, Asp59, Glu230, and Tyr342. On the other hand, Phthaloyl group was found at the mouth of TcTS catalytic pocket with carbonyl group near to key amino acid residues Tyr119 and Trp312 of TcTS. To produce stronger interaction, hydrophilic substituents  $-\text{COOH}$  and hydrophobic  $-\text{CH}_3$  at the 4<sup>th</sup> position of Phthaloyl moiety was also considered. To understand the binding mode of the enzyme with molecules, 3-aryl propionic acid and Phthaloyl moiety were considered separately **Fig. 30**.

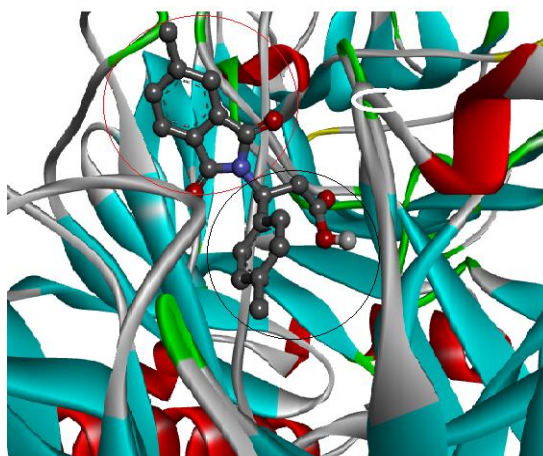


**Fig. 30.** The orientation of Phthaloyl derivative of 3-amino-3-arylpropionic acids inside the TcTS catalytic cavity (ribbons showing TcTS enzyme 1MS8), the red circle is showing Phthaloyl group, at the mouth of the cavity and black circle showing 3-amino-3-arylpropionic acids part, deep inside the cavity. The 3D image was produced by Discovery studio visualizer R-2 client 2017 version.

To understand and establish the interaction of the designed molecules with key amino acids residues on the catalytic pocket of TcTS (PDB code 1MS8), molecular docking studies were performed to explore the best predicted binding affinities. The TcTS natural ligand DANA was used as reference obtaining a predicted binding affinity value of -7.8 Kcal/mol.

From series **A** (**Table. 3**) only six compounds showed the same predicted binding affinities or better than reference DANA(-7.8 Kcal/mol). The compounds A-3 and A-5 showed similar binding affinities as DANA ~~reference~~ but only bind to the two amino acid residue Arg35 and Tyr342 via conventional hydrogen bonding, while Asp96 and Glu230 showed salt bridge interaction. However, compound A-5 showed unfavourable interaction with Arg53 and Asp59 but in contrast, Glu230 was bound via hydrogen bonding with NO<sub>2</sub> substituents. Compound A-11 (**Fig.31, 31-a**) showed the highest predicted binding affinity (-9.0 Kcal/mol) in this series, the hydrogen bonding was found between Tyr342, Arg53 and Arg35 and a carboxylic oxygen atom, hydroxyl oxygen and the amino group of the 3-amino-3-arylpropionic acid chain. **The  $\pi$ - $\pi$  stacking interaction between Val95, and the aromatic ring of naphthalene of compound A-11 but hydrophobic interaction was found Tyr119 and Trp312** (no entiendo redacción). The rest of compounds A-9, A-10, and A-12 with highest predicted binding affinity compared to reference DANA only showed interaction with two key amino acids Arg245 and Glu230 but with other amino acid showed the hydrophobic interaction with TcTS catalytic cavity. Therefore, from the docking analysis of series **A**, concluded that 3-amino-3-arylpropionic acid chain has only ability to bind with two or three amino acid residues but ~~no-one~~ none of the compounds showed the interaction with Tryp312 and other essential amino acid residues in catalytic cavity of TcTS, even they are small molecules and can be deep inside the catalytic cavity of TcTS.

In series **B**, the compound B-11 showed the highest binding affinities (-10.8 Kcal/mol) compared to reference DANA (-7.8 Kcal/mol) (**Table. 3**). The binding interaction of B-11 (**Fig 31. 31-b**), in TcTS cavity, showed that the arginine triad (Arg35, Arg245 and Arg314) of TcTS, was engaged by carbonyl group of Phthaloyl moiety via hydrogen bonding. Asp96 and Asp59 were attracted via  $\pi$ -anion interaction with naphthyl and phthaloyl groups of B-11 and Glu230 ~~were~~ was found in interaction with naphthyl group via  $\pi$ -anion. Additionally hydrogen bonding between Glu230 and -OH of carboxylic acid group of B-11 was also observed, while Tyr342 was bound via hydrogen bonding with carbonyl group of Phthaloyl, these three amino acid residues Asp59, Glu230 and Tyr342 were reported very important to stabilize the transition state during catalytic mechanism of TcTS ~~for~~ in the transfer of sialic acid (reference). Trp312, which contribute to the formation of hydrophobic pocket, facilitating ~~on~~ ~~of~~ the sialic acid transfer mechanism over hydrolysis and the formation of acceptor binding sites, was found in interaction with Phthaloyl ring of B-11 via strongest classical parallel  $\pi$ - $\pi$  stacking. Furthermore, other residue Tyr119, Trp120, Val95 and Leu176 that are involved in *trans* glycosylase activity and exclusion of water from hydrophobic pocket were attracted by B-11 with hydrophobic interaction. Compound B-2 showed the second highest predicted binding affinity (-9.9 kcal/mol) in this series, but the binding pattern was found totally different as compared to B-11. Only two key residues Asp59 and Tyr342, which plays important role in protonation and deprotonation of TcTS enzyme in transition state, was bound via hydrogen bonding with the carbonyl group of Phthaloyl and the carbonyl group of carboxylic acid, respectively. The arginine triad only showed ~~the~~ weak Van der Waals forces. Val 95 and Asp96 other important residues showed  $\pi$  -sigma and  $\pi$  -anion interaction with phthaloyl ring. Compounds B-6, B7 and B-8 which have halogen substituents showed the lower predicted binding affinity values as compared to B-1, B-2 and B-3, which have electron donating substituents. On the other hand, compounds B-5 and B-13 with -NO<sub>2</sub>

group at *para* and *meta* position of 3-arylpropionic acid, respectively, showed a big difference in large-predicted binding affinity values difference and binding pattern. The binding pattern of compound B-5 showed the three hydrogen bonding interactions, -NO<sub>2</sub> interaction with Trp312 and Arg245, carboxylic group interaction with Tyr342 and carbonyl group of Phthaloyl interaction with Arg53, but in compound B-13 unfavourable interaction of Glu230 was observed with carboxylic acid, while, -NO<sub>2</sub> group showed the hydrogen bonding with Tyr342, Arg53, which is a totally different interaction compared to compound B-5. Compounds B-14 and B-15 containing the furanyl and thienyl heterocyclic groups showed the same binding pattern like compound B-5 except the oxygen and sulphur atom showed an additional hydrogen bonding with Tyr342 and Arg245. When the binding pattern of compound B-4 with predicted binding affinity (-9.3 kcal/mol) was compared to other compounds of this series B, only Trp120 showed the hydrogen bonding between the oxygen atom of the hydroxyl group at aryl moiety of propionic acid and all other residues showed only hydrophobic interaction. The compound B-12, with bi-phenyl ring, showed the lower predicted binding affinity values (-9.0 kcal/mol), compared to B-11 even both have two aromatic rings, because the orientation pattern of B-12 in the catalytic cavity of the enzyme was found different as compared to other compounds, the biphenyl ring did not show the strong interaction like naphthalene ring of compound B-11. Only hydrogen bonding was found between carboxylic group and Tyr119.

The docking study of series C and D (**Table. 3**), showed the same binding pattern and orientation in catalytic pocket of TcTS as found for B series with some exception due to the presence of carboxyl and methyl substituents at the 4<sup>th</sup> carbon (it is correct use a superscript letter?) of Phthaloyl group. The one of the highest ranked compound C-11 with predicted binding affinity (-11.1 Kcal/mol) (**Fig.31, 31-c**) showed an extra interaction due to presence of carboxylic acid group at 4<sup>th</sup> carbon of Phthaloyl ring, bound the two extra amino acid

residue Tyr364, and Glu362 that were not reported as essential amino acid on TcTS catalytic process but are present in the catalytic pocket. Moreover Glu230 of compound C-11 showed the  $\pi$ -anion interaction with naphthyl ring, but in contrast, same amino acid (Glu230) was bound by hydrogen bonding with –O atom of the hydroxyl group of the carboxylic group of propionic acid part of the compound B-11.

The compound D-11, (**Fig. 31, 31-d**) with highest predicted binding affinity (-11.1 Kcal/mol) (**Table. 3**) possessing a methyl group at 4<sup>th</sup> carbon of Phthaloyl moiety showed exactly the exact same binding pattern as shown by the compound C-11, only one more  $\pi$ - $\pi$  stacking interaction was observed in the by methyl group at phthaloyl moiety with Trp312. In case of compound D-4 with hydroxyl substituent on the aryl moiety of propionic acid, hydrogen bonding was found between H atom of hydroxyl and O atom of Asp96, and O atom of hydroxyl group showed the hydrogen bonding with Arg53. In the comparison of compound D-4 with C-4, the same binding pattern was observed for –OH group at *para* position of aryl moiety of propionic acid chain, but oxygen atom in carboxyl group of propionic acid of compound C-4 showed hydrogen bonding with Tyr119 and Arg245, while the same carboxylic group oxygen in D-4 compound showed hydrogen bonding with Glu230. The hydrophobic interaction was observed for Tyr119 and Arg245 of compound D-4. Beside of this all the rest of compounds of series C and D showed the same binding pattern as was discussed for series B.

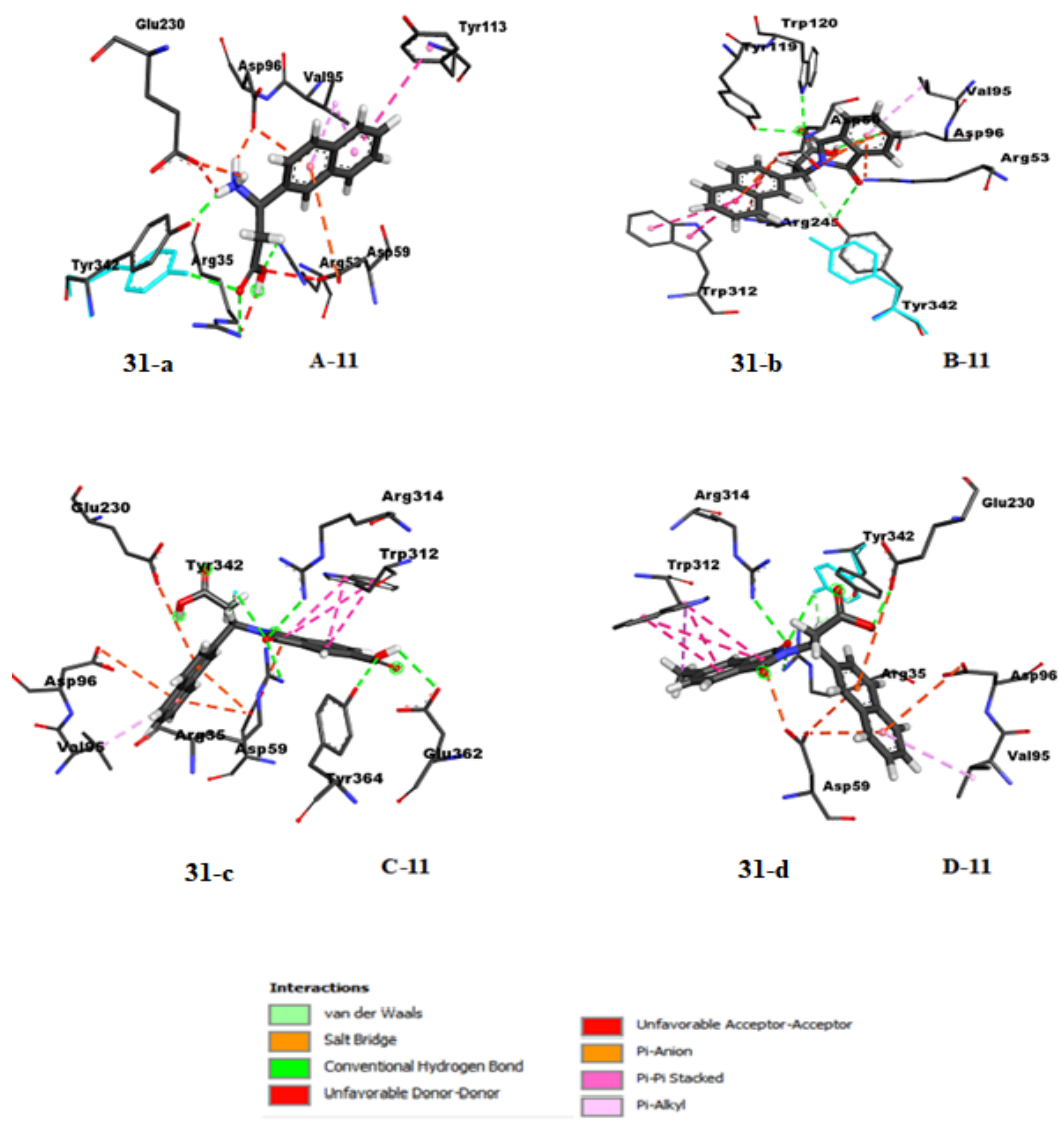


**Fig. 31.** 3D interaction of compounds with highest predicted binding affinities, 31-a (series A, A-11), 31-b (series B, B-11), 31-c (series C, C-11) and 31-d (series D, D-11) compared to reference DANA -7.8 Kcal/mol. The 3D image was produced by Discovery studio visualizer R-2 client 2017 version.

**3.1.4. Design and molecular docking studies of novel phenyl carbamoyl derivatives of, 3-nitrophthalic anhydride, Benzene-1,2,4-tricarboxylic anhydride, 5-methylphthalic anhydride and methylhexahydrophthalic anhydride**



One hundred ten (110) novel compounds of phenyl carbamoyl benzoic acid were designed by substituted anilines and phthalic anhydrides (a), 3-nitro phthalic anhydride, series **E** (b), 4-carboxy phthalic anhydride, series **F** (c) 4-methyl phthalic anhydride, series **G** (d) 4-methylhexahydrophthalic anhydride series, **H**. The presence of different substituents on aniline and phthalic anhydride give the best orientation in the catalytic pocket of TcTS with highest predicted affinity values (-Kcal/mol) compared to reference DANA. The Two-dimensional (2D) and three dimensional (3D) interaction of compounds which possesses the highest predicted binding affinity values showed hydrogen bond, **pi-pi**  $\pi$   $\pi$ stacking, **pi**-anion and hydrophobic interaction with TcTS active amino acid residues Arg35, Arg245, Arg314, Asp59, Asp96, Glu230, Tyr342, Trp120, Tyr119 and Trp312 which have vital role in the transfer of sialic acid from host to *T. cruzi* surface. For the ease to understand the binding interaction, each compound was considered into two parts (a), amide linkage part (b), and phthalic acid part.

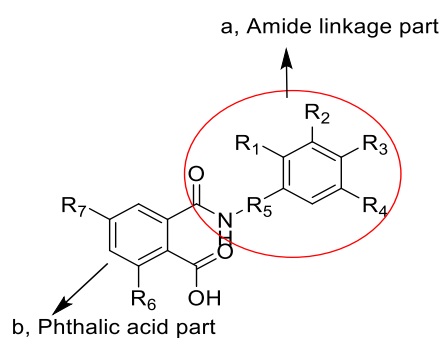


**Figure. 32.** The general structure of phenyl carbamoyl derivatives. (a), the Red circle is showing amide linkage part,(b), shows phthalic acid part

#### 3.1.4.1. Molecular docking analysis of 3-Nitro phenyl carbamoyl benzoic acid (series E)

In this series twenty-five (25) compounds were docked on active sites of TcTS enzyme and their binding pattern was analyzed, all compounds showed ~~the~~ a predicted binding affinity (free energy) in range of -8.5 to -10.1 kcal/mol which are ~~found~~ greater than the predicted binding energy of reference DANA -7.8 kcal/mol. The highest predicted binding affinity -10.1 kcal was shown by compound E-7 and the lowest corresponding to -8.5 kcal/mol was shown by compound E-23 (**Table 4**). In compound E-7, with highest predicted binding energy of five amino acid Arg35, Arg314, Tyr119, Tyr342 and Trp120 showed the hydrogen bonding with a carboxy group, or amide and phthalic acid phenyl group. ~~Other~~ amino acids Asp59, Asp96, Glu230 and Trp312 showed the hydrophobic interaction and no  $\pi$ - $\pi$  stacking was observed (**Figure 33-a**). The second highest predicted binding affinities -9.7 kcal/mol was shown by compounds E-4 and E-12. In compound E-4 Arg245 and Tyr342 were found in hydrogen bond interaction with the carbonyl group of amide and carboxy group, while Tyr119 showed the  $\pi$ - $\pi$  stacking with a phenyl group and other essential amino acid showed the hydrophobic interaction. In the case of compound E-12 only four essential amino acid residues Arg35, Arg314 and Tyr 342 showed the hydrogen bonding with carbonyl group, while Tyr119 showed hydrogen bonding with hydrogen atom -NH group of the amide. The hydrophobic interaction was shown by other amino acid residues. For compounds E-14, E-15, E-16, and E-22, where phenyl ring was substituted with pyridine, showed the -9.0, -9.4, -9.3 and -9.3kcal/ mol predicted binding affinity, respectively. From these pyridine derivatives only compound E-14 showed the best binding pattern in which Arg35, Arg341, Tyr342, Tyr119 and Asp59 showed the hydrogen bonding with carbonyl group and the rest of active amino acid showed ~~to~~ hydrophobic interaction; ~~while in~~ compound E-15 exhibit the same binding pattern and ~~was found but for~~ compounds E-16 and E-21 showed unfavourable interactions ~~was observed~~ for Glu230 and Arg53. Extra  $\pi$ - $\pi$  stacking was observed in compound E-16 for Trp312 and Trp120 and a phenyl group which was found absent for other

pyridine derivatives. The compound E-24 and E-25, where the phenyl group was replaced by benzimidazole and benzothiazole, showed the -9.6 and -9.1 kcal/mol predicted binding affinity values. Both compounds showed the slightly different binding interaction in the TcTS pocket. The benzothiazole showed a most promising binding pattern, in which six amino acid residue Arg53, Arg245, Arg314, Asp59, Glu230, and Arg53 showed the hydrogen bonding interaction with carbonyl, hydrogen atom of amide and Sulphur, while the Trp312 showed the  $\pi$ - $\pi$  stacking with phenyl group of carbamoyl moiety. On the other hand Arg35, Tyr314, Tyr342, and Tyr119 showed hydrogen bonding interaction with carbonyl group for compound E-24 and Trp312 was found in a  $\pi$ - $\pi$  stacking interaction with benzimidazole moiety.

#### *3.1.4.2. Molecular docking analysis of 4-carboxy phenyl carbamoyl benzoic acid (series F)*

In this series, the carboxyl group was introduced at the fourth carbon (carbon-4) of phthalic acid moiety, and twenty-five (25) compounds were designed with same substituents as described for series E and docking analysis on active sites of TcTS enzyme were studied. All compounds showed the predicted binding affinity value (free energy) in the range of -8.3 to -10.3 kcal/mol which is higher than reference DANA -7.8 kcal/mol. The highest binding affinity (-10.3 kcal/mol) was shown by compound F-4 and lowest predicted binding affinity shown by F-2 (-8.3 kcal/mol) (**Table 4**) which is different compared to series E compounds. The compound F-4 did not show the best interaction pattern with active amino acid even this compound has the highest binding predicted value. Only three essential amino acid residues, Tyr342, Trp120, and Tyr119 showed the hydrogen bonding interaction and unfavourable interaction was shown by Arg53 and asp96 this amino acid residue also a play important role in the catalytic process. The Glu230, Arg245, Trp312, and Arg35 showed the hydrophobic

interaction. The most promising interaction with active amino acid residue in catalytic pocket of TcTS was shown by compounds F-1, F-2, F-7, F-8, and F-12 where seven amino acid residues were found in hydrogen bond interaction with carbonyl and carboxyl moieties, for example in compounds F-7, F-8 and F-12 where Arg35, Arg314, and Tyr342 were found in binding with carbonyl oxygen atom of amide linkage, while Trp312 showed hydrogen bonding and  $\pi$ - $\pi$  interaction with carboxy group of phthalic acid moiety and phenyl group, respectively. Trp120, Asp96, and Tyr119 showed the hydrogen bonding with the carboxyl group of aniline part while Glu230 and Arg245 showed the hydrophobic interaction (**Figure 33-b**). The compounds F1, F-2, F-8, and F-12 also showed the interaction with same amino acid as discussed for compound F-7 but orientation pattern of the compound was found totally different in the TcTS catalytic pocket. In the comparison of compounds F-7 and E-8 the compound, F-7 showed better interaction and occupy all the essential amino acid, while compound E-7 bound only 5 amino acid residue even this E-7 has highest predicted binding affinity -10.1 Kcal/mol compared to F-7 and F-8. When phenyl group of aniline part was substituted by pyridine, and their docking analysis was performed the compound F-14, F-15, F-16, and F-22 showed the -8.5, -9.4, -9.2 and -10.0 kcal/mol predicted binding affinities values respectively. The binding pattern of compounds F-14 and F-22 were found much better compared to F-15, F-16 and also E series compounds E-14, E15, E-16, and E-22. In compound F-14 and F-22 about six and seven amino acid residues Arg35, Arg53, Asp59, Tyr119, Glu230, Arg314 and Tyr342 which have a vital role in catalytic mechanism were found in hydrogen bond interaction with different substituents. Trp312 was found in  $\pi$ - $\pi$  interaction with pyridine moiety. The compound F-24 and F-25 which have the benzimidazole and benzothiazole moieties showed the predicted binding affinity -9.7 and -9.5 kcal/mol, the binding pattern of compound F-24 was found better than the F-25. The hydrogen bonding was observed with six amino acid residues Asp59, Tyr119, Trp120,

Gln195, Glu230 and Tyr342 with carbonyl moiety and the hydrogen atom of the carboxyl group. The Tyr342 showed hydrogen bonding with the carbonyl group and the hydrogen atom of –NH moiety. The Trp312 was found in  $\pi$ - $\pi$  stacking with phenyl group of benzimidazole, while for compound F-25 only four amino acid residues Tyr119, Trp120, Glu230 and Tyr342 in TcTS pocket and other amino acid showed the hydrophobic interaction. In the comparison with E-24 and E-25, the interaction pattern of compound E-25 was found about similar to the F-25 but better than F-24.

#### *3.1.4.3. Molecular docking analysis of 4-methyl phenyl carbamoyl benzoic acid (series G)*

In this series, the methyl (–CH<sub>3</sub>) group was introduced on the fourth position of the phthalic acid moiety to know the effect of electron donating moiety on binding interaction compared to series E and F which have –NO<sub>2</sub> and –COOH electron withdrawing the groups. In this series thirty (30) compounds were designed and docked in catalytic pocket of TcTS and all the compounds showed the predicted binding affinities in the range of -10.0 to -8.0 kcal/mol (**Table 4**) which are higher than reference DANA -7.8 kcal/mol. The highest predicted binding affinity was shown by compound G-6 (-10.0 Kcal/mol) and lowest predicted binding energy (-8.0 kcal/mol) was found for compound G-11. The compound G-6 showed most favourable interaction in catalytic pocket of TcTS in which eight amino acid residues, Asp59, Asp96, Tyr119, Trp120, Glu230, Trp312, Arg314 and Trp312 out of ten active amino acid residue showed the hydrogen bonding interaction with carbonyl, carboxyl moiety and the hydrogen atom of –NH group. The methyl group at the 4<sup>th</sup> carbon of phthalic acid showed the extra  $\pi$ - $\pi$  stacking with Trp312. The two amino acid residues Arg35 and Arg245 showed hydrophobic interaction (**Figure 33-c**). The interaction pattern of the G-6 compound was also found better in comparison to the E and F series where most interacted compounds only occupy the six and seven amino acid residues as discussed in these series. The other

compounds G-2, G-6, G-12 and G-18 with predicted binding affinity value -9.8, -8.9, -8.8 and -9.0 kcal/mol respectively showed most promising interaction as compared to other compounds. In these compounds, seven amino acid residues Arg35, Asp59, Asp96, Glu230, Trp312, Arg314 and Tyr342 out of ten showed the hydrogen bonding interaction and here methyl group again participate in  $\pi$ - $\pi$  stacking with Trp312 same as compound G-6. When pyridine group was introduced in place of phenyl group of amide part, the compounds G-14, G-15, G-16 and G-22 showed predicted binding affinities value -9.1, -9.2, -9.5 and -8.9 kcal/mol which was found less as compared to compounds series E and F compounds 14-16 and 22. From these G-14 to G-16 and G22 compounds only G-15 compound showed best interaction in catalytic pocket, where four amino acid residues Arg35, Asp59, Arg314 and Tyr342 showed the hydrogen bond interaction and Trp312 was found  $\pi$ - $\pi$  stacking with phenyl and methyl group of phthalic acid. In the comparison to series E and F, the compounds with the same scaffold showed in series F showed the better interactions. The compound G-24 and G-25 where benzimidazole and benzothiazole group was introduced showed the predicted binding affinity value -9.5 and -9.7 kcal/mol. The binding interaction of these compound in catalytic pocket of TcTS was found poor as compared to series E and F compounds 24 and 25. Herein compound G-24 showed hydrogen bond interaction only with three essential amino acid residues Tyr119, Glu230 and Tyr342. The Trp312 was found in  $\pi$ - $\pi$  stacking with both phenyl ring of phthalic acid and benzimidazole. Only one amino acid residue Arg35 was found in hydrogen bonding interaction with the carbonyl group and N of benzothiazole for compound G-25.

#### ***3.1.4.4. Molecular docking analysis of 4-methylcyclohexane carbamoyl benzoic acid (series H)***

In this series, 4-methylhexahydrophthalic anhydride was used with substituted anilines to design the mixed phenyl and cyclohexane carbamoyl derivatives. The strategy to design the compound was to understand the interaction of more saturated ring cyclohexane due to the presence of more hydrogen atom which can play a role to enhance the hydrogen bonding and other physical force of attractions. Thirty (30) compounds were designed and docking analysis was carried out in catalytic pocket of TcTS enzyme. All compounds showed the predicted binding affinity values in the range of -10.0 to -8.1 kcal/mol which is greater than the reference DANA -7.8 kcal/mol. The highest binding affinity (-10.0 kcal/mol) was shown by compound H-22 and lowest value (-8.1 kcal/mol) was shown by compound H-10 (**Table 4**). The binding pattern of highest binding affinity compound in the TcTs pocket was not found satisfactory, because only three amino acid residues, Arg53, Asp96 and Trp120 which have an essential role in transfer mechanism, showed the hydrogen bond interaction with carbonyl oxygen and the hydrogen atom of the carboxyl group. The Trp312 showed the  $\pi$ - $\pi$  interaction with a methyl group on cyclohexane. The compounds E-22, F-22 and G-22 which have the same amide linkage part and different substituents at phthalic acid were found better as compared to H-22, by occupying the more amino acid residues via hydrogen bonding and other physical forces which is due to the involvement of phenyl ring. The most favourable interaction in catalytic pocket TcTS for this series H was shown by compounds H-2, H-4, H-7, H-11, H-13 and H-26 which have the predicted binding affinity values -9.9, -9.9, -9.7, -8.3, -8.1 and -9.5 kcal/mol. These compounds showed the hydrogen bonding interaction with five catalytically active amino acid residues. For example compound H-26, where Asp96, Trp120, Tyr119, Glu230 and Tyr342 showed the hydrogen bonding interaction with carbonyl, carboxyl acid hydrogen atom and H atom of -NH group (**Figure 33-d**). The compound H-7 which has a similar group at amide linkage part as in compound E-7, F-7 and G-7 showed the hydrogen bond interaction with Arg35, Trp120, Tyr314, Tyr342 and Tyr119

and Trp312 showed  $\pi$ - $\pi$  stacking with a methyl group on cyclohexane. The interaction pattern of compound E-7, F-7 and G-7, in TcTS catalytic pocket was found much better than compound H-7. The compound H-24 and H-25, where benzimidazole and benzothiazole was substituted for phenyl group showed the very poor interaction with active amino acid residues compared to compounds E-24, E-25, F-24, F-25, G-24 and G-25 even these H-24 and H-25 compound has shown the best predicted binding affinity values -9.9 and -9.0 kcal/mole. The binding pattern analysis showed only one amino acid residue, Asp96 showed hydrogen bond interaction and other amino acid residue showed the hydrophobic and unfavourable interaction. Most of the compounds in this series showed least predicted binding affinity values and poor binding interaction compared to series E, F and G which may be due to lack of  $\pi$ - $\pi$  interaction due to absence of one phenyl ring compared to other series and due to less rigidity of cyclohexane ring compared to phenyl ring because during energy minimization the cyclohexane changed to chaired conformer which leads to unfavourable interaction.



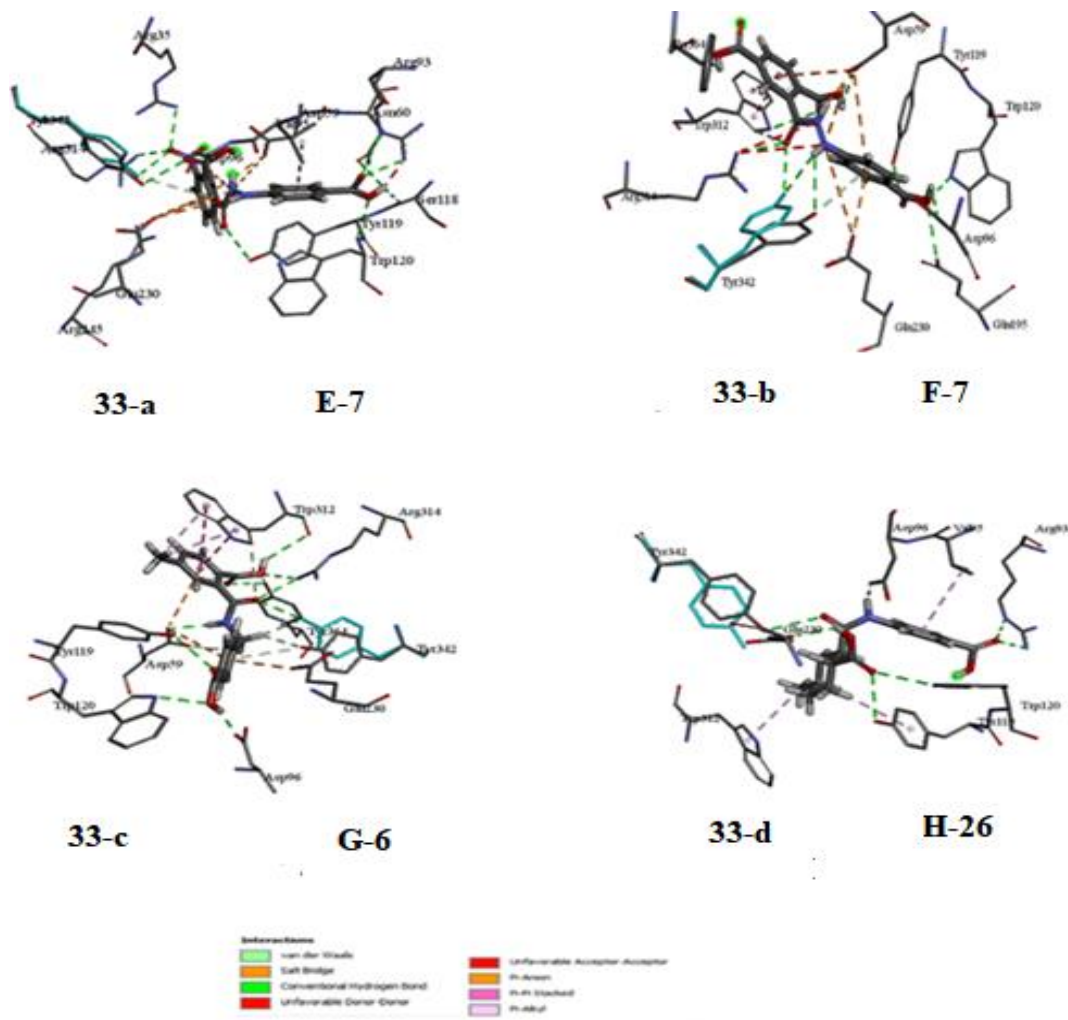


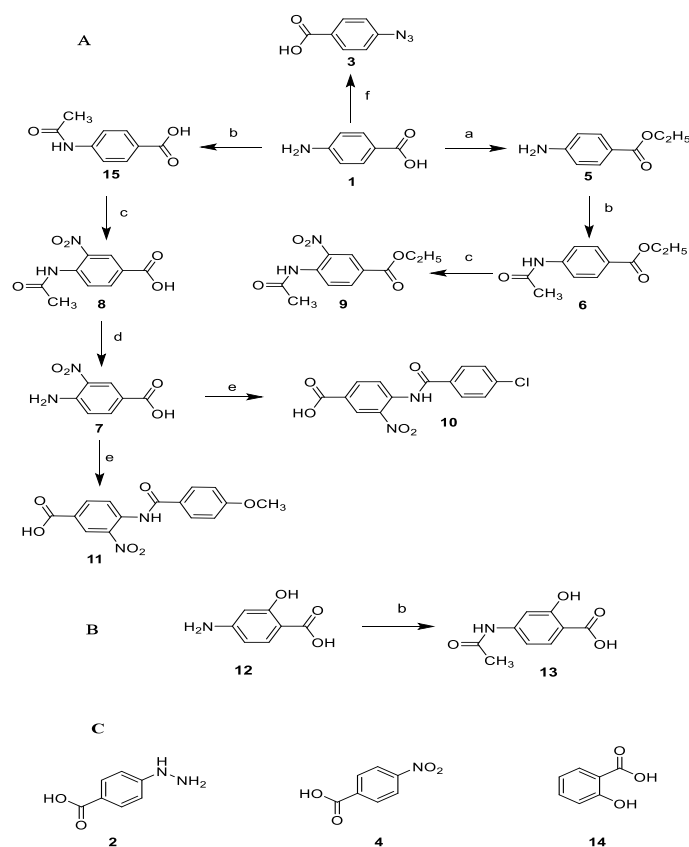
**Fig. 33.** 3D interaction of compounds with highest predicted binding affinities, 32-a (series E, E-7), 32-b (series F, F-7), 32-c (series G, G-6) and 31-d (series H, H-26) compared to reference DANA -7.8 Kcal/mol. The 3D image was produced by Discovery studio visualizer R-2 client 2017 version.

### 3.2. Synthesis and spectroscopic characterization

Three series, one hundred eighty derivatives (180) of a carboxylic/benzoic acid having different scaffold were synthesised after molecular docking and binding pattern analysis of compounds in TcTS active sites.

#### 3.2.1. *Synthesis and spectroscopic characterization of para-aminobenzoic acid*

In this series, ten (10) derivatives of *para-aminobenzoic derivatives* were synthesised by the reported procedure in literature as described in **scheme 1** and five were purchased from Sigma Aldrich. Our strategy was based on a molecular simplification of the purchased compounds 1, 2, 4, 12 and 14, by performing slightly, but chemically sensitive changes in the *meta* and *para* positions to the carboxylate group. We started from *para-aminobenzoic acid* (PABA) (1), and by esterification, acylation, nitration obtained the simple derivatives (1-15).



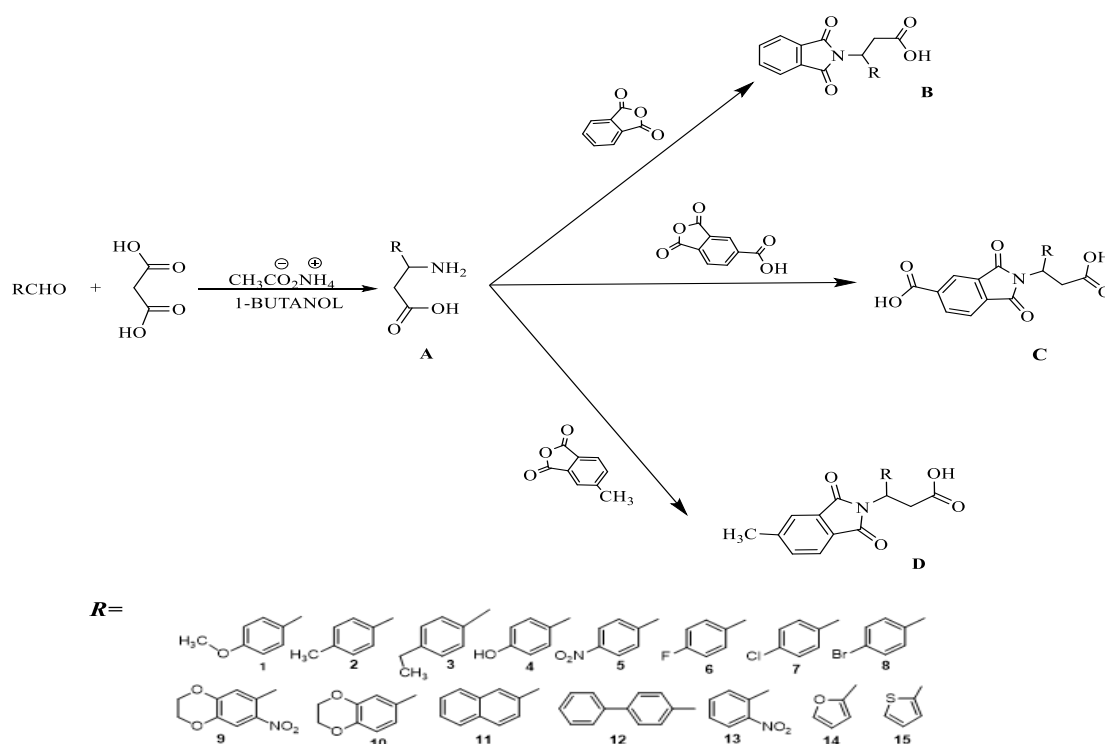
**Scheme 1.** (A, B) Compounds designed and synthesized in this work. *Reagents and condition:* (a) dry  $\text{CH}_3\text{CH}_2\text{OH}$ , conc  $\text{H}_2\text{SO}_4$ ,  $\Delta$ ; (b)  $\text{CH}_3\text{CO}_2\text{H}/(\text{CH}_3\text{CO})_2\text{O}$ ,  $\Delta$ ; (c)  $\text{HNO}_3$  and conc  $\text{H}_2\text{SO}_4$ ,  $\Delta$ ; (d)  $\text{H}_2\text{SO}_4$ ,  $\Delta$ ; (e) *p*- $\text{ClC}_6\text{H}_4\text{COCl}$ ,  $\text{Et}_3\text{N}$  (**10**), *p*- $\text{CH}_3\text{OC}_6\text{H}_4\text{COCl}$ ,  $\text{Et}_3\text{N}$  (**11**); (f)  $\text{HCl}$ ,  $\text{NaNO}_2$ , and  $\text{CH}_3\text{COONa}/\text{NaN}_3$  in  $\text{H}_2\text{O}$ ; (C) Compounds acquired from Sigma-Aldrich, Mexico.

These synthesised compounds were confirmed by spectroscopic analysis, FTIR and NMR. In FTIR analysis, the presence of a broad peak in the range of  $3500\text{-}3000$  ( $\nu \text{ cm}^{-1}$ ) confirms the presence of  $-\text{OH}$  group of carboxylic acid. The presence of sharp  $-\text{NH}$  peak in the range of  $3370\text{-}3300$  ( $\nu \text{ cm}^{-1}$ ) confirmed the amide linkage. The  $-\text{C-H}$   $\text{sp}^2$  hybridized and  $-\text{C-H}$   $\text{sp}^3$  hybridized was confirmed by a peak in the  $3050\text{-}2850$  ( $\nu \text{ cm}^{-1}$ ). These synthesized compounds were also characterized and confirmed by NMR spectroscopy. The  $-\text{OH}$  proton of carboxylic acid showed the chemical shift in the range of  $12.1$  to  $12.8$   $\delta$  ppm by singlet.

The –NH proton was confirmed by singlet peak in the range of 10 to 9.5  $\delta$  ppm. The –NH<sub>2</sub> proton showed the chemical shift at 7.6 to 8.5  $\delta$  ppm. The benzene ring proton showed the multiples in the 8.00 to 6.99  $\delta$  ppm. The detailed procedure and spectroscopic characterization are described in experimental part (Annexure 1).

### 3.2.2. Synthesis of novel phthaloyl derivatives of the 3-amino-3-aryl propionic acid

Compounds from series A, B, C, and D (fifteen for each series) were synthesized according to scheme 2, which are described as 3-amino-3-aryl propionic acids derivatives (series A) and were synthesized by following the procedure as described in methodology chapter. The Phthalic anhydride (series B), trimellitic anhydride (series C) and 4-methylphthalic anhydride (series D), Phthaloyl derivatives of 3-amino-3-aryl propionic acids were synthesized by the fused reaction as described in experimental section.



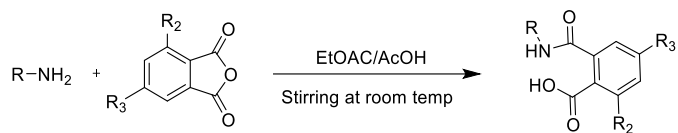
**Scheme 2.** Synthesised compounds and reaction conditions. Serie A obtained by reflux for 2-3 h; Series B, C and D fused reaction in the equimolar ratio at 250 °C.

The FTIR spectra of series **A**, showed the broad –OH peak in the range of 3300-2900  $\text{cm}^{-1}$  and absence of –NH<sub>2</sub> peak due to interchangeable hydrogen atom between –OH and –NH<sub>2</sub>. Also, carbonyl (C=O) peaks in 1650-1600 (short)  $\text{cm}^{-1}$  confirmed the synthesis. Furthermore, the <sup>1</sup>H-NMR showed the peak in the range of chemical shift 4.60 – 4.40 (singlet) ppm due to interchangeable hydrogen atom between –OH and –NH<sub>2</sub> also confirmed the synthesis.

The Phthaloyl derivatives of 3-amino-3-aryl propionic acids were confirmed by FTIR, phthalimide peaks in the range of C<sub>2</sub>O<sub>2</sub>N (phthalimido): 1770 asymmetric, 1690 symmetric  $\text{cm}^{-1}$  and carbonyl (C=O) peak in the range of 1650-1610  $\text{cm}^{-1}$ . The –OH proton peak of the carboxylic acid of  $\beta$ -amino acid part in <sup>1</sup>H-NMR was found in a range of 13.20-11.90 ppm and singlet peak of proton of CH-N of phthalamide in range of 5.80-5.30 ppm also strength the synthesis of compounds. Further, detail about synthesis, spectroscopic characterization of each compound is described in experimental part (Annexure 1).

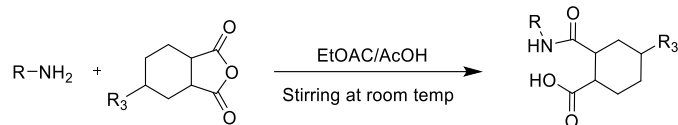
### ***3.2.3. Synthesis of novel phenyl carbamoyl derivatives of 3-nitrophthalic anhydride, 4-carboxy phthalic anhydride, 5-methylphthalic anhydride, methylhexahydrophthalic anhydride.***

Compounds from series E, F, G, and H (twenty five for series E and F and thirty for series G and H) were synthesized according to scheme **3**, which are described as *3-Nitro phenyl carbamoyl benzoic acid* (series **E**), *4-carboxyphenylcarbamoylterephthalic acid* (series **F**), *4-methylphenylcarbamoylbenzoic acid* (series **G**) and *4-methylcyclohexanecarbamoyl benzoic acid* (series H). All compounds were obtained in 85-90% and purity of the product was determined by TLC plates. The synthesis and spectroscopic characterization of each compound is described in detail in experimental part (Annexure 1)



R2 = -NO2 for series E

R3 = -COOH and -CH3 for series F and G



R3 = -CH3 for series H

where, R= 1-25 for E and F and

1-30 for Gand H

R=

Code	R	Code	R	Code	R
1		11		21	
2		12		22	
3		13		23	
4		14		24	
5		15		25	
6		16		26	
7		17		27	
8		18		28	
9		19		29	
10		20		30	

**Scheme 3.** Synthesised compounds (110) and reaction conditions. Series E, F, G and H were obtained by stirring at room temperature

The synthesis of compounds was confirmed by spectroscopic analysis, FTIR and NMR. In FTIR analysis, a number of peaks were obtained but most important to confirm the presence of presence of –OH, –NH and –C=O are considered here. The –OH group of a carboxylic acid moiety was confirmed by the presence of a broad peak in the range of 3500-2900 ( $\nu$   $\text{cm}^{-1}$ ). The amide-linked –NH group showed the sharp peak in the range of 3400-3150 ( $\nu$   $\text{cm}^{-1}$ ). The –CH  $\text{sp}^2$  hybridized and –CH<sub>3</sub> hybridized was confirmed by a peak in the 3050-2850 ( $\nu$   $\text{cm}^{-1}$ ). The presence of a sharp peak in the range 1750-1650 (asymmetrical) ( $\nu$   $\text{cm}^{-1}$ ) confirmed the presence of –C=O group.

In <sup>1</sup>H, NMR the proton of O-H of carboxylic acid (-COOH) showed a chemical shift in the range of 10.0 -13.5 ppm and -NH proton chemical shift was found 7.5-9.5 ppm. The benzene proton showed the multiplet at 7.0-8.5 ppm. The methane and methylene signal was found at 1.6-2.5 range singlet and doublet depending upon the environment of the proton. The synthesised molecules were also confirmed by <sup>13</sup>C NMR analysis.

### 3.3. *In vitro* trypanocidal activity

All synthesised compounds from series, *para*-amino benzoic acid derivatives were screened at 1 mM, and compounds from series A, B, C, D, E, F, G, and H were screened at a concentration of 10 µg/mL to determine their trypanocidal effect (% lysis) and LC<sub>50</sub> values to determine for the fifty percent population lysis, on blood sample of CD-1 mice, infected with trypomastigotes from NINOA and INC-5 strains of *T. cruzi*. Additionally, C log P values of all series were calculated from online server swissADME [139] to determine the lipophilic and hydrophilic character of compounds. All compounds showed C log P values < 5, which showed that these derivatives have best lipophilic characters and showed the best agreement with Lipinski rules for drugs development.

#### 3.3.1. Trypanocidal activity by *para*-amino benzoic acid derivatives

Initially, the lytic effect of the benzoic acid derivatives and reference drugs (Nfx and Bnz) on mouse blood trypomastigotes was evaluated *in vitro*, using INC-5 and NINOA *T. cruzi* strains (**Table 5**) [111]. Furthermore, 4-acetamidobenzoic acid (**15**) previously assayed by Neres et al. (2007) for TcTS inhibition has been studied.

Biological activity showed that both reference compounds Nfx and Bnz have a similar 50% lysis concentration of the population (LC<sub>50</sub>)(this abbreviation is before in the text) in each strain: 0.21–0.29 µM against the NINOA strain and 0.62–0.68 µM against the INC-5 strain. As shown in Table 5, amongst the tested compounds, the ethyl benzoate derivatives **5** (benzocaine, a known anesthetic agent), **6**, and **9** displayed significant trypanocidal activities in the range of 0.02–0.34 µM against the NINOA strain and 0.10–0.22 µM against the INC-5 strain, comparing to those of the corresponding carboxylic acid precursors **1**, **15**, and **8**, respectively: 0.52–1.39 µM and 0.21–1.24 µM in the NINOA and INC-5 strains, respectively. Thus, the introduction of a hydrophobic group such as ethyl showed an increase



of activity. In fact, these compounds presented trypanocidal activity comparable to the reference Bzn and Nfx against the NINOA strain and significantly higher against the INC-5 strain.

Compound **10**, showing significant trypanocidal activity against the NINOA strain (0.14  $\mu\text{M}$ ) and the highest activity against the INC-5 strain (0.0008  $\mu\text{M}$ ), became a lead structure of the benzoic derivative series. The subsequent modification of this structure by replacing the chloride substituent by the acceptor methoxide group **11** did not improve the activity in both the NINOA (0.61  $\mu\text{M}$ ) and INC-5 (0.43  $\mu\text{M}$ ) strains.

Compound **1** is a simplification of the structures synthesized by Neres et al [111] displaying moderate trypanocidal activity against the NINOA (0.52  $\mu\text{M}$ ) and INC-5 (1.24  $\mu\text{M}$ ) strains. The structure-activity relationship (SAR) of these compounds showed that the replacement of the *para*-amino group by nitro (**4**), hydrazine (**2**), or azide (**3**) groups showed comparable trypanocidal activities against the NINOA strain (0.47–0.66  $\mu\text{M}$ ) and an improvement against the INC-5 strain (0.46–0.58  $\mu\text{M}$ ). On the other hand, the *meta*-nitration of compound **1** afforded compound **7** to display a notably reduced activity against the NINOA strain (1.37  $\mu\text{M}$ ), whereas it increased the activity against the INC-5 strain (0.63  $\mu\text{M}$ ). Alternatively, *ortho*-hydroxylation afforded compound **12** to display significant trypanocidal activity against the NINOA (0.27  $\mu\text{M}$ ) and INC-5 (0.26  $\mu\text{M}$ ) strains. Compound **12** presented a higher trypanocidal activity than references Bzn and Nfx. Thus, the incorporation of a hydrophilic group as a hydroxyl in the *ortho* position of the *para*-amino benzoic acid moiety may provide a centre for H-bond interactions and it might be positively affecting the biological activity. In fact, the elimination of the *para*-amino group generated compound **14** with lower trypanocidal activities (0.57  $\mu\text{M}$  and 0.72  $\mu\text{M}$  against the NINOA and INC-5 strains, respectively) and in addition, the *N*-acetylation of this group (compound **13**)

significantly reduced the biological activity (1.28  $\mu\text{M}$  in both strains). This was partially observed in compounds **15** and **8**, which did not reflect an improvement of the activity in relation to the *para*-aminobenzoic acid precursors **1** and **7** against the NINOA strain ( $> 1.0 \mu\text{M}$ ) but showed better trypanocidal activities against the INC-5 strain (0.87 and 0.21  $\mu\text{M}$ , respectively). It is remarkable that a different drugs sensitivity ~~trypanocidal activities tendency~~ was observed in both strains. Finally, three compounds (**5**, **9**, and **10**) showed more potent trypanocidal activity than the commercially available drugs Nfx and Bnz in both strains:  $\text{LC}_{50} < 0.15 \mu\text{M}$  in the NINOA strain and  $\text{LC}_{50} < 0.22 \mu\text{M}$  in the INC-5 strain. Compounds 5 and 9 share ~~all of them sharing~~ the modified *para*-aminobenzoic ester moiety ~~except 10~~. These structures can be used as references for current and future studies for the synthesis of new anti-Chagas compounds. We have demonstrated that the incorporation of *ortho*-hydroxyl groups in *para*-aminobenzoic acid derivatives successfully provided a more potent compound (**21**). The esterification of the carboxylic acid (**5**, **6**, and **9**) generating a hydrophobic moiety to increase the activity could be a good strategy in these compounds. However, the introduction of a *meta*-nitro group did not initially generate a more active compound (**7**), although subsequent structural modifications finally modulated the activity and improved it. Further assays are required to understand the electronic and steric properties of *meta* and *ortho* substituents in the *para*-aminobenzoic derivative structures.

### **3.3.2. Trypanocidal activity by 3-amino-3-aryl propionic acid (series A) and their novel Phthaloyl derivatives of ~~3-amino-3-aryl propionic acids~~ (series B, C, and D).**

#### **3.3.2.1. Trypanocidal activity by 3-amino-3-aryl propionic acids series A**

We began our investigation using 3-amino-3-arylpropionic acids derivatives series **A**, modification of substituents on aryl part of 3-arylpropionic acids showed ~~the~~ different lytic

effect on both NINOA and INC-5 strains. In series **A**, compounds A-1, A-2 and A-3 with electron donating substituents as -OCH<sub>3</sub>, -CH<sub>3</sub> and -C<sub>2</sub>H<sub>5</sub> at *para* position on phenyl ring showed 83, 78 and 65% lysis for NINOA strain, respectively (**Table. 6**), which are higher than the reference drugs Bzn (46.30%) and (Nfx 40.74%). This showed that the alkyl substituent (methoxy) with electronegative oxygen atom increases the lysis, which may be due to more polarizability compared to methyl substituent, however ~~but~~ a comparison of methyl and ethyl substituents showed that increase in chain length decrease in lysis. The electron withdrawing substituents as -OH and -NO<sub>2</sub> in compounds A-4 and A-5, respectively, at *para* position on the phenyl ring, showed 50% lysis, but compound A-13 with -NO<sub>2</sub> substituent at *ortho* position showed 23% lysis. This result suggest that the nitro substituent at the *para* position of phenyl ring is more favourable for lysis due to low steric effect compared to *ortho*, even such type of compounds have the ability for making hydrogen bonding and free radical production.

For compounds A-6 to A-8, with halogen substituents -F, -Cl and -Br at the *para* position of the aryl group propionic acid, respectively, showed the least lysis values of 35, 13 and 20% which is less than reference drugs, and also that of ~~as well as~~ compounds A-1 to A-5. Substitution with benzodioxane (A-9) and 6-nitro benzodioxane (A-10) in  $\beta$ -amino acid chain it also did not show better lysis. When substitution was made with naphthyl (A-11) and biphenyl (A-12) groups, ~~the~~ only compound A-11 showed 60% lysis, which is better than reference drugs; compound A-12 showed the lower percentage of lysis, which indicates that aromatic polarizability and conformers also have an important impact on lysis. When modification was made with heterocyclic groups as furanyl (A-14) and thienyl (A-15), compound A-14 showed 50% of lysis, which is better than reference drugs, however compound A-15 showed the least activity, which may be due to high electronegativity of

oxygen atom which can form H-bonding with different amino acid residues compared to sulphur atom.

The compounds A-1 to A-3 with electron donating substituents, showed the lowest percentage of lysis 54, 59 and 50%, respectively for INC-5 strain, which is almost ~~about to equal~~ the same as the reference drugs Bzn 50% and Nfx 56% and less than the % lysis of these compounds for NINOA strain, this contrast in results, may be due to different proteins expression level of both strains in trypanomastigotes. In INC-5 strains the compounds A-4, A-5 and A-13 with electron withdrawing substituent –OH and –NO<sub>2</sub>, showed 76, 68 and 63% lysis which are better than the lysis produced in ~~of these compounds for~~ NINOA strain. These lysis results indicate that electron withdrawing substituents favours lysis in INC-5. The compounds A-6 and A-7 with halogen atoms as –F and –Cl also showed good lysis 62 and 73%, respectively, in contrast when modification was made with –Br (compound A-8) it exhibited only 18% lysis, this behaviour showed that halogens with moderate electronegativity and moderate atomic radii as –Cl are favourable for INC-5 strain. The benzodioxane compounds A-9 and A-10 showed the poor lysis of both strains INC-5 and NINOA. Interestingly, the compound A-11 with naphthyl group showed 60% lysis which is exactly similar to the NINOA strain, which suggested that the fused aromatic ring or bulky aromatic moiety is favourable for both strain, the compound A-12 with bi-phenyl group showed the least lysis 37% which is similar to lysis for NINOA strain, which strengthens that bi-phenyl conformer is not suitable for both strains. The compound A-14 with furanyl group showed 50% lysis value which is better than compound A-15, for both strain, but for INC-5 strain compound, A-15 showed slightly increase in lysis 32%, which is better than for NINOA strain by this compound.

### 3.3.2.2. Trypanocidal activity of phthaloyl derivatives of 3-amino-3-aryl propionic acids (series B)

In series B, the modification was made on  $-\text{NH}_2$  group of a 3-amino-3-arylpropionic acids of series A derivatives by introducing the Phthaloyl group, which results in an increase the C log P value (Table. 7). The compounds B-4, B-5, B-13 and B-6 with  $-\text{OH}$ ,  $-\text{NO}_2$  (*meta* for B-13), and  $-\text{F}$  at *para* position on phenyl ring showed 77, 62, 63 and 56% of lysis, respectively, for NINOA strain (Table. 3), which is greater than references drugs Bzn (46%) and Nfx (40%) and also better than compounds A-4, A-5, A-6 and A-13 for NINOA strain. The lipophilic groups as  $-\text{OCH}_3$ ,  $-\text{CH}_3$  and  $-\text{C}_2\text{H}_5$  in compounds B-1, B-2 and B-3 respectively, showed very low % lysis for NINOA strain in series B, while these group has shown highest % lysis for NINOA strain in series A (A-1 to A-3). These results showed that the introduction of Phthaloyl moiety on  $-\text{NH}_2$  group of the  $\beta$ -amino acid chain has the best ~~better~~ influence on electron withdrawing groups compared to lipophilic groups. The compound B-11 with naphthyl group showed 60% lysis for NINOA strain which is similar to compound A-11 in series A, which showed that naphthyl moiety is unaffected by this Phthaloyl addition.

The phthaloyl group addition produced the same effect on INC-5 strain in series B as discussed above, the hydrophilic group (electron withdrawing ), B-4, B-5, B-7 and B-13 with  $-\text{OH}$ ,  $-\text{NO}_2$ , and  $-\text{Cl}$  group showed the 68, 80, 70 and 68% lysis respectively, but activity of B-6 compound with  $-\text{F}$  group decreased and B-7 with  $-\text{Cl}$  group increase as compared to NINOA which may be due to biological difference between the two ~~in~~ strains. In comparison to series A, the compounds A-4 to A-7 and A-13 showed about the same behaviour for the INC-5 strain. While in series B only compounds B-1 to B-3 showed the consistency in results for INC-5 as showed for NINOA strain. The compound B-11 with naphthyl group showed

the nearly similar 62% lysis, compared to lysis for NINOA strain as compound A-11 showed in series A. The rest of compounds did not show better lysis than reference drugs.

### ***3.3.2.3 Trypanocidal activity of carboxylic phthaloyl derivatives 3-amino-3-aryl propionic acids (series C)***

In series C,  $-\text{COOH}$  group was added at 4<sup>th</sup> carbon of phthaloyl moiety of series B, this addition showed decrease in C log P values for all compounds as compared to series B. In series C,  $-\text{COOH}$  group was introduced at 4<sup>th</sup> carbon of phthaloyl moiety, this addition showed decrease in C log P values for all compounds as compared to series B. The compound C-2, with  $-\text{CH}_3$ , substituent at *para* position on phenyl ring showed the highest lysis 85% for NINOA strain (**Table 8**), which is greater compared to all compounds in series C and B. The compound C-1, with methoxy substituent at aryl ring showed second highest value of lysis 72% which found about to same as compound C-1 but greater than compared to compound B-1. This result showed that the addition of  $-\text{COOH}$  at the 4<sup>th</sup> carbon of phthaloyl moiety produced the better effect on lipophilic substituents on the aryl ring. The compound C-3 showed 23% lysis which similar to compound B-2, which indicate that increase in chain length of alkyl substituents is unaffected by  $-\text{COOH}$  addition at Phthaloyl moiety. The compound C-4 and C-5 and C-13 with  $-\text{OH}$  and  $-\text{NO}_2$  substituents at *para* position and  $-\text{NO}_2$  at *ortho* for C-13, of aryl ring, showed the 43, 23 and 48 % lysis respectively, which is very less compared to compounds B-4, B-5 and B-13 which have the same scaffold except  $-\text{COOH}$  at Phthaloyl moiety. This result indicates the decrease in electron density in aryl ring and Phthaloyl moiety due to the presence of electron withdrawing substituents is unfavourable for lysis. The halogen-substituted compounds C-6 to C-8 also showed the decrease in lysis compared to B-6 to B-8 compounds. A decrease in lysis was observed for compounds C-9 and C-10 compared to series B compounds which have the benzodioxane at

aryl ring. Compound C-11 and C-12, with naphthyl and biphenyl ring at aryl part of the propionic acid part, showed the 42 and 17% lysis, which is less compared to compound B-11 and B-12, which showed that addition of electron withdrawing group at Phthaloyl moiety decrease in lysis due to a decrease in electron density. The addition of  $-\text{COOH}$  group at Phthaloyl moiety produced the appreciable effect on lysis value of compounds C-14 and C-15 with heterocyclic moieties as furanyl and thienyl at aryl part of propionic acid. These compounds showed the 77 and 67 % lysis which is much better than the lysis produced by ~~compared to~~ B-14 and B-15 compounds.

Compound C-1 and C-2 with methoxy and methyl substituents at aryl part showed a decrease in the lysis of 32 and 59% for INC-5 strain compared to NINOA, but for  $-\text{C}_2\text{H}_5$  group in compound C-3 a reasonable increase in lysis of 61% was observed (**Table. 8**). In a comparison of lysis compounds C- to C-3 with compounds B-1 to B-3 for INC-5 strain, it was observed that addition of  $-\text{COOH}$  at Phthaloyl moiety is better for INC-5 strains. The compound C-4, C-5 and C-13 with  $-\text{OH}$  and  $-\text{NO}_2$  substituents at *para* and *meta* for C-13 showed 71, 63 and 68 % lysis for INC-5 strain, which is greater compared to lysis of these compounds for NINOA strain but in comparison with series B compounds B-4, B-5 and B-13, the compound C-4 showed slightly lower lysis and compound C-5 slightly higher. Compounds C-6 to C-8 with halogen substituents like  $-\text{F}$ ,  $-\text{Cl}$ , and  $-\text{Br}$  respectively, showed the 63, 67 and 69 % lysis which is better than lysis of these compounds for NINOA and also better than series B compounds B-6 to B-8. The compound C-11 with naphthyl group at aryl part of propionic acid showed the 24% lysis which is less than compound B-11 for INC-5 strain but increase in lysis value for compound C-13 was observed for INC-5 strain compared to lysis of the same compound for NINOA strain and B-12. The heterocyclic compounds C-14 and C-15 showed ~~the~~ 51 and 19% lysis for INC-5 strain but less than lysis of these compounds for NINOA strain.

#### 3.3.2.4. Trypanocidal activity of 4- Methyl phthaloyl derivatives of 3-amino-3-aryl propionic acids (series D)

In series D, the  $-\text{CH}_3$  group was added at the 4<sup>th</sup> carbon of phthaloyl moiety, which showed an increase in C log P values for all compounds compared to series B and C (**Table. 9**). The compound D-1, D-2 and D-3 with lipophilic substituent  $-\text{OCH}_3$ ,  $-\text{CH}_3$  and  $-\text{C}_2\text{H}_5$  at *para* position on the phenyl ring of propionic acid, ~~part~~ showed 78, 73 and 65% lysis for NINOA strain compared to reference drugs Bzn (46%) and Nfx (40%) (**Table 9**). These compounds D-1–D-3 showed the better %age lysis compared to series B compounds B1 – B-3. In comparison with series C compounds, C-1 and C-2, the series D compounds showed the lightly better or equal lysis, but D-3 compound showed higher lysis value compared to a C-3 compound which showed that the introduction of the lipophilic substituent on Phthaloyl group enhances the trypanocidal effect for ethyl group at ~~phenyl ring of propionic acid part~~ propionic acid phenyl ring. The compounds D-4 and D-5 with hydrophilic substituents  $-\text{OH}$  and  $-\text{NO}_2$  group at ~~phenyl ring of propionic acid part~~ showed the 38 and 45% lysis for NINOA, which is similar to compounds C-4 and C-5 of the series C, but least than the compounds B-4 and B-5 of series B. This behaviour showed that the introduction of hydrophilic or lipophilic substituents as  $-\text{COOH}$  or  $-\text{CH}_3$  respectively, at the 4<sup>th</sup> carbon of phthaloyl moiety has no appreciable effect on lysis. Compounds D-6 to D-8 with halogen substituents (hydrophilic)  $-\text{F}$ ,  $-\text{Cl}$ , and  $-\text{Br}$  at the *para* position of the phenyl ring of propionic acid part showed 63, 62 and 65% lysis respectively, for NINOA strain which is higher than the series C compounds C-6 to C-8. In a comparison of series D compound D-6, with series B compound B-6 showed ~~the~~ a similar lysis but compound D-7 and D-8 showed ~~the~~ a higher lysis than B-7 and B-8. These result of series D showed that  $-\text{CH}_3$  substituent at the 4<sup>th</sup> carbon of Phthaloyl increases the lysis of halogenated substituents.



The  $-CH_3$  (electron donating) on phthaloyl moiety produced ~~the~~ a good effect on lytic activity of compound D-11 which has naphthyl group, showed ~~the~~ 63% lysis in NINOA compared to C-11 compound which beard  $-COOH$  group at 4<sup>th</sup> position on phthaloyl moiety and showed similar lysis like the B-11 compound of series B. The heterocyclic compounds D-14 and D-15 showed decrease in activity 27 and 47% respectively, which is similar to series B compounds B-14 and B-15 but less than series C compounds C-14 and C-15, which showed that the electron withdrawing group at Phthaloyl moiety can produce good effect on lysis activity for heterocyclic groups.

For INC-5 strain the compounds D-1 to D-3 with lipophilic substituents  $OCH_3$ ,  $-CH_3$  and  $-C_2H_5$  at *para* position on the phenyl ring of propionic acid part, showed 57, 67 and 59% lysis activity which is better than the series B compounds B-1 to B-3 and approximately similar to series C compounds C-1 to C-3 and reference drugs Bzn (56%) and Nfx (50%) (Table. 5), which indicate that the substituent on Phthaloyl moiety can enhance the lytic effect for INC-5 strain, compared to series B but no significant difference in lytic activity was observed for  $-COOH$  and  $-CH_3$  substituent on phthaloyl moiety. The compound D-4 and D-5 with  $-OH$  and  $-NO_2$  at phenyl ring of  $\beta$ -amino part showed 15 and 25% lysis, which is **very less** compared to the series B and series compounds B-4, B-5, C-4, and C-5. This decrease in lysis showed that lipophilic substituent at Phthaloyl group is not favourable for  $-OH$  and  $-NO_2$  but in contrast, the compound D-13 which has  $-NO_2$  at *meta* position showed 65% lysis which is better than compound D-5. ~~The comparison of the Compounds D-13 compound with series C and B compounds C-13 and B-13 respectively,~~ showed ~~the~~ similar lysis for INC-5 strain which showed that *meta* position is most favourable for  $-NO_2$  substituent. Compounds D-6 to D-8 with halogen substituent at phenyl ring of propionic acid part showed similar lysis to reference drugs. The compound D-11 with naphthyl group showed the 65% lysis which is greater than a C-11 compound in series C and similar to a B-11 compound in series B, which

provides evidence that the addition of more lipophilic substituent on phthaloyl moiety can give appreciable result to increase lytic effect in INC-5 strain. The decrease in lysis of compound D-12, with a bi-phenyl substituent, was observed compared to C-12. Rest of compounds showed the consistent behaviour as they have shown in series B and C for INC-5 series.

The different lytic effect of compounds in both NINOA (I see that the correct is Ninoia, please check it )and INC-5 strains showed that there are different protein expression (how do you know that?) and biochemical pathways [140] with different mechanism of action for each compound in each series except to compounds with naphthyl group in series A, B and D which have shown the same consistency in results for both strains.

(I think it is necessary to talk about the biological difference between both strains, and tried to explain the difference in sensibility with the different compounds)

### **3.3.2.5. Trypanocidal activity of substituted 3 Nitro phenyl carbamoyl benzoic acid (series E)**

In this series novel, twenty-five (25) 3 Nitro phenyl carbamoyl benzoic acid derivatives were screened but no compound showed the prominent biological activity in both strains (**Table 10**) compared to reference drugs **Nfx** and **Bzn** (NINOA,  $33.14 \pm 5.4$  and  $37.24 \pm 6.3$ ) and (INC-5,  $27.74 \pm 6.4$  and  $24.65 \pm 7.1$ ) respectively. The only compound 24 (2-[(1H-1,3-benzothiazole-2-yl)carbamoyl]-6-nitrobenzoic acid) showed only 20.1 and 19.23% trypanocidal activity for INC-5 and NINOA strain respectively but very poor compared to reference drugs. If we consider the scaffold of this series E, the phthalic acid part contains the  $-\text{NO}_2$  group, which have the ability to show the best biological activity due to production of free radicals and amide linkage part contains the  $-\text{COOH}$ , Cl, Br, F,  $-\text{CH}_3$ , pyridine,  $-\text{C}_2\text{H}_5$  and  $-\text{OH}$  groups but failed to show the best biological activity. We conclude from these

results the position of  $-\text{NO}_2$  at *ortho* position respect to the phthalic acid group may be unfavourable. If we compare the biological activity with free binding affinity values these molecules have shown the best free binding energy compared to reference DANA (-7.8 kcal/mol).

### **3.3.2.6. Trypanocidal activity substituted, 4-carboxy phenyl carbamoyl terephthalic acid (series F)**

In this series novel twenty-five (25), 4-carboxyphenylcarbamoylterephthalic acid derivatives were screened to determine the trypanocidal activity or % lysis effect. In this series F, the amide linkage part for each molecule was same like to E series but in phthalic acid part, a carboxyl group was introduced at 4<sup>th</sup> carbon instead of  $-\text{NO}_2$  group. This series F, molecules showed an increase in biological activity, which found greater than reference drugs and also better than the E, series. The two compounds F-5 and F-10 showed the 59.7 and 56.9 for NINOA strain compared to **Nfx** and **Bzn** (NINOA,  $33.14 \pm 5.4$  and  $37.24 \pm 6.3$ ) and (INC-5,  $27.74 \pm 6.4$  and  $24.65 \pm 7.1$ ) respectively (**Table 11**). The compound F-5, 2-((4-carboxy-3-chlorophenyl) carbamoyl) terephthalic acid, if we consider the scaffold of this molecule, it consists of  $-\text{Cl}$  at *meta* position reference to amide linkage and  $-\text{COOH}$  group at the 4<sup>th</sup> carbon of phthalic acid. In comparison to compound F-9 which has the  $-\text{Br}$  substituent at but at *ortho* position showed the reference to amide linkage showed the only 1.2% lysis value for NINOA. This behavior showed that the moderate size and electronegativity of halogen is favourable compared to the bigger size and least electronegative. The second compound F-10, 2-((4-(methoxycarbonyl) phenyl)carbamoyl) terephthalic acid with % lysis greater than 50% contains the ethyl acetate group at *para* position reference to amide linkage can play an important role to enhance the activity. The compound F-1, which contains the  $-\text{OH}$  group at *meta* position respect to amide linkage showed the 31.9 % lysis for NINOA strain, while the

compound F-2 which has the –OH substituent at *ortho* position compared to F-1, showed only 1.3% lysis, this shows that –OH position at *meta* position is favorable. The rest of compounds showed the activity less than the reference drugs.

For INC-5 strain, only the compound F-10 showed the 39.3% lysis which is greater than the reference drugs Nfx and Bzn (INC-5,  $27.74 \pm 6.4$  and  $24.65 \pm 7.1$ ) respectively (**Table 11**). This compound has the ethyl acetate group at para position reference to the amide linkage and the same compound has also shown the 56.94 % lysis for NINOA strain. This behavior showed that by substituting more active groups on this molecule, the lysis value can be enhanced. The second highest percentage lysis for INC-5 strain was shown by compound F-12, which was found 35.86%, which is better than the reference drugs but showed only 7.69 % lysis for the NINOA strain. This F-12, compounds contain the –NH<sub>2</sub> substituents at the para position of the phenyl ring in reference to amide linkage. The compound F-24, which has benzimidazole part at amide linkage showed the 32.5% lysis for INC-5 and 27.22% for the NINOA strain. While the compound F-25, benzthiazole substituents showed 20.45 for INC-5 and 22.68% for NNOA, which showed that benzimidazole group can play a better role to enhance the activity. Rest of compound showed the activity less than the reference drugs.

### **3.3.2.7. Trypanocidal activity substituted 4-methyl phenyl carbamoyl benzoic acid (series G)**

In this series novel thirty (30), *4-methylphenylcarbamoylbenzoic acid* derivatives were screened to determine the trypanocidal activity or % lysis effect. In this series in first twenty five compounds have the same amide linkage part as described for series E and F but methyl group was introduced at 4<sup>th</sup> carbon of phthalic acid part compared to series E and F. In this series only compounds G-27, G-2 and G-12 showed the  $38.10 \pm 1.8$ ,  $35.71 \pm 6$ , and  $32.03 \pm 7$  % lysis which was found slightly greater than or equal to reference drugs **Nfx** and **Bzn**

(NINOA,  $33.14 \pm 5.4$  and  $37.24 \pm 6.3$ ), respectively (**Table 12**). The compound G-27 with 38.10 % lysis molecule has benzyl group at amide linkage as compare to G-2 and G-12 molecule, which have –OH and - NH<sub>2</sub> group at ortho and para position, respectively reference to amide linkage. If we consider molecules structure, the compounds G-2, G-12, G-5, G-10, G-8 and G-16 which contains more biological active substituents failed to show the highest activity which is surprising.

The same behaviour was observed for the INC-5 strain lytic activity. No one compound showed the most prominent activity, only compounds G-2 and G-25 showed the  $37.06 \pm 6$  and  $34.41 \pm 2.8$  which is higher than the reference drug Nfx and Bzn (INC-5,  $27.74 \pm 6.4$  and  $24.65 \pm 7.1$ ) (**Table 12** ). Rest of compounds in this series showed the lysis less than the reference drugs.

#### **3.3.2.8. Trypanocidal activity substituted 4-methylcyclohexane carbamoyl benzoic acid (series H)**

In this series thirty (30) novel, *substituted 4-methylcyclohexanecarbamoyl benzoic acid* derivatives were screened determine the trypanocidal activity or % lysis effect. In this series compounds from 1-25 have the same amide linkage part as described for series E, F and G but on the phthalic acid part, here we use the cyclohexane, instead of phenyl. No compound among this series showed the trypanocidal activity greater than the reference drugs reference drugs **Nfx** and **Bzn** (NINOA,  $33.14 \pm 5.4$  and  $37.24 \pm 6.3$ ), respectively (**Table 13**). Only two compounds H-18 and H-25 showed the  $31.39 \pm 6$  and  $32.25 \pm 2.09$  %age lysis which is less than the reference drugs.

For INC-5 series, only compound G-7, G-9 and G-12 showed the  $40.09 \pm 6$ ,  $31.06 \pm 4$  and  $28.03 \pm 1$  %age lysis, which were found slightly higher than the reference drugs **Nfx and Bzn** (INC-5,  $27.74 \pm 6.4$  and  $24.65 \pm 7.1$ ) respectively (**Table 13**). The rest of compound of this series showed the trypanocidal effect less than the reference drugs. The compound G-7 contains the hydrazine group at amide linkage which may be involved to enhance the activity.

### 3.4. *Trans*-sialidase inhibition

*Trans*-sialidase inhibition of synthesized compounds was carried out by employing the two methods (a), the continuous fluorometric method was used to determine the TcTS inhibition for *para*-aminobenzoic acid series and (b), high-performance anion exchange chromatography with pulsed amperometric detection (HPAEC-PAD) for series A-H to determine the TcTS inhibition.

#### 3.4.1. TcTS inhibition by *para*-aminobenzoic acid derivatives

TcTS inhibition screening results, including percentage inhibition values for a series of substituted benzoic acid derivatives, are given in (**Table 4**) The percentage inhibition at 1 mM concentration is the average of at least three independent experiments. The enzymatic inhibition assay was performed using a continuous fluorometric method based on the TcTS-catalyzed hydrolysis of 2-(4-methylumbelliferyl)- $\alpha$ -D-N-acetylneuraminic acid (MuNANA). As a control, the activities of pyridoxal phosphate (Pyr) and compound **15** (Neres et al. [111])

were measured in the same concentrations of the target compounds due to their respective moderate [141] and weak activities on TcTS.

Pyridoxal has been reported as a non-competitive TcTS inhibitor with a  $K_i = 7.3$  mM, reference [142] showing a moderate inhibition (73% at 1.0 mM in the presence of MuNANA 0.1 mM). In this work, the inhibition percentage of pyridoxal phosphate was 64%, similar to previous studies [119]. On the other hand, contrary to results described by Neres et al. [111], the inhibition of compound **15** was 30% instead of 0%. These differences could be mainly associated with the enzymatic assays' particularities. Nonetheless, this compound shows a weak inhibition, lower than pyridoxal phosphate.

The numbers in all graph are small and without color

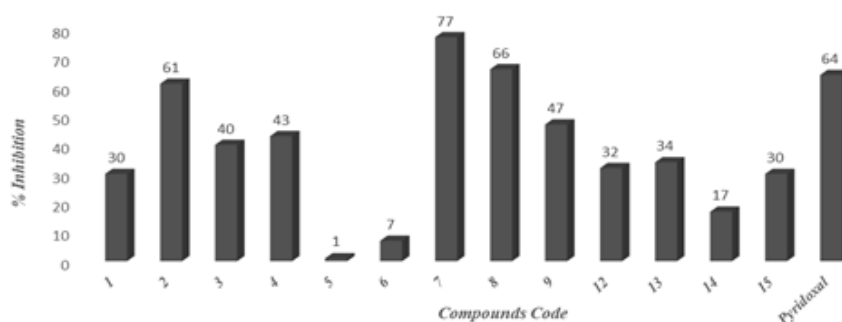


**Figure 34.** Graph showing the TcTS inhibition data of *para-amino benzoic acid* determined by the *continuous fluorometric* method. \*11, 12 were not tested due to low solubility in DMSO.

According to (Table 4), compounds 1–15 showed a variable influence on TcTS enzyme inhibition. All of the substances displayed a lower inhibitory activity against TcTS than pyridoxal, excepting compounds 2 and 8 which blocked 61 and 66% of the enzyme activity,

respectively, with the same inhibitory effect as that of pyridoxal, and compound **7** showed the best inhibitory activity (77%). Based on the inhibitory activity of these compounds, the *para*-amino-*meta*-nitrobenzoic acid core may have a relevant role in TcTS inhibition. Accordingly, compound **9**, obtained from the ethyl esterification of compound **8**, also showed moderate results (47%); however, esterification decreases the activity. This behaviour also can be observed in compounds **1** and **15**, where the activity decreases as compared with their ethyl ester analogues **5** and **6**, respectively. The lack of the nitro substituent reduced notably the inhibition activity of these compounds. Consequently, the *ortho*-hydroxyl benzoic acid derivative compounds **12–14** and the *para*-aminobenzoic acid/benzoate derivative compounds **1**, **5**, and **6** showed weak inhibition results in the range of 1–34%. However, the replacement of the *para*-amino group of the benzoic acid by hydrazine (**2**), azide (**2**), or nitro (**4**) groups lead to moderate results, with 61, 40, and 43% of inhibition, respectively. Again, the nitro group observed in compound **4** plays an important role in the interaction with the TcTS active site. Compounds **10–11** were not tested due to a low solubility in DMSO 1.0% in the well.

The significant TcTS inhibition shown by compounds **2**, **7**, and **8** (> 60% inhibition) may direct the development of new derivatives as TcTS inhibitors, pointing out the necessity to maintain benzoic acid/benzoate core and nitrogenous moieties (amine, *N*-acetyl, nitro, azide, or hydrazine) for an efficient inhibition of this enzyme.

In summary, we can observe that there is no correlation between trypanocidal activity and TcTS inhibition. For example, of the benzoate derivatives **5**, **6** and **8–10** showing moderate trypanocidal activities (0.10–0.028  $\mu\text{M}$  in the NINOA strain and 0.0008–0.22  $\mu\text{M}$  in the INC-5 strain), only compound **6** moderately blocked the TcTS enzyme as expected with 47%, whereas the other compounds inhibited less than 7%. Nevertheless, the importance of *para*-



amino carboxylic derivatives acting as TcTS inhibitors or lysing trypomastigotes via other biological mechanisms against *T. cruzi* has been demonstrated.

### **3.4.2. TcTS inhibition by novel Phthaloyl derivative of 3-amino-3-aryl propionic acids (series A-D)**

After molecular docking, twelve compounds were selected by highest, intermediate and lowest predicted binding affinity values, from series A, B, C and D to determine their inhibitory properties towards the TcTS enzyme and to measure their capacity to inhibit the sialylation of N-acetyllactosamine in the reaction. A mixture of 3'-sialyllactose (1 mM) donor, N-acetyllactosamine (1 mM) acceptor, and TcTS was prepared in the absence or presence of inhibitor (1 mM) and analyzed by high-performance anion exchange chromatography with pulsed amperometric detection (HPAEC-PAD) [69].

Inhibition of enzyme was calculated comparing the amount of 3'-sialyl-N-acetyllactosamine in the presence or absence of selected compounds. When the equimolar concentration of donor substrate 3'-sialyllactose and inhibitors were used, inhibition values ranged between 1.4 and 86.9% (**Fig. 35**). Compounds D-11 and D-4 exhibited the strongest inhibition against the TcTS with 86.9 and 82.5% value, respectively. Furthermore, the compound B-14, C-11, B-11 and C-4 showed 76.5, 66.9, 65.8 and 53% enzyme inhibition, respectively. Compounds from series A failed to show the better inhibition values.

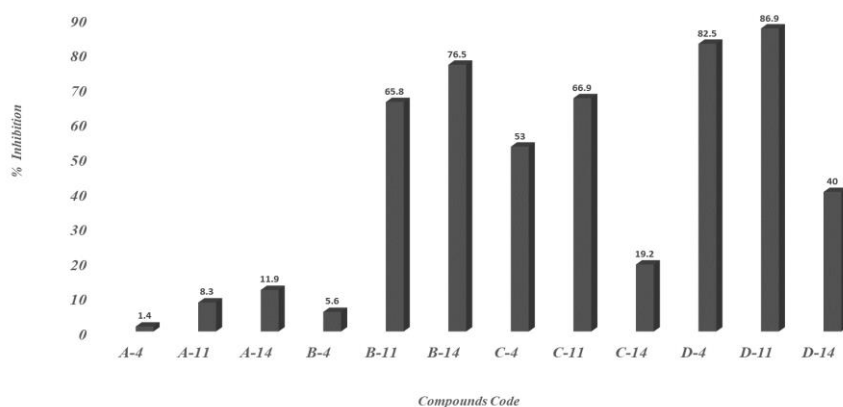


**Figure 35.** Graph showing the TcTS inhibition data of selected compounds of series A-D determined by (HPAEC-PAD).

Interestingly, the compound D-11 with highest 86.9% inhibition value, also has shown the highest predicted binding affinity -11.1 Kcal/mol compared to reference DANA (-7.8 Kcal/mol) but the compound C-11 which also has the same predicted binding affinity exhibited 66.9% enzyme inhibition. Both these compounds D-11 and C-11, bearing the same substituents on the aryl group of the propionic acid part but different substituents -CH<sub>3</sub> and -COOH at the 4<sup>th</sup> carbon of phthaloyl group, respectively (**Table-5**). On the other hand, the compound B-11 with the same substituent on the aryl group, like the compound D-11 and C-11 but no substituents on phthaloyl group showed 65.8% enzyme inhibition which is only one percent less than compound C-11. These results suggest that addition of lipophilic or electron donating substituents on Phthaloyl moiety are favourable for enzyme inhibition and TcTS inhibition values can be increased by the addition of such types of substituents.

Compound D-11 with 86.9% inhibition value showed the interaction with most essential amino acids of TcTS (**Fig. 36**) as follows: The carbonyl moiety of phthaloyl group was found in binding with two arginines (Arg35 and Arg314) and Tyr342 via hydrogen bond. A classical parallel  $\pi$ - $\pi$  stacking was observed between methyl group at Phthaloyl moieties and

phthaloyl ring with Trp312. The naphthyl moiety at propionic acid and phthaloyl group showed  $\pi$ - $\pi$  stacking and  $\pi$ -anion interaction with Val95 and Asp59, Asp96, respectively. The amino acid Glu230 was found in hydrogen bonding with a proton of the hydroxyl group of the carboxylic acid of the propionic acid part and amino acid residues Tyr119, Trp120 and Arg245 were found in interaction via Van der Waals forces. The molecular docking analysis of compound C-11 and B-11 with 66.9 and 65.8% respectively, also showed the same pattern of interaction as shown by compound D-11, except the interaction of Glu230, which was found absent in compound C-11 (**Fig. 36**), but additional hydrogen bond interaction of Arg245, Tyr119 was observed in compound C-11 which was absent in compound D-11.

Compound D-4, (**Fig.36**) with the second highest inhibition value 82.5%, the docking analysis showed the same binding interaction for Arg35, Arg314, Asp59, Trp312, Glu230 and Tyr342 as compound D-11, except that the amino acid residues Asp96, and Arg53 which showed the hydrogen bond interaction with *para* substituted hydroxyl group on phenyl ring, at propionic acid part of compound D-4.

On the other hand compound C-4 which has the same scaffold as D-4, except the -COOH substituent at the 4<sup>th</sup> carbon of Phthaloyl, showed the 53% inhibition. The binding pattern of both compound C-4 and D-4 is found about to same, except Glu230, which was found in hydrogen bond interaction with a carboxylic group of a propionic acid part in D-4, but in compound C-4, Glu230 was found in  $\pi$ -anion interaction with the phenyl ring. The compound B-4 with the same scaffold-like compounds C-4 and D-4, but no substituents on Phthaloyl moiety showed only 5.6% inhibition even it has shown the better trypanocidal activity (77% for NONOA and 68% INC-5) as compared to compound C-4 & D-4 and also have good predicted binding affinity value. The interaction pattern of this compound B-4 only showed

the hydrophobic interaction with key amino acid residues in TcTS catalytic pocket compared to interaction pattern of compounds C-4 and D-11.

The compound B-14 with furanyl ring showed third highest TcTS enzyme inhibition 76.5% (**Fig.36**), compared to compounds C-14 and D-14, which have 40% and 19.2% respectively. The interaction pattern of this compound B-14 was found similar to compounds D-11 and D-4. Herein, Trp312 showed the  $\pi$ - $\pi$  stacking with furanyl ring and hydrogen bonding with carbonyl of Phthaloyl moiety. Furthermore, Tyr119 also showed the  $\pi$ - $\pi$  stacking and hydrogen bonding with Phthaloyl moiety but in compound D-11, D-4 and C-11 the Tyr 119 was found in hydrophobic interaction.

In case of series A, the compound A-11, which also has shown the highest predicted binding affinity (-9.0 Kcal/mol) compared to DANA, showed the least value of enzyme inhibition (8.3 %). If we compare the interaction of A-11, with compounds which have highest enzyme inhibition values (**Fig.36**), we found A-11 showed the least interaction with essential amino acids residues and also showed the unfavourable interaction bumps, compared to other compounds interactions with highest predicted binding affinity and enzyme inhibition values. From this comparison of enzyme inhibition and docking analysis, we suggest that compounds with strong interaction with Glu230, Trp312 and Tyr342 are showing strong inhibition as compared to other interaction and presence of lipophilic substituents (-CH<sub>3</sub>) on 4<sup>th</sup> position of Phthaloyl moiety is another factor.

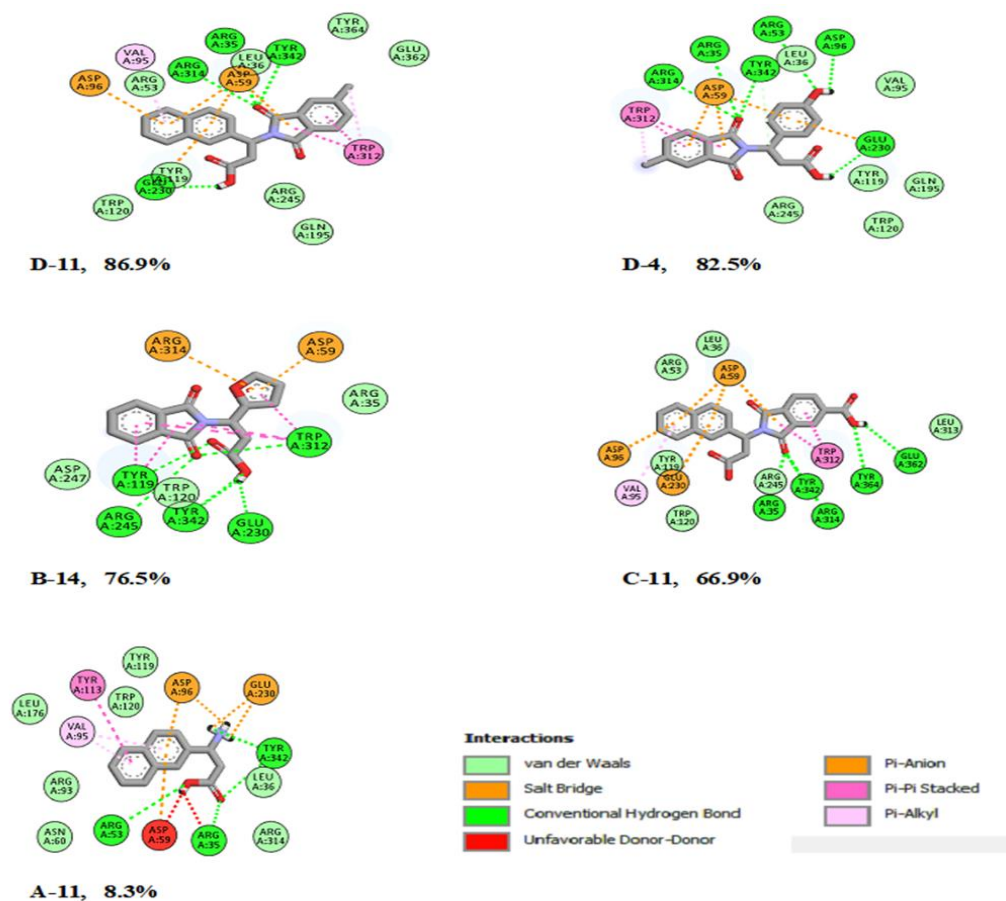


**Figure. 36.** 2D interaction of series D, B, C and A compounds with TcTS active residues, with highest to lowest TcTS inhibition is expressed as percentage . The 2D image was produced by Discovery studio visualizer R-2 client 2017 version. Color boxes indicated the interaction.

### 3.4.3. *Trans-sialidase enzyme inhibition assay of series E, F, G and H*

After the predicted binding energy calculation and binding pattern analysis in catalytic pocket of TcTS enzyme, sixteen compounds (16) were selected out of one hundred ten (110). The selection criteria were adopted depending upon the highest to lowest predicted binding

affinities value and number of active amino acid residues occupied by molecules in the TcTS pocket.

From a selected derivative of phenyl carbamoyl benzoic acid (E, F and G) and cyclohexane carbamoyl benzoic acid (H) (**Table-6**), the compound F-7 (2-(2-(4-carboxyphenyl) hydrazine-1-carbonyl) terephthalic acid) showed the 97%, TcTS enzyme inhibition value which was found highest values from all the series. Other compounds showed enzyme inhibition less than 50%, the compound E-4 (2-[(4-carboxy-2-chlorophenyl) carbamoyl]-6-nitrobenzoic acid) showed 48.1 %, compound H-15 (4-methyl-2-((pyridine-2-ylmethyl) carbamoyl) cyclohexane carboxylic acid) showed 46.1%, compound E-12 (2-[(4-aminophenyl)carbamoyl]-6-nitrobenzoic acid) showed 42.5%, compound E-13 (2-nitro-6-[(4-nitrophenyl) carbamoyl]benzoic acid) showed 41.7% and compound E-10 (2-[[4-(ethoxy carbonyl)phenyl] carbamoyl]-6-nitrobenzoic acid) showed 35.8%. Remaining compounds F-2, F-14, F-22, G-2, G-11, G-23, H-2, H-11, H-16, and H-25 showed very low TcTS inhibition in the range of 5.4% to 13.6% (**Fig. 37**) even these compounds have better predicted binding affinity values as compared to reference DANA.

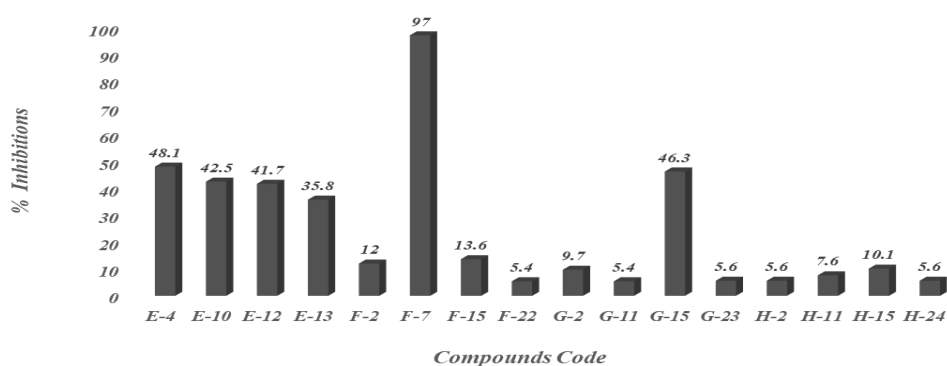


**Figure. 37.** Graph showing the TcTS inhibition data of selected compounds of series E-H determined by (HPAEC-PAD).

In the comparison with molecular docking and binding pattern of compounds **F- 7** in catalytic pocket of TcTS enzyme, this compound has shown the -9.5 kcal/mol predicted binding affinity and occupied most of the essential amino acid residues (**Fig. 38**). In compound F-7, terephthalic acid plays an important role and amide linkage part which contain the hydrazide group and carboxyl group at *para* position reference to hydrazide or amide linkage also participate to occupy the essential amino acid residues by different interactions. The arginine triad (Arg35, Arg245, and Arg314) which contribute to binding of a carboxylic group of sialic acid [], two of them Arg35, and Arg314 showed the hydrogen bonding with the carbonyl group of amide linkage and Arg245 showed the hydrophobic interaction. The amino acid residue Tyr342 was found in hydrogen bonding with the hydrogen atom of hydrazine group and Glu230 was found in hydrophobic and  $\pi$  anion attraction with phenyl moiety. Both these Tyr342 and Glu230 are reported to stabilize the transition state. Asp96 which occupied the amide part the sialic acid in catalytic pocket of TcTS was attracted by a hydrogen bond with the oxygen atom of the carboxylic acid group on phenyl moiety of an amide linkage. Two most important amino acid residues Tyr119 and Trp312 which are present at the mouth of catalytic pocket and reported as a gatekeeper to control the entrance of the substrate or allow the substrate in control manner into the pocket of TcTS enzyme [124] showed the hydrogen bonding with the oxygen atom of the carboxylic moiety. The Trp312 was attracted by hydrogen bonding with carboxylic group oxygen atom as well as classical parallel  $\pi$ - $\pi$  stacking with phenyl ring of phthalic acid part while Tyr119 was occupied by hydrogen bonding with a carboxylic group of phenyl ring in amide linkage part. The side chain residue Trp120 which also contribute to the formation of hydrophobic pocket was found in hydrogen bond interaction [124] with the oxygen atom of the carboxylic acid of amide linkage part. Furthermore, Glu195 and Tyr364 were also found in hydrogen bond interaction with the oxygen atom of the carboxylic acid moiety.

The compound **E-4** with the free energy value  $-9.7$  kcal/mole, which is greater than the compound **F-7** showed the 48.1% TcTS inhibition. The series E, compounds contains the 3-nitro ( $-\text{NO}_2$ ) of the phthalic acid ring. The  $-\text{NO}_2$  group did not show prominent interaction with any amino acid residues compared to carboxyl group for compound **F-7**. This behaviour shows that substituents at the 4<sup>th</sup> carbon of phthalic acid are more favourable. The amide linkage part contains the  $-\text{Cl}$  and  $-\text{COOH}$  showed the hydrogen bond interaction with two amino acid residues. The binding pattern of **E-4** displayed, the interaction with only two essential amino acid residues Arg245 and Tyr342. The Tyr119 was found in  $\pi$ - $\pi$  stacking T shaped (**Fig. 38**). An unfavourable interaction was found between Trp120 and carboxylic group of amide linkage part. Rest of the amino acid residues in TcTS catalytic pocket showed the hydrophobic interaction. The **G**, series compounds, which contains the  $-\text{CH}_3$  substituents at the 4<sup>th</sup> carbon of phthalic acid part, one of the compounds **G-15**, with  $-9.2$  kcal/mol free energy value showed the 46.3% TcTS inhibition value. The binding pattern of this compound revealed that only three essential amino acids Arg35, Arg314 and Tyr342 showed the hydrogen bonding interaction. A  $\pi$ - $\pi$  stacking was observed between methyl and phenyl ring of phthalic acid part of compound **G-15** and Trp312 residue (**Fig. 38**). From the comparison of compound **G-15** and **E-4**, both compounds occupy the equal amino acid residues via different physical forces but compound **E-4** has a higher TcTS binding which can be due to the presence of carboxy and  $-\text{Cl}$  phenyl ring and more hydrophobic interaction compared to pyridine. Compounds from series **H**, which has the cyclohexane ring in one part and phenyl ring in amide linkage part showed the least inhibition values even these compounds have the better predicted free energy value. For example compound **H-24** which has shown the best predicted binding affinity value  $-9.9$  kcal/ mol, which was found highest from compound **F-7**, **E-4**, and **G-15** showed the 5.6% TcTS inhibition value which was found very less than compound **F-7** which has 97%. The binding pattern comparison of both **H-24** and **F-7** in



TcTS pocket showed the compound **F-7** has occupied more amino acid residues, which due to the presence of two phenyl ring but in compound **H-24**, the cyclohexane ring transform into chair shaped conformer after energy minimization. Four amino acid residues Asp96, Trp120, Tyr119 and Tyr342 showed the hydrogen bond interaction with carbonyl and carboxylic acid moiety while the Trp312 showed  $\pi$ -alkyl interaction with a methyl group at cyclohexane ring (**Fig. 38**).

Form these selected compounds, a well-defined correlation were not found between predicted binding affinity values and TcTS inhibitions. Most of the compounds have the excellent predicted binding affinity but least inhibition and vice versa. A partial correlation was found between molecular docking and TcTS inhibition for phthaloyl derivatives of 3-amino-3-aryl propionic acids, series **A-D**.

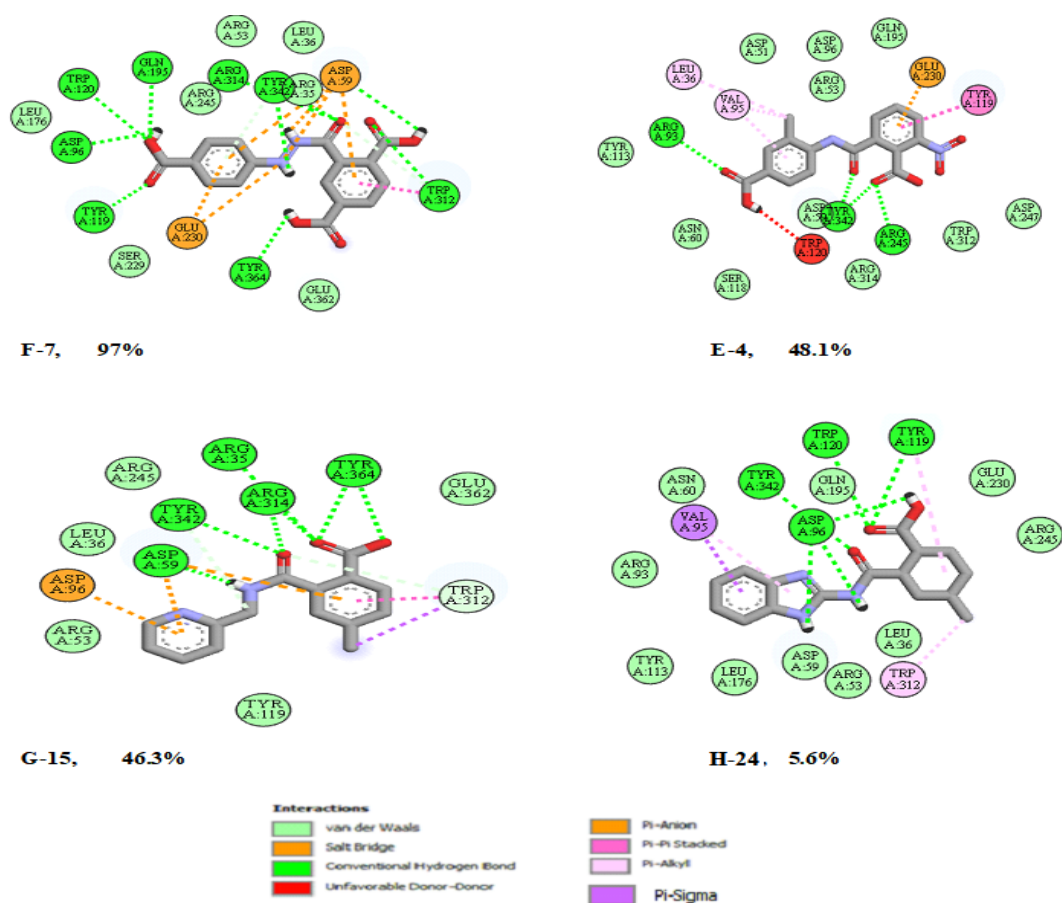


**Figure. 38.** 2D interaction of series F, E, G and H compounds with TcTS active residues, with highest to lowest TcTS inhibition percentage. The 2D image was produced by Discovery studio visualizer R-2 client 2017 version.

If we compare the TcTS inhibition of the selected compounds of series E-F with trypanocidal activity, the compound F-7 with 97% TcTS inhibition only showed the  $12.5 \pm 7.61$  and  $22.73 \pm 6$  % lysis for NINOA and INC-5 strain, respectively. The compounds E-4, G-15 and H-24 also showed the same behaviour for trypanocidal activity and no correlation was found between TcTS and lysis.

## CONCLUSIONS

The objective of this work was to design and synthesize a new carboxylic/benzoic acid derivatives compounds as potential trans-sialidase inhibitors taking advantage of ~~due to the advantage~~ of phenyl ring over the sugar moiety ring. The ease of synthesis, substitution of different groups, and rigidity of phenyl ring over the sugar moiety with  $\pi$ -electron resonance in phenyl ring made carboxylic/benzoic acid derivative attractive for TcTS inhibitor.

In this reported work, one hundred seventy five 175?? o 180 (180), benzoic/carboxylic acid derivative, para-aminobenzoic acid derivatives, 3-amino-3-aryl propionic acids (series A), phthaloyl derivatives of 3-amino-3-aryl propionic acids (series B-D), and phenyl carbamoyl benzoic acid derivatives (series E-H) were designed by molecular docking in catalytic pocket of trans-sialidase enzyme. All these designed compounds showed the best pose and interaction with essential amino acid in the TcTS pocket and predicted binding affinity of these compounds was found greater than the reference DANA. The compounds C-11 and D-11 from series C and respectively showed the -11 kcal/mol predicted binding affinity compared to reference DANA (-7.8 kcal/mol). These designed carboxylic acid derivatives were synthesized successfully and reaction completion was confirmed by TLC. All these synthesized compounds were confirmed by FTIR,  $^1\text{H}$  NMR, and  $^{13}\text{C}$  NMR spectroscopic techniques. All these compounds were screened for trypanocidal effects and  $\text{LC}_{50}$  determination on infected blood with trypomastigotes of NINOA and INC-5 strain of *T. cruzi*. The phthaloyl derivative of 3-amino-3-aryl propionic acids was found best among all series, some compound showed the 85% lytic activity but for the individual strain. The compounds A-1, A-5, C-2, B-4, B-4, B-5, B-11, D-1, D-2, D-3, and D-11 from series B and D showed, best trypanocidal activity for both NINOA and INC-5 strain with best  $\text{LC}_{50}$  values. From series (E-H), only compound F-10 showed the tolerable trypanocidal activity for bot strain.

The best TcTS enzyme inhibition was showed by compound F-7, 97% which is highest among all series and second D series compounds D-11, D-4 showed the 85.6 and 82% respectively. Furthermore, the compounds with highest TcTS inhibition showed the best correlation between predicted binding affinity and TcTS. But no prominent correlation was found between trypanocidal activity and TcTS inhibition. Only a partial correlation was shown by compound D-11 with predicted binding affinity -11 kcal/mol, trypanocidal effect (% lysis  $63 \pm 4$  and  $LC_{50}$   $18.94 \pm 2.1$  for NINOA) and (% lysis  $65 \pm 2$  and  $LC_{50}$   $16.60 \pm 2.3$  for INC-5) respectively and 86.9% TcTS inhibition.

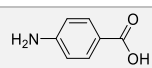
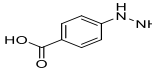
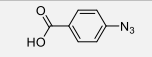
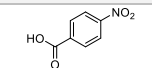
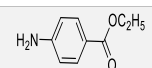
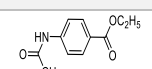
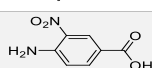
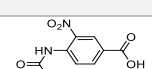
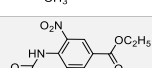
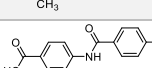
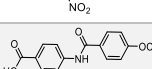
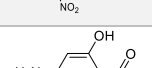
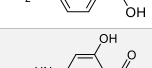
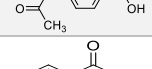
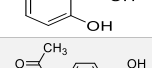
These compounds with best trypanocidal activity and TcTS inhibition can be used as starting point for the development of new anti-Chagas drugs and by further modification of substituents by reviewing the pattern style of these compound in catalytic pocket, we can find the more appropriate correlation among molecular docking, trypanocidal activity (NINOA and INC-5) and TcTS inhibition.



## CHAPTER FOUR

### Tables

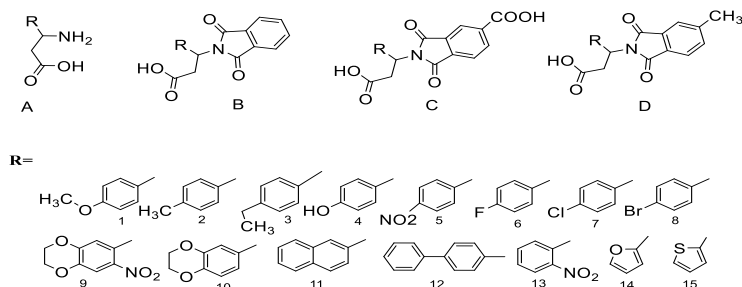
**Table 2.** Predicted binding affinities of *para-amino benzoic acid (PABA) derivatives*, Predicted by using Auto Dock Vina version 4.2 and MGL tool using natural ligand DANA as

Code	Compound structure	Lowest energy conformation		Binding mode for the top nine low energy conformations						
		Bind	Score	Bind (A2)	A	Bind B	Bind C	Max. Score	Min. Score	Mean Score
1		B	-5.8	1		6	2	-5.8	-4.9	-5.3
2		B	-6.3	1		6	2	-6.3	-5.6	-5.9
3		A2	-6.9	4 (3)		0	5	-6.9	-6.2	-6.5
4		B	-5.9	2 (2)		2	5	-5.9	-5.7	-5.8
5		B	-6.0	1		4	4	-6.0	-5.1	-5.6
6		A	-6.8	3		0	6	-6.8	-5.7	-6.1
7		A2	-6.3	4 (2)		0	5	-6.3	-5.9	-6.1
8		A2	-7.4	5 (3)		0	4	-7.4	-6.5	-6.8
9		A2	-7.4	5 (3)		0	4	-7.4	-6.5	-7
10		A2	-8.0	1 (1)		0	8	-8.0	-6.9	-7.4
11		C	-7.8	0		1	8	-7.8	-6.7	-7.1
12		B	-5.9	1		3	5	-6.9	-6.4	-5.5
13		C	-6.9	2		2	5	-6.9	-6.4	-6.6
14		C	-5.8	0		2	7	-5.8	-5.1	-5.4
15		A, B	-6.3	2		1	6	-6.3	-5.8	-6.0

a reference

**Table 3.** Predicted binding affinities of series A-D, Predicted by using Auto Dock Vina

version 4.2 and MGL tool using natural ligand DANA as a reference.

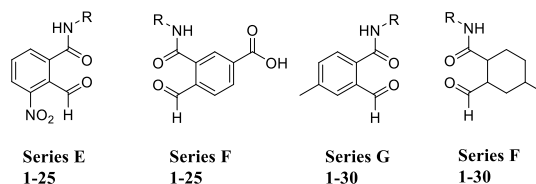


Series A	Predicted binding affinity Kcal/mol	Series B	Predicted binding affinity Kcal/mol	Series C	Predicted binding affinity Kcal/mol	Series D	Predicted binding affinity Kcal/mol
A-1	-7.4	B-1	-9.1	C-1	-9.9	D-1	-9.6
A-2	-7.5	B-2	-9.9	C-2	-9.9	D-2	-9.7
A-3	-7.8	B-3	-9.4	C-3	-10.1	D-3	-10.0
A-4	-7.2	B-4	-9.3	C-4	-9.9	D-4	-9.6
A-5	-7.8	B-5	-9.5	C-5	-9.6	D-5	-9.6
A-6	-7.2	B-6	-9.2	C-6	-9.8	D-6	-9.0
A-7	-7.4	B-7	-9.3	C-7	-9.8	D-7	-9.6
A-8	-7.5	B-8	-9.2	C-8	-9.8	D-8	-9.7
A-9	-8.1	B-9	-9.8	C-9	-10.4	D-9	-10.5
A-10	-8.2	B-10	-9.4	C-10	-10.6	D-10	-10.5
A-11	-9.0	B-11	-10.8	C-11	-11.1	D-11	-11.1
A-12	-8.2	B-12	-9.0	C-12	-9.5	D-12	-9.4
A-13	-7.5	B-13	-9.2	C-13	-9.6	D-13	-9.6
A-14	-6.2	B-14	-8.0	C-14	-9.2	D-14	-8.8
A-15	-6.0	B-15	-7.0	C-15	-8.0	D-15	-8.2
<b>DANA</b>	<b>-7.8</b>	<b>DANA</b>	<b>-7.8</b>	<b>DANA</b>	<b>-7.8</b>	<b>DANA</b>	<b>-7.8</b>

**Table 4.** Predicted binding affinities of series E, F, G and H. Predicted by using Auto Dock

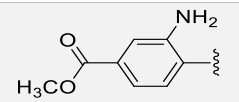
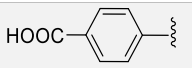
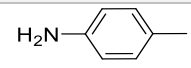
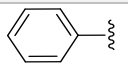
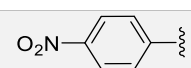
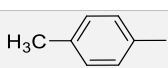
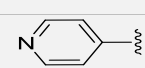
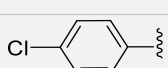
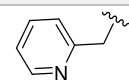
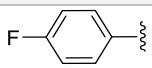
*Vina version 4.2* and MGL tool using natural ligand DANA as a reference

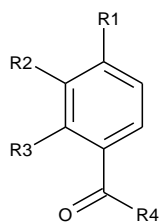
General structures



Code	R	Predicted binding affinity – Kcal/mol				Code	R	Predicted binding affinity – Kcal/mol			
		E	F	G	H			E	F	G	H
1		-9.3	-9.0	-9.2	-9.8	16		-9.3	-9.2	-9.5	-9.0
2		-9.7	-9.2	-8.8	-9.9	17		-9.5	-9.5	-9.5	-9.5
3		-8.6	-8.8	-8.9	-8.9	18		-9.4	-9.2	-9.0	-8.7
4		-9.7	-10.3	-9.2	-9.9	19		-9.5	-9.7	-8.7	-9.5
5		-8.9	-9.1	-8.9	-9.1	20		-8.9	-9.2	-8.7	-8.7
6		-9.5	-9.5	-10.0	-9.5	21		-8.8	-8.7	-9.5	-8.3
7		10.1	-9.5	-9.6	-9.7	22		-9.3	-10.0	-8.9	-10.0
8		-9.0	-8.4	-8.4	-8.3	23		-8.5	-8.6	-8.9	-8.9
9		-9.5	-8.7	-8.6	-8.7	24		-9.6	-9.7	-9.5	-9.9
10		-9.1	-8.5	-8.6	-8.1	25		-9.1	-9.5	-9.7	-9.0



<b>11</b>		-9.1	-8.3	-8.0	-8.1	<b>26</b>		-	-	-9.0	-9.5
<b>12</b>		-9.7	-9.0	-8.8	-8.3	<b>27</b>		-	-	-8.6	-8.7
<b>13</b>		-9.0	-8.8	-8.2	-8.3	<b>28</b>		-	-	-8.2	-8.7
<b>14</b>		-9.0	-8.5	-9.1	-8.5	<b>29</b>		-	-	-8.3	-8.6
<b>15</b>		-9.4	-9.4	-9.2	-8.9	<b>30</b>		-	-	-8.5	-8.7

**Table 5.** TcTS inhibition values of benzoic acid derivatives.

<i>Code</i>	<i>R<sub>1</sub></i>	<i>R<sub>2</sub></i>	<i>R<sub>3</sub></i>	<i>R<sub>4</sub></i>	<i>NINOA LC<sub>50</sub> (μM)</i>	<i>INC-5 LC<sub>50</sub> (μM)</i>
<b>1</b>	NH <sub>2</sub>	H	H	OH	0.52 ± 0.19	1.24 ± 1.0
<b>2</b>	NHNH <sub>2</sub>	H	H	OH	0.66 ± 0.39	0.58 ± 0.4
<b>3</b>	N <sub>3</sub>	H	H	OH	0.60 ± 0.46	0.47 ± 0.35
<b>4</b>	NO <sub>2</sub>	H	H	OH	0.47 ± 0.16	0.46 ± 0.38
<b>5</b>	NH <sub>2</sub>	H	H	OCH <sub>2</sub> CH <sub>3</sub>	0.10 ± 0.041	0.10 ± 0.047
<b>6</b>	NHCOCH <sub>3</sub>	H	H	OCH <sub>2</sub> CH <sub>3</sub>	0.34 ± 0.18	0.21 ± 0.1
<b>7</b>	NH <sub>2</sub>	NO <sub>2</sub>	H	OH	1.37 ± 0.56	0.63 ± 0.3
<b>8</b>	NHCOCH <sub>3</sub>	NO <sub>2</sub>	H	OH	1.10 ± 0.58	0.21 ± 0.1
<b>9</b>	NHCOCH <sub>3</sub>	NO <sub>2</sub>	H	OCH <sub>2</sub> CH <sub>3</sub>	0.02 ± 0.012	0.22 ± 0.09
<b>10</b>	NHCOC <sub>6</sub> H <sub>4</sub> - <i>p</i> -Cl	NO <sub>2</sub>	H	OH	0.14 ± 0.08	0.0008 ± 0.0001
<b>11</b>	NHCOC <sub>6</sub> H <sub>4</sub> -OCH <sub>3</sub>	NO <sub>2</sub>	H	OH	0.61 ± 0.3	0.43 ± 0.28
<b>12</b>	NH <sub>2</sub>	H	OH	OH	0.27 ± 0.10	0.26 ± 0.09
<b>13</b>	NHCOCH <sub>3</sub>	H	OH	OH	1.28 ± 0.26	1.28 ± 0.31
<b>14</b>	H	H	OH	OH	0.576 ± 0.32	0.721 ± 0.42
<b>15</b>	NHCOCH <sub>3</sub>	H	H	OH	1.39 ± 0.75	0.878 ± 0.55
<b>Nfx</b>					<b>0.213 ± 0.08</b>	<b>0.68 ± 0.17</b>
<b>Bzn</b>					<b>0.292 ± 0.12</b>	<b>0.62 ± 0.28</b>

**Table 6.** %age lysis of trypomastigotes of NINOA and INC-5 strains, LC<sub>50</sub> and C log P

values of series A.

Compound code	C log P	<i>T. cruzi</i> NINOA		<i>T. cruzi</i> INC-5	
		% Lysis at 10 µg/mL	LC <sub>50</sub> (µg/mL)	% Lysis at 10 µg/mL	LC <sub>50</sub> (µg/mL)
<b>A-1</b>	0.59	83 ± 6	19.822 ± 1.15	54 ± 9	>50
<b>A-2</b>	0.92	78 ± 6	32.920 ± 2.81	59 ± 7	>50
<b>A-3</b>	1.20	65 ± 8	21.855 ± 1.58	50 ± 7	>50
<b>A-4</b>	0.15	50 ± 8	27.455 ± 2.35	76 ± 2	23.080 ± 2.53
<b>A-5</b>	-0.22	50 ± 5	26.265 ± 2.26	68 ± 3	52.382 ± 4.06
<b>A-6</b>	0.85	35 ± 4	<i>Nd</i>	62 ± 9	<i>Nd</i>
<b>A-7</b>	1.09	13 ± 13	<i>Nd</i>	73 ± 1	<i>Nd</i>
<b>A-8</b>	1.18	20 ± 10	<i>Nd</i>	18 ± 5	<i>Nd</i>
<b>A-9</b>	-0.53	07 ± 6	<i>Nd</i>	15 ± 6	<i>Nd</i>
<b>A-10</b>	1.04	37 ± 8	<i>Nd</i>	52 ± 3	<i>Nd</i>
<b>A-11</b>	1.38	60 ± 6	21.280 ± 2.78	60 ± 3	22.147 ± 3.542
<b>A-12</b>	1.96	32 ± 6	<i>Nd</i>	37 ± 1	<i>Nd</i>
<b>A-13</b>	-0.44	23 ± 6	<i>Nd</i>	63 ± 4	<i>Nd</i>
<b>A-14</b>	-0.39	53 ± 2	15.370 ± 2.23	50 ± 5	35.542 ± 3.059
<b>A-15</b>	0.27	8 ± 5	<i>Nd</i>	32 ± 6	<i>Nd</i>
<b>DANA</b>	<b>-2.08</b>	-	-	-	-
<b>Bzn</b>	-	<b>46.30 ± 3.1</b>	<b>33.72 ± 5.1</b>	<b>56 ± 7</b>	<b>32.19 ± 4.51</b>
<b>Nfx</b>	-	<b>40.74 ± 6.4</b>	<b>25.72 ± 4.6</b>	<b>50 ± 6</b>	<b>22.19 ± 2.11</b>

**Table 7.** %age lysis of trypomastigotes of NINOA and INC-5 strains, LC<sub>50</sub> and C log P values of series B.

Compound code	C log P	<i>T. cruzi</i> NINOA		<i>T. cruzi</i> INC-5	
		% Lysis at 10 µg/mL	LC <sub>50</sub> (µg/mL)	% Lysis at 10 µg/mL	LC <sub>50</sub> (µg/mL)
<b>B-1</b>	1.99	24 ± 3	<i>Nd</i>	09 ± 2	<i>Nd</i>
<b>B-2</b>	2.36	23 ± 3	<i>Nd</i>	22 ± 1	<i>Nd</i>
<b>B-3</b>	2.68	22 ± 3	<i>Nd</i>	08 ± 3	<i>Nd</i>
<b>B-4</b>	<b>1.61</b>	<b>77 ± 4</b>	<b>22.221 ± 2.88</b>	<b>68 ± 1</b>	<b>28.231 ± 2.10</b>
<b>B-5</b>	1.32	62 ± 5	18.203 ± 2.98	80 ± 1	40.391 ± 3.86
<b>B-6</b>	2.34	63 ± 2	28.45 ± 2.99	52 ± 3	79.129 ± 2.56
<b>B-7</b>	2.56	36 ± 7	<i>Nd</i>	70 ± 3	<i>Nd</i>
<b>B-8</b>	2.65	08 ± 1	<i>Nd</i>	15 ± 3	<i>Nd</i>
<b>B-9</b>	1.12	54 ± 6	<i>Nd</i>	13 ± 3	<i>Nd</i>
<b>B-10</b>	1.90	24 ± 5	<i>Nd</i>	41 ± 3	<i>Nd</i>
<b>B-11</b>	2.96	57 ± 2	33.595 ± 1.62	62 ± 4	40.497 ± 5.32
<b>B-12</b>	3.30	31 ± 3	<i>Nd</i>	22 ± 5	<i>Nd</i>
<b>B-13</b>	1.26	56 ± 6	<i>Nd</i>	68 ± 5	<i>Nd</i>
<b>B-14</b>	1.32	16 ± 1	<i>Nd</i>	21 ± 6	<i>Nd</i>
<b>B-15</b>	2.00	22 ± 3	<i>Nd</i>	25 ± 4	<i>Nd</i>
<b>DANA</b>	<b>-2.08</b>	-	-	-	-
<b>Bzn</b>		<b>46.30 ± 13.12</b>	<b>33.72 ± 5.1</b>	<b>56 ± 7</b>	<b>32.19 ± 4.51</b>
<b>Nfx</b>		<b>40.74 ± 6.4</b>	<b>25.72 ± 4.6</b>	<b>50 ± 6</b>	<b>22.19 ± 2.11</b>

**Table 8.** %age lysis of trypomastigotes of NINOA and INC-5 strains,  $LC_{50}$  and C log P

values of series C.

Compound code	C log P	<i>T. cruzi</i> NINOA		<i>T. cruzi</i> INC-5	
		% Lysis at 10 $\mu$ g/mL	$LC_{50}$ ( $\mu$ g/mL)	% Lysis at 10 $\mu$ g/mL	$LC_{50}$ ( $\mu$ g/mL)
C-1	1.59	72 $\pm$ 6	<i>Nd</i>	32 $\pm$ 8	<i>Nd</i>
C-2	1.91	85 $\pm$ 5	38.693 $\pm$ 1.62	55 $\pm$ 2	14.091 $\pm$ 3.25
C-3	2.10	23 $\pm$ 6	<i>Nd</i>	61 $\pm$ 2	<i>Nd</i>
C-4	1.13	43 $\pm$ 7	<i>Nd</i>	71 $\pm$ 3	<i>Nd</i>
C-5	0.84	23 $\pm$ 8	<i>Nd</i>	63 $\pm$ 6	<i>Nd</i>
C-6	1.89	10 $\pm$ 8	<i>Nd</i>	67 $\pm$ 6	<i>Nd</i>
C-7	1.13	03 $\pm$ 6	<i>Nd</i>	69 $\pm$ 6	<i>Nd</i>
C-8	1.71	23 $\pm$ 3	<i>Nd</i>	56 $\pm$ 8	<i>Nd</i>
C-9	0.69	40 $\pm$ 4	<i>Nd</i>	59 $\pm$ 10	<i>Nd</i>
C-10	1.46	33 $\pm$ 4	<i>Nd</i>	47 $\pm$ 8	<i>Nd</i>
C-11	1.91	42 $\pm$ 4	<i>Nd</i>	24 $\pm$ 8	<i>Nd</i>
C-12	1.99	17 $\pm$ 6	<i>Nd</i>	57 $\pm$ 2	<i>Nd</i>
C-13	0.85	48 $\pm$ 7	<i>Nd</i>	68 $\pm$ 4	<i>Nd</i>
C-14	0.91	77 $\pm$ 6	25.543 $\pm$ 2.85	55 $\pm$ 3	33.457 $\pm$ 2.01
C-15	1.57	67 $\pm$ 8	<i>Nd</i>	19 $\pm$ 2	<i>Nd</i>
<b>DANA</b>	<b>-2.08</b>	-	-	-	-
<b>Bzn</b>		<b>46.30 <math>\pm</math> 13.12</b>	<b>33.72 <math>\pm</math> 5.1</b>	<b>56 <math>\pm</math> 7</b>	<b>32.19 <math>\pm</math> 4.51</b>
<b>Nfx</b>		<b>40.74 <math>\pm</math> 6.4</b>	<b>25.72 <math>\pm</math> 4.6</b>	<b>50 <math>\pm</math> 6</b>	<b>22.19 <math>\pm</math> 2.11</b>

**Table 9.** %age lysis of trypomastigotes of NINOA & INC-5 strains, LC<sub>50</sub> and C log P values

of series D.

Compound code	C log P	<i>T. cruzi</i> NINOA		<i>T. cruzi</i> INC-5	
		% Lysis at 10 µg/mL	LC <sub>50</sub> (µg/mL)	% Lysis at 10 µg/mL	LC <sub>50</sub> (µg/mL)
<b>D-1</b>	2.36	78 ± 7	22.23 ± 3.7	57 ± 4	20.18 ± 3.9
<b>D-2</b>	2.69	73 ± 8	27.67 ± 2.8	67 ± 6	14.09 ± 2.9
<b>D-3</b>	3.01	65 ± 4	<i>Nd</i>	59 ± 5	<i>Nd</i>
<b>D-4</b>	2.01	38 ± 7	<i>Nd</i>	15 ± 4	<i>Nd</i>
<b>D-5</b>	1.72	45 ± 8	<i>Nd</i>	25 ± 5	<i>Nd</i>
<b>D-6</b>	2.99	63 ± 6	14.79 ± 4.0	56 ± 6	24.43 ± 6.5
<b>D-7</b>	2.77	52 ± 6	12.96 ± 3.9	51 ± 7	17.88 ± 2.6
<b>D-8</b>	3.08	65 ± 6	9.55 ± 4.3	50 ± 6	8.94 ± 3.9
<b>D-9</b>	1.55	47 ± 5	<i>Nd</i>	63 ± 7	<i>Nd</i>
<b>D-10</b>	2.31	47 ± 7	<i>Nd</i>	40 ± 5	<i>Nd</i>
<b>D-11</b>	3.34	63 ± 4	18.94 ± 2.1	65 ± 2	16.60 ± 2.3
<b>D-12</b>	3.78	25 ± 6	<i>Nd</i>	25 ± 4	<i>Nd</i>
<b>D-13</b>	1.65	22 ± 7	<i>Nd</i>	65 ± 5	<i>Nd</i>
<b>D-14</b>	1.77	27 ± 8	<i>Nd</i>	40 ± 3	<i>Nd</i>
<b>D-15</b>	2.44	47 ± 6	<i>Nd</i>	48 ± 5	<i>Nd</i>
<b>DANA</b>	<b>-2.08</b>	-	-	-	-
<b>Bzn</b>		<b>46.30 ± 13.12</b>	<b>33.72 ± 5.1</b>	<b>56 ± 7</b>	<b>32.19 ± 4.51</b>
<b>Nfx</b>		<b>40.74 ± 6.4</b>	<b>25.72 ± 4.6</b>	<b>50 ± 6</b>	<b>22.19 ± 2.11</b>

**Table 10.** %age lysis of trypomastigotes of NINOA & INC-5 strains, LC<sub>50</sub> and C log P

values of series **E**.

Code	C log P	<i>T. cruzi</i> NINOA		<i>T. cruzi</i> INC-5	
		% Lysis at 10 µg/mL	LC <sub>50</sub> (µg/mL)	% Lysis at 10 µg/mL	LC <sub>50</sub> (µg/mL)
E-1	0.41	5.16 ± 2.5	Nd	7.2±3.1	Nd
E-2	0.54	3.99 ± 1.8	-	4.22±1.5	-
E-3	1.94	7.74 ± 3.2	-	8.3 ± 1.5	-
E-4	1.58	3.99 ± 2.2	-	5.4 ± 3.1	-
E-5	1.42	4.69 ± 3.2	-	4.4 ± 3.0	-
E-6	1.08	6.10 ± 2.5	-	8.2 ± 1.1	-
E-7	0.59	10.09 ± 1.8	-	9.10 ± 2.2	-
E-8	0.15	4.69 ± 2.1	-	3.2 ± 2.1	-
E-9	1.43	5.86 ± 1.7	-	4.44 ± 2.2	-
E-10	1.46	11.26 ± 2.5	-	13.1 ± 3.0	-
E-11	0.78	13.84 ± 1.8	-	10.4 ± 3.3	-
E-12	0.58	12.44 ± 3.1	-	14.1 ± 1.7	-
E-13	0.41	6.33 ± 2.5	-	8.1 ± 2.2	-
E-14	0.55	5.39 ± 2.2	-	4.72 ± 1.2	-
E-15	0.55	11.73 ± 3.2	Nd	9.4 ± 3.1	Nd
E-16	0.07	12.67 ± 2.5	-	11.5 ± 2.0	-
E-17	0.9	8.45 ± 2.9	-	6.1 ± 1.9	-
E-18	0.91	5.39 ± 2.9	-	6.10 ± 1.1	-
E-19	-0.48	10.56 ± 2.6	-	5.2 ± 2.2	-
E-20	1.11	1.5 ± 1.8	-	3.2 ± 1.8	-
E-21	1.32	3.1 ± 1.1	-	2.1 ± 1.7	-
E-22	0.36	5.63 ± 3.3	-	7.2 ± 1.8	-
E-23	1.32	1.87 ± 3.2	-	3.45 ± 1.1	-
E-24	1.02	19.23 ± 1.5	-	20.1 ± 1.8	-
E-25	1.89	16.92 ± 2.0	-	14. ± 2.7	-
<i>Bzn</i>		<b>37.24 ± 6.3</b>	<b>47.65 ± 4.2</b>	<b>24.65± 7.1</b>	<b>58.66 ± 6.9</b>
<i>Nfx</i>		<b>33.14 ± 5.4</b>	<b>28.56± 3.2</b>	<b>27.74 ± 6.4</b>	<b>33.66 ± 4.7</b>

**Table 11.** %age lysis of trypomastigotes of NINOA & INC-5 strains, LC<sub>50</sub> and C log Pvalues of series **F**.

<i>Code</i>	<b>C log P</b>	<i>T. cruzi</i> <b>NINOA</b>		<i>T. cruzi</i> <b>INC-5</b>	
		<b>% Lysis at 10 µg/mL</b>	<b>LC<sub>50</sub> (µg/mL)</b>	<b>% Lysis at 10 µg/mL</b>	<b>LC<sub>50</sub> (µg/mL)</b>
<b>F-1</b>	1.13	31.94 ± 9.8	27.32 ± 3.1	7.07 ± 7.6	<i>Nd</i>
<b>F-2</b>	0.83	1.39 ± 5.89	<i>Nd</i>	5.56 ± 3.2	<i>Nd</i>
<b>F-3</b>	2.24	29.17 ± 1.96	31.23 ± 4.5	21.21 ± 12.4	45.31 ± 5.4
<b>F-4</b>	2.01	8.33 ± 7.50	<i>Nd</i>	6.57 ± 4.6	<i>Nd</i>
<b>F-5</b>	1.71	59.72 ± 9.82	24.76 ± 4.2	7.58 ± 3.0	<i>Nd</i>
<b>F-6</b>	1.12	18.06 ± 9.82	35.27 ± 4.1	33.33 ± 3.0	31.22 ± 3.8
<b>F-7</b>	1.35	12.5 ± 7.61	<i>Nd</i>	22.73 ± 13.2	<i>Nd</i>
<b>F-8</b>	0.82	22.22 ± 11.79	<i>Nd</i>	11.62 ± 11.4	<i>Nd</i>
<b>F-9</b>	0.42	0	<i>Nd</i>	6.57 ± 11.4	<i>Nd</i>
<b>F-10</b>	1.85	56.94 ± 1.96	18.93 ± 2.9	39.39 ± 0.3	34.25 ± 3.9
<b>F-11</b>	1.97	6.94 ± 1.96	<i>Nd</i>	13.64 ± 5.2	<i>Nd</i>
<b>F-12</b>	1.08	7.69 ± 1.57	45.27 ± 5.3	35.86 ± 6.3	38.17 ± 2.6
<b>F-13</b>	1.21	14.40 ± 1.49	42.51 ± 3.3	28.28 ± 3.8	39.73 ± 3.8
<b>F-14</b>	0.69	29.98 ± 1.81	29.29 ± 3.6	11.11 ± 8.3	<i>Nd</i>
<b>F-15</b>	0.88	4.93 ± 1.81	<i>Nd</i>	5.05 ± 5.3	<i>Nd</i>
<b>F-16</b>	0.96	1.58 ± 0.90	<i>Nd</i>	2.27 ± 3.2	<i>Nd</i>
<b>F-17</b>	0.46	14.20 ± 2.71	<i>Nd</i>	10.61 ± 6.1	<i>Nd</i>
<b>F-18</b>	1.28	5.92 ± 2.13	<i>Nd</i>	0	<i>Nd</i>
<b>F-19</b>	1.25	21.30 ± 2.37	<i>Nd</i>	9.09 ± 9.9	<i>Nd</i>
<b>F-20</b>	0.01	13.81 ± 2.08	<i>Nd</i>	0	<i>Nd</i>
<b>F-21</b>	1.67	21.10 ± 2.08	<i>Nd</i>	3.03 ± 5.2	<i>Nd</i>
<b>F-22</b>	1.54	14.00 ± 1.81	<i>Nd</i>	27.27 ± 4.5	43.22 ± 4.4
<b>F-23</b>	0.89	26.23 ± 2.67	<i>Nd</i>	5.30 ± 1.1	<i>Nd</i>
<b>F-24</b>	1.63	27.22 ± 2.13	31.15 ± 3.2	32.58 ± 1.1	38.45 ± 4.1
<b>F-25</b>	2.2	22.68 ± 2.39	<i>Nd</i>	20.45 ± 1.1	<i>Nd</i>
<b>Bzn</b>		<b>37.24 ± 6.3</b>	<b>47.65 ± 4.2</b>	<b>24.65 ± 7.1</b>	<b>58.66 ± 6.9</b>
<b>Nfx</b>		<b>33.14 ± 5.4</b>	<b>28.56 ± 3.2</b>	<b>27.74 ± 6.4</b>	<b>33.66 ± 4.7</b>

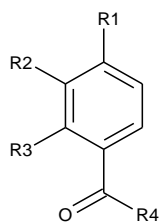


**Table 12.** %age lysis of trypomastigotes of NINOA & INC-5 strains, LC<sub>50</sub> and C log P values of series G

Code	C log P	<i>T. cruzi</i> NINOA		<i>T. cruzi</i> INC-5	
		% Lysis at 10 µg/mL	LC <sub>50</sub> (µg/mL)	% Lysis at 10 µg/mL	LC <sub>50</sub> (µg/mL)
G-1	1.9	11.04 ± 9.09	Nd-	17.64 ± 5.2	Nd-
G-2	1.9	35.71 ± 6.75		12.64 ± 4.1	
G-3	3.06	7.14 ± 4.29		37.06 ± 5.7	
G-4	2.85	8.23 ± 7.80		5.88 ± 3.5	
G-5	2.55	8.01 ± 6.88		8.53 ± 3.1	
G-6	2.13	22.08 ± 8.49		1.47 ± 2.2	
G-7	1.67	0		11.47 ± 4.5	
G-8	1.28	6.71 ± 8.22		0	
G-9	2.68	10.17 ± 4.17		0.29 ± 0.9	
G-10	2.68	27.27 ± 7.35		21.17 ± 4.9	
G-11	2.77	24.24 ± 4.79		7.64 ± 3.4	
G-12	1.9	32.03 ± 7.24		11.17 ± 3.6	
G-13	1.95	11.45 ± 1.87		24.12 ± 4.0	
G-14	1.79	5.11 ± 2.77		13.82 ± 4.4	
G-15	1.76	7.36 ± 1.23		17.64 ± 1.3	
G-16	1.16	22.29 ± 1.87		9.41 ± 3.6	
G-17	2.04	16.77 ± 2.15		4.70 ± 3.4	
G-18	1.95	24.13 ± 2.15		8.23 ± 2.7	
G-19	0.73	16.77 ± 1.87		23.23 ± 6.2	
G-20	2.5	22.90 ± 1.87		0.88 ± 2.1	
G-21	2.35	19.84 ± 1.87		10.88 ± 3.1	
G-22	1.62	13.8 ± 2.15		11.3 ± 1.8	
G-23	2.46	20.2 ± 2.1		14.3 ± 1.5	
G-24	2.06	5.73 ± 1.54		16.47 ± 4.4	
G-25	2.88	24.54 ± 2.45		34.41 ± 2.8	
G-26	2.05	9.52 ± 4.70		3.23 ± 2.1	
G-27	2.59	38.10 ± 1.87		5.88 ± 2.3	
G-28	2.83	11.45 ± 2.77		9.11 ± 2.9	
G-29	3.04	6.13 ± 2.21		8.23 ± 2.4	
G-30	2.77	18.00 ± 1.87	Nd-	1.76 ± 2.1	Nd-
<i>Bzn</i>		<b>37.24 ± 6.3</b>	<b>47.65 ± 4.2</b>	<b>24.65 ± 7.1</b>	<b>58.66 ± 6.9</b>
<i>Nfx</i>		<b>33.14 ± 5.4</b>	<b>28.56 ± 3.2</b>	<b>27.74 ± 6.4</b>	<b>33.66 ± 4.7</b>

**Table 13.** %age lysis of trypomastigotes of NINOA & INC-5 strains, LC<sub>50</sub> and C log P values of series H

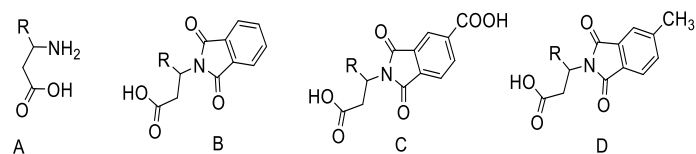
Code	C log P	<i>T. cruzi</i> NINOA		<i>T. cruzi</i> INC-5	
		% Lysis at 10 µg/mL	LC <sub>50</sub> (µg/mL)	% Lysis at 10 µg/mL	LC <sub>50</sub> (µg/mL)
1	1.4	9.74 ± 5.96	Nd-	18.1 ± 1.8	Nd-
2	1.39	11.26 ± 5.52		6.3 ± 2.3	
3	2.82	15.80 ± 6.5		10.85 ± 3.2	
4	2.33	25.32 ± 4.06		1.88 ± 6.7	
5	1.76	6.93 ± 3.12		6.13 ± 1.3	
6	1.76	3.25 ± 6.49		20.75 ± 3.1	
7	1.28	7.14 ± 6.84		40.09 ± 6.8	
8	1.09	9.09 ± 8.74		5.19 ± 1.3	
9	2.44	8.66 ± 5.49		31.60 ± 4.3	
10	2.55	13.42 ± 8.22		12.26 ± 4.3	
11	1.63	25.76 ± 10.5		5.42 ± 2.9	
12	1.63	8.23 ± 2.89		28.30 ± 7.8	
13	1.4	3.90 ± 4.50		14.86 ± 6.4	
14	1.42	17.97 ± 0.99		21.1 ± 2.1	
15	1.52	9.74 ± 0.65		5.89 ± 3.3	
16	0.84	1.30 ± 4.68		5.4 ± 1.5	
17	1.81	4.76 ± 0.37		18.16 ± 3.1	
18	1.6	31.39 ± 6.24		9.67 ± 2.1	
19	0.45	13.20 ± 4.61		18.12 ± 2.0	
20	2.18	3.03 ± 0.75		5.7 ± 2.8	
21	2.13	14.07 ± 4.87		16.04 ± 4.6	
22	1.38	13.11 ± 2.4		8.22 ± 1.8	
23	2.17	17.22 ± 2.1		19.10 ± 2.1	
24	1.8	14.29 ± 2.98		4.95 ± 2.3	
25	2.65	32.25 ± 2.09		15.09 ± 4.3	
26	1.71	3.90 ± 4.06		3.54 ± 5.0	
27	2.15	4.11 ± 1.35		4.48 ± 3.3	
28	2.51	11.4 ± 2.0		2.83 ± 4.5	
29	2.71	3.91 ± 4.68		4.71 ± 1.4	
30	2.49	7.58 ± 5.04	Nd-	9.43 ± 3.7	Nd-
<i>Bzn</i>		<b>37.24 ± 6.3</b>	<b>47.65 ± 4.2</b>	<b>24.65 ± 7.1</b>	<b>58.66 ± 6.9</b>
<i>Nfx</i>		<b>33.14 ± 5.4</b>	<b>28.56 ± 3.2</b>	<b>27.74 ± 6.4</b>	<b>33.66 ± 4.7</b>

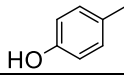
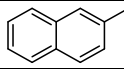
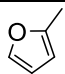
**Table 14. TcTS inhibition values of benzoic acid derivatives**

Code	R1	R2	R3	R4	% Inhib. at 1 mM
1	NH <sub>2</sub>	H	H	OH	30
2	NHNH <sub>2</sub>	H	H	OH	61
3	N <sub>3</sub>	NO <sub>2</sub>	H	OH	40
4	NO <sub>2</sub>	H	H	OH	43
5	NH <sub>2</sub>	H	H	OCH <sub>2</sub> CH <sub>3</sub>	1
6	NHCOCH <sub>3</sub>	H	H	OCH <sub>2</sub> CH <sub>3</sub>	7
7	NH <sub>2</sub>	NO <sub>2</sub>	H	OH	77
8	NHCOCH <sub>3</sub>	NO <sub>2</sub>	H	OH	66
9	NHCOCH <sub>3</sub>	NO <sub>2</sub>	H	OCH <sub>2</sub> CH <sub>3</sub>	47
10	NHCOC <sub>6</sub> H <sub>4</sub> - <i>p</i> -Cl	NO <sub>2</sub>	H	OH	Not tested *
11	NHCOC <sub>6</sub> H <sub>4</sub> - <i>p</i> -OCH <sub>3</sub>	NO <sub>2</sub>	H	OH	Not tested *
12	NH <sub>2</sub>	H	OH	OH	32
13	NHCOCH <sub>3</sub>	H	OH	OH	34
14	H	H	OH	OH	17
15	NHCOCH <sub>3</sub>	H	H	OH	30
Pyr					64

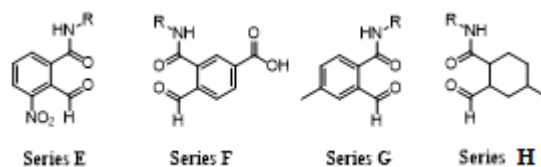
\* Not tested due to low solubility. The standard deviation for each experiment was < 5%.

**Table 15** TcTS inhibition values of selected compounds of series A-D



<i>Code</i>	<i>R</i>	<i>% TcTS inhibition Series A</i>	<i>% TcTS inhibition Series B</i>	<i>% TcTS inhibition Series C</i>	<i>% TcTS inhibition Series D</i>
4		1.4	5.6	53	82.5
11		8.3	65.8	66.9	86.6
14		11.9	76.5	19.2	33.7

**Table 16. TcTS inhibition values of selected compounds of series E-H**



Code	R	% TcTS inhibition
E-4		48.1
E-10		35.8
E-12		42.5
E13		41.7
F-2		12
F-7		97
F-15		13.6
F-22		5.4
G-2		9.7
G-11		5.4
G-15		46.3
G-23		7.8
H-2		5.6
H-11		7.6
H-16		10.1
H-24		5.6



## REFERENCES

1. Chagas C. Nova tripanozomíase humana: estudos sobre a morfologia e o ciclo evolutivo do *Schizotrypanum cruzi* n. gen., n. sp., agente etiológico de nova entidade morbida do homem. Memórias do Instituto Oswaldo Cruz. 1909; 1(2):159-218.
2. Carbajal-de-la-Fuente AL, Yadón ZE. A scientometric evaluation of the Chagas disease implementation research programme of the PAHO and TDR. *PLOS Negl Trop Dis*. 2013; 7(11):e2445.
3. Lent H, Wygodzinsky P. Revision of the Triatominae (Hemiptera, Reduviidae), and their significance as vectors of Chagas' disease. *Bulletin of the American Museum of Natural History*. 1979; 163(3):123-520. Complete journal name or abbreviations??
4. Valente SA, Valente VD, Fraiha Neto H. Considerations on the epidemiology and transmission of Chagas disease in the Brazilian Amazon. Memórias do Instituto Oswaldo Cruz. 1999; 94:395-8. Name of the journal is missing
5. Dias J.C.P.; Brener, Z.; Andrade Z.A.; Barral-Netto M, editors.; *Epidemiologia of Trypanosoma Cruzi e Doença de Chagas*. Rio de Janeiro, Brazil: Guanabara Koogan S/A; 2000; 48–74.
6. Carlier Y, Torrico F. Congenital infection with *Trypanosoma cruzi*: from mechanisms of transmission to strategies for diagnosis and control. *Revista da Sociedade Brasileira de Medicina Tropical*. 2003; 36:767-71.
7. Dias JP, Bastos C, Araújo E, Mascarenhas AV, Martins Netto E, Grassi F, Silva M, Tatto E, Mendonça J, Araújo RF, Shikanai-Yasuda MA. Acute Chagas disease outbreak

associated with oral transmission. *Revista da Sociedade Brasileira de Medicina Tropical*. 2008; 41(3):296-300.

8. Cruz-Reyes A, Pickering-López JM. Chagas disease in Mexico: an analysis of geographical distribution during the past 76 years-A review. *Memorias do Instituto Oswaldo Cruz*. 2006; 101(4):345-54.
9. Bern C, Kjos S, Yabsley MJ, Montgomery SP. *Trypanosoma cruzi* and Chagas' disease in the United States. *Clinical microbiology reviews*. 2011; 24(4):655-81.
10. Hotez PJ, Dumonteil E, Cravioto MB, Bottazzi ME, Tapia-Conyer R, Meymandi S, Karunakara U, Ribeiro I, Cohen RM, Pecoul B. An unfolding tragedy of Chagas disease in North America. *PLoS Negl Trop Dis*. 2013; 7(10):e2300.
11. Hanford EJ, Zhan FB, Lu Y, Giordano A. Chagas disease in Texas: recognizing the significance and implications of evidence in the literature. *Social science & medicine*. 2007; 65(1):60-79.
12. Moncayo Á, Silveira AC. Current epidemiological trends for Chagas disease in Latin America and future challenges in epidemiology, surveillance and health policy. *Memórias do Instituto Oswaldo Cruz*. 2009; 104:17-30.
13. Bern C, Montgomery SP. An estimate of the burden of Chagas disease in the United States. *Clinical Infectious Diseases*. 2009; 49(5):e52-4.
14. Basile L, Jansa JM, Carlier Y, Salamanca DD, Angheben A, Bartoloni A, Seixas J, Van Gool T, Canavate C, Flores-Chavez M, Jackson<sup>10</sup> Y. Chagas disease in European countries: the challenge of a surveillance system. *Chagas disease in Europe*. 2011; 16(37):19968.



15. Guerri-Guttenberg RA, Grana DR, Ambrosio G, Milei J. Chagas cardiomyopathy: Europe is not spared!†. *European heart journal*. 2008; 29, 2587–2591.
16. Reporte sobre la enfermedad de Chagas, World Health Organization, Buenos Aires, Argentina, 2007.
17. Lee BY, Bacon KM, Bottazzi ME, Hotez PJ. Global economic burden of Chagas disease: a computational simulation model. *The Lancet infectious diseases*. 2013; 13(4):342-8.
18. RASSI JR, Anis; RASSI, Anis; MARIN-NETO, José Antonio. Chagas disease. *The Lancet*, 2010;375:1388-1402.
19. Barrett, M. P., Burchmore, R. J., Stich, A., Lazzari, J. O., Frasc, A. C., Cazzulo, J. J., & Krishna, S. The trypanosomiasis. *The Lancet*, 2003; 362:1469-1480. cursive
20. CDC, 2007 Centers for Disease Control and Prevention (CDC) New global effort to eliminate Chagas disease *Wkly. Epidemiol. Rec.*, 2007;82:259-260
21. Coura, J.R.; Dias, J.C. Epidemiology, control and surveillance of Chagas disease: 100 years after its discovery. *Mem. Inst. Oswaldo Cruz* 2009;104: 31–40.
22. World Health Organization (WHO). Chagas disease (American trypanosomiasis) fact sheet (revised in June 2010). *Wkly Epidemiol. Rec.* 2010;85:, 334–336.
23. Salomon, C.J. First century of Chagas' disease: An overview on novel approaches to nifurtimox and benznidazole delivery systems. *J. Pharm. Sci.* 2012: 101: 888–894.
24. Castro, J.A.; de Mecca, M.M.; Bartel, L.C. Toxic side effects of drugs used to treat Chagas' disease (American trypanosomiasis). *Hum. Exp. Toxicol.* 2006; 25:, 471–479.

25. Viotti, R.; Vigliano, C.; Lococo, B.; Alvarez, M.G.; Petti, M.; Bertocchi, G.; Armenti, A. Side effects of benznidazole as treatment in chronic Chagas disease: Fears and realities. *Expert Rev Anti Infect. Ther.* 2009;7: 157–163.
26. Altcheh, J.; Moscatelli, G.; Moroni, S.; Bournissen, G.F.; Freilij, H. Adverse events after the use of benznidazole in infants and children with Chagas disease. *Pediatrics* 2011; 127: 212–218.
27. Santos, V.P.; Barrias, E.S.; Santos, J.F.; Barros Moreira, T.L.; De Carvalho, T.M.; Urbina, J.A.; De Souza, W. Effects of amiodarone and posaconazole on the growth and ultrastructure of *Trypanosoma cruzi*. *Int. J. Antimicrob. Agent* 2012; 40: 61–71.
28. Chamond, N.; Coatnoan, N.; Minoprio, P. Immunotherapy of *Trypanosoma cruzi* infections. *Curr. Drug Targets Immune Endocr. Metab. Disord.* 2002; 2: 247–254.
29. Filardi LS, Brener Z. Susceptibility and natural resistance of *Trypanosoma cruzi* strains to drugs used clinically in Chagas disease. *Transactions of the Royal Society of Tropical Medicine and Hygiene.* 1987;81:755-9.
30. Maya JD, Cassels BK, Iturriaga-Vásquez P, Ferreira J, Faúndez M, Galanti N, Ferreira A, Morello A. Mode of action of natural and synthetic drugs against *Trypanosoma cruzi* and their interaction with the mammalian host. *Comparative Biochemistry and Physiology Part A: Molecular & Integrative Physiology.* 2007;146:601-20.
31. Apt W. Current and developing therapeutic agents in the treatment of Chagas disease. *Drug design, development and therapy.* 2010;4:243.
32. Padilla AM, Brandan CP, Basombrío MA. Vaccine development for Chagas disease. In *American Trypanosomiasis Chagas Disease (Second Edition).* 2017; 22:773-796.

33. de Lana M, de Menezes Machado EM. Biology of *Trypanosoma cruzi* and biological diversity. In *American Trypanosomiasis* 2010;16:339-363).
34. de Souza W. Special organelles of some pathogenic protozoa. *Parasitology research*. 2002 ;88:1013-25.
35. Brener Z, Alvarenga NJ. Life cycle of *T. cruzi* in the vector. *American Trypanosomiasis Research*. PAHO Sci Public. 1976; 318: 83-8.
36. Sanchez-Sanchez M, Rivera G, A Garcia E, Bocanegra-Garcia V. Therapeutic Targets for the Development of Anti-*Trypanosoma Cruzi* Drugs: A Brief Review. *Mini-Reviews in Organic Chemistry*. 2016; 13(3):227-43.
37. Gonzales-Perdomo M, de Castro SL, Meirelles MN, Goldenberg S. *Trypanosoma cruzi* proliferation and differentiation are blocked by topoisomerase II inhibitors. *Antimicrobial agents and chemotherapy*. 1990; 34(9):1707-14.
38. Fragoso SP, Mattei D, Hines JC, Ray D, Goldenberg S. Expression and cellular localization of *Trypanosoma cruzi* type II DNA topoisomerase. *Molecular and biochemical parasitology*. 1998; 94(2):197-204.
39. Neres J, Bryce RA, Douglas KT. Rational drug design in parasitology: trans-sialidase as a case study for Chagas disease. *Drug discovery today*. 2008; 13(3):110-7.
40. Chamond N, Goytia M, Coatnoan N, Barale JC, Cosson A, Degraeve WM, Minoprio P. *Trypanosoma cruzi* proline racemases are involved in parasite differentiation and infectivity. *Molecular microbiology*. 2005; 58(1):46-60.

41. Duschak VG, Couto AS. Cruzipain, the major cysteine protease of *Trypanosoma cruzi*: a sulfated glycoprotein antigen as relevant candidate for vaccine development and drug target. A review. *Current medicinal chemistry*. 2009; 16(24):3174-202.
42. Khan OF. Trypanothione reductase: a viable chemotherapeutic target for antitrypanosomal and antileishmanial drug design. *Drug target insights*. 2007; 2:129.
43. G Duschak V. A decade of targets and patented drugs for chemotherapy of Chagas disease. *Recent patents on anti-infective drug discovery*. 2011; 6(3):216-59.
44. Belluti F, Uliassi E, Veronesi G, Bergamini C, Kaiser M, Brun R, Viola A, Fato R, Michels PA, Krauth-Siegel RL, Cavalli A. Toward the Development of Dual-Targeted Glyceraldehyde-3-phosphate Dehydrogenase/Trypanothione Reductase Inhibitors against *Trypanosoma brucei* and *Trypanosoma cruzi*. *ChemMedChem*. 2014; 9(2):371-82.
45. Zuccotto F, Martin AC, Laskowski RA, Thornton JM, Gilbert IH. Dihydrofolate reductase: a potential drug target in trypanosomes and leishmania. *Journal of computer-aided molecular design*. 1998; 12(3):241-57.
46. Khare S, Nagle AS, Biggart A, Lai YH, Liang F, Davis LC, Barnes SW, Mathison CJ, Myburgh E, Gao MY, Gillespie JR. Proteasome inhibition for treatment of leishmaniasis, Chagas disease and sleeping sickness. *Nature*. 2016; 537:229-33.
47. Marino C, de Lederkremer RM. Galactose configurations in Nature with emphasis on the biosynthesis of Galactofuranose in glycans. *Galactose: Structure and Function in Biology and Medicine*. 2014:107-34.
48. Zuma AA, Cavalcanti DP, Zogovich M, Machado AC, Mendes IC, Thiry M, Galina A, de Souza W, Machado CR, Motta MC. Unveiling the effects of berenil, a DNA-binding

- drug, on *Trypanosoma cruzi*: implications for kDNA ultrastructure and replication. *Parasitology research*. 2015; 114(2):419-30.
49. de Souza W, Rodrigues JC. Sterol biosynthesis pathway as target for anti-trypanosomatid drugs. *Interdisciplinary perspectives on infectious diseases*. 2009; 5:2009.
50. Pilatte Y, Bignon J, Lambré CR. Sialic acids as important molecules in the regulation of the immune system: pathophysiological implications of sialidases in immunity. *Glycobiology*. 1993; 3(3):201-18.
51. dC-Rubin SS, Schenkman S. *Trypanosoma cruzi* trans-sialidase as a multifunctional enzyme in Chagas' disease. *Cellular microbiology*. 2012; 14(10):1522-30.
52. Schenkman S, Eichinger D, Pereira ME, Nussenzweig V. Structural and functional properties of *Trypanosoma* trans-sialidase. *Annual Reviews in Microbiology*. 1994; 48(1):499-523.
53. Ming M, Chuenkova M, Ortega-Barria E, Pereira ME. Mediation of *Trypanosoma cruzi* invasion by sialic acid on the host cell and trans-sialidase on the trypanosome. *Molecular and biochemical parasitology*. 1993; 59(2):243-52.
54. Buschiazzo A, Alzari PM. Structural insights into sialic acid enzymology. *Current opinion in chemical biology*. 2008; 12(5):565-72.
55. Agustí R, Giorgi ME, de Lederkremer RM. The trans-sialidase from *Trypanosoma cruzi* efficiently transfers  $\alpha$ -(2 $\rightarrow$ 3)-linked N-glycolylneuraminic acid to terminal  $\beta$ -galactosyl units. *Carbohydrate research*. 2007; 342(16):2465-9.
56. Freitas LM, Dos Santos SL, Rodrigues-Luiz GF, Mendes TA, Rodrigues TS, Gazzinelli RT, Teixeira SM, Fujiwara RT, Bartholomeu DC. Genomic analyses, gene expression

and antigenic profile of the trans-sialidase superfamily of *Trypanosoma cruzi* reveal an undetected level of complexity. *Plos one*. 2011; 6(10):e25914.

57. Cremona ML, Sánchez DO, Frasch AC, Campetella O. A single tyrosine differentiates active and inactive *Trypanosoma cruzi* trans-sialidases. *Gene*. 1995; 160(1):123-8.
58. Chiurillo MA, Cortez DR, Lima FM, Cortez C, Ramírez JL, Martins AG, Serrano MG, Teixeira MM, da Silveira JF. The diversity and expansion of the trans-sialidase gene family is a common feature in *Trypanosoma cruzi* clade members. *Infection, Genetics and Evolution*. 2016; 37:266-74.
59. Risso MG, Garbarino GB, Mocetti E, Campetella O, Cappa SM, Buscaglia CA, Leguizamn SM. Differential expression of a virulence factor, the trans-sialidase, by the main *Trypanosoma cruzi* phylogenetic lineages. *Journal of Infectious Diseases*. 2004; 189(12):2250-9.
60. Zingales B, Carniol C, de Lederkremer RM, Colli W. Direct sialic acid transfer from a protein donor to glycolipids of trypomastigote forms of *Trypanosoma cruzi*. *Molecular and biochemical parasitology*. 1987; 26(1):135-44.
61. Chaves LB, Briones MR, Schenkman S. Trans-sialidase from *Trypanosoma cruzi* epimastigotes is expressed at the stationary phase and is different from the enzyme expressed in trypomastigotes. *Molecular and biochemical parasitology*. 1993; 61(1):97-106.
62. Briones MR, Egima CM, Schenkman S. *Trypanosoma cruzi* trans-sialidase gene lacking C-terminal repeats and expressed in epimastigote forms. *Molecular and biochemical parasitology*. 1995; 70(1):9-17.

63. Jäger AV, Muiá RP, Campetella O. Stage-specific expression of *Trypanosoma cruzi* trans-sialidase involves highly conserved 3' untranslated regions. *FEMS microbiology letters*. 2008; 283(2):182-8.
64. Agusti R, Couto AS, Campetella OE, Frasch AC, De Lederkremer RM. The trans-sialidase of *Trypanosoma cruzi* is anchored by two different lipids. *Glycobiology*. 1997; 7(6):731-5.
65. Buschiazzo A, Amaya MF, Cremona ML, Frasch AC, Alzari PM. The crystal structure and mode of action of trans-sialidase, a key enzyme in *Trypanosoma cruzi* pathogenesis. *Molecular cell*. 2002; 10(4):757-68.
66. Pollevick GD, Affranchino J, Frasch AC, Sánchez DO. The complete sequence of a shed acute-phase antigen of *Trypanosoma cruzi*. *Molecular and biochemical parasitology*. 1991; 47(2):247-50.
67. Vandekerckhove F, Schenkman S, de Carvalho LP, Tomlinson S, Kiso M, Yoshida M, Hasegawa A, Nussenzweig V. Substrate specificity of the *Trypanosoma cruzi* trans-sialidase. *Glycobiology*. 1992; 2(6):541-8.
68. Watts AG, Damager I, Amaya ML, Buschiazzo A, Alzari P, Frasch AC, Withers SG. *Trypanosoma cruzi* trans-sialidase Operates through a Covalent Sialyl-Enzyme Intermediate: Tyrosine Is the Catalytic Nucleophile. *Journal of the American Chemical Society*. 2003; 125(25):7532-3.
69. Todeschini AR, Mendonça-Previato L, Previato JO, Varki A, van Halbeek H. *Trans-sialidase* from *Trypanosoma cruzi* catalyzes sialoside hydrolysis with retention of configuration. *Glycobiology*. 2000; 10(2):213-21.

70. Buschiazzo A, Tavares GA, Campetella O, Spinelli S, Cremona ML, París G, Amaya MF, Frasch AC, Alzari PM. Structural basis of sialyltransferase activity in *trypanosomal* sialidases. *The EMBO Journal*. 2000; 19(1):16-24.
71. Pierdominici-Sottile G, Roitberg AE. Proton transfer facilitated by ligand binding. An energetic analysis of the catalytic mechanism of *Trypanosoma cruzi trans*-sialidase. *Biochemistry*. 2011; 50(5):836-42.
72. Demir O, Roitberg AE. Modulation of Catalytic Function by Differential Plasticity of the Active Site: Case Study of *Trypanosoma cruzi trans*-Sialidase and *Trypanosoma rangeli* Sialidase†. *Biochemistry*. 2009; 48(15):3398-406.
73. Mitchell FL, Miles SM, Neres J, Bichenkova EV, Bryce RA. Tryptophan as a molecular shovel in the glycosyl transfer activity of *Trypanosoma cruzi trans*-sialidase. *Biophysical journal*. 2010; 98(9):L38-40.
74. Nesmelova IV, Ermakova E, Daragan VA, Pang M, Menéndez M, Lagartera L, Solís D, Baum LG, Mayo KH. Lactose binding to galectin-1 modulates structural dynamics, increases conformational entropy, and occurs with apparent negative cooperativity. *Journal of molecular biology*. 2010; 397(5):1209-30.
75. Miller III BR, Roitberg AE. *Trypanosoma cruzi trans*-sialidase as a drug target against Chagas disease (American trypanosomiasis). *Future medicinal chemistry*. 2013; 5(15):1889-900.
76. Blume A, Neubacher B, Thiem J, Peters T. Donor substrate binding to *trans*-sialidase of *Trypanosoma cruzi* as studied by STD NMR. *Carbohydrate research*. 2007; 342(12):1904-9.



77. Paris G, Ratier L, Amaya MF, Nguyen T, Alzari PM, Frasch AC. A sialidase mutant displaying *trans*-sialidase activity. *Journal of molecular biology*. 2005; 345(4):923-34.
78. Goldstein IJ, Winter HC, Poretz RD, Montreuil J, Vliegthart JF, Schachter H. in: *New Comprehensive Biochemistry Glycoproteins II*. Elsevier, Amsterdam, 1997; 29b:243-402.
79. Engstler M, Reuter G, Schauer R. The developmentally regulated *trans*-sialidase from *Trypanosoma brucei* sialylates the procyclic acidic repetitive protein. *Molecular and biochemical parasitology*. 1993; 61(1):1-3.
80. Tiralongo E, Schrader S, Lange H, Lemke H, Tiralongo J, Schauer R. Two *trans*-sialidase forms with different sialic acid transfer and sialidase activities from *Trypanosoma congolense*. *Journal of Biological Chemistry*. 2003; 278(26):23301-10.
81. Ferrero GMA, Sánchez DO, Frasch AC, Parodi AJ. The effect of pyridoxal 5 phosphate and related compounds on *Trypanosoma cruzi trans*-sialidase. *An. Asoc. Quim. Arg.*, 1993; 8(1): 127–132.
82. Carvalho ST, Sola-Penna M, Oliveira IA, Pita S, Gonçalves AS, Neves BC, Sousa FR, Freire-de-Lima L, Kurogochi M, Hinou H, Nishimura SI. A new class of mechanism-based inhibitors for *Trypanosoma cruzi trans*-sialidase and their influence on parasite virulence. *Glycobiology*. 2010; 20(8):1034-45.
83. Buchini S, Buschiazzo A, Withers SG. A New Generation of Specific *Trypanosoma cruzi trans*-Sialidase Inhibitors. *Angewandte Chemie International Edition*. 2008; 47(14):2700-3.
84. Harrison JA, Kartha KR, Turnbull WB, Scheuerl SL, Naismith JH, Schenkman S, Field RA. Hydrolase and sialyltransferase activities of *Trypanosoma cruzi trans*-sialidase

- towards NeuAc- $\alpha$ -2, 3-Gal- $\beta$ -O-PNP. *Bioorganic & medicinal chemistry letters*. 2001; 11(2):141-4.
85. Vandekerckhove F, Schenkman S, de Carvalho LP, Tomlinson S, Kiso M, Yoshida M, Hasegawa A, Nussenzweig V. Substrate specificity of the *Trypanosoma cruzi* trans-sialidase. *Glycobiology*. 1992; 2(6):541-8.
86. Agustí R, París G, Ratier L, Frasch AC, de Lederkremer RM. Lactose derivatives are inhibitors of *Trypanosoma cruzi* trans-sialidase activity toward conventional substrates in vitro and in vivo. *Glycobiology*. 2004; 14(7):659-70.
87. Agustí R, Giorgi ME, Mendoza VM, Gallo-Rodriguez C, de Lederkremer RM. Comparative rates of sialylation by recombinant trans-sialidase and inhibitor properties of synthetic oligosaccharides from *Trypanosoma cruzi* mucins-containing galactofuranose and galactopyranose. *Bioorganic & medicinal chemistry*. 2007; 15(7):2611-6.
88. Brouillette WJ, Atigadda VR, Luo M, Air GM, Babu YS, Bantia S. Design of benzoic acid inhibitors of influenza neuraminidase containing a cyclic substitution for the N-acetyl grouping. *Bioorganic & medicinal chemistry letters*. 1999; 9(14):1901-6.
89. Carvalho I, Andrade P, Campo VL, Guedes PM, Sesti-Costa R, Silva JS, Schenkman S, Dedola S, Hill L, Rejzek M, Nepogodiev SA. 'Click chemistry' synthesis of a library of 1, 2, 3-triazole-substituted galactose derivatives and their evaluation against *Trypanosoma cruzi* and its cell surface trans-sialidase. *Bioorganic & medicinal chemistry*. 2010; 18(7):2412-27.
90. Campo VL, Ivanova IM, Carvalho I, Lopes CD, Carneiro ZA, Saalbach G, Schenkman S, da Silva JS, Nepogodiev SA, Field RA. Click chemistry oligomerisation of azido-alkyne-

functionalised galactose accesses triazole-linked linear oligomers and macrocycles that inhibit *Trypanosoma cruzi* macrophage invasion. *Tetrahedron*. 2015; 71(39):7344-53.

91. Harrison JA, Kartha KR, Fournier EJ, Lowary TL, Malet C, Nilsson UJ, Hindsgaul O, Schenkman S, Naismith JH, Field RA. Probing the acceptor substrate binding site of *Trypanosoma cruzi* trans-sialidase with systematically modified substrates and glycoside libraries. *Organic & biomolecular chemistry*. 2011; 9(5):1653-60.
92. Cano ME, Agusti R, Cagnoni AJ, Tesoriero MF, Kovensky J, Uhrig ML, de Lederkremer RM. Synthesis of divalent ligands of  $\beta$ -thio- and  $\beta$ -N-galactopyranosides and related lactosides and their evaluation as substrates and inhibitors of *Trypanosoma cruzi* trans-sialidase. *Beilstein journal of organic chemistry*. 2014; 10(1):3073-86.
93. Giorgi ME, Ratier L, Agusti R, Frasch AC, de Lederkremer RM. Improved bioavailability of inhibitors of *Trypanosoma cruzi* trans-sialidase: PEGylation of lactose analogs with multiarm polyethyleneglycol. *Glycobiology*. 2012; 22(10):1363-73.
94. Agustí R, Cano ME, Cagnoni AJ, Kovensky J, de Lederkremer RM, Uhrig ML. Multivalent sialylation of  $\beta$ -thio-glycoclusters by *Trypanosoma cruzi* trans sialidase and analysis by high performance anion exchange chromatography. *Glycoconjugate journal*. 2016; 33(5):809-18.
95. Hader S, Watts AG. The synthesis of a series of deoxygenated 2, 3-difluoro-N-acetylneuraminic acid derivatives as potential sialidase inhibitors. *Carbohydrate research*. 2013; 374:23-8.
96. Silva BL, José Filho DS, Andrade P, Carvalho I, Alves RJ. Design, synthesis and enzymatic evaluation of 3-O-substituted aryl  $\beta$ -d-galactopyranosides as inhibitors of

- Trypanosoma cruzi* trans-sialidase. *Bioorganic & medicinal chemistry letters*. 2014; 24(18):4529-32.
97. Blaney J. A very short history of structure-based design: how did we get here and where do we need to go?. *Journal of computer-aided molecular design*. 2012; 1;26:13-4.
98. Mandal S, Moudgil MN, Mandal SK. Rational drug design. *European journal of pharmacology*. 2009;25;625:90-100.
99. Fang Y. Ligand–receptor interaction platforms and their applications for drug discovery. *Expert opinion on drug discovery*. 2012;1:969-88.
100. Kahsai AW, Xiao K, Rajagopal S, Ahn S, Shukla AK, Sun J, Oas TG, Lefkowitz RJ. Multiple ligand-specific conformations of the  $\beta$  2-adrenergic receptor. *Nature chemical biology*. 2011;7(10):692.
101. Shoichet BK, Kobilka BK. Structure-based drug screening for G-protein-coupled receptors. *Trends in pharmacological sciences*. 2012; 33(5):268-72.
102. Chandrika BR, Subramanian J, Sharma SD. Managing protein flexibility in docking and its applications. *Drug discovery today*. 2009;14:394-400.
103. Durrant JD, McCammon JA. Computer-aided drug-discovery techniques that account for receptor flexibility. *Current opinion in pharmacology*. 2010;10(6):770-4.
104. Fischer E. Einfluss der Configuration auf die Wirkung der Enzyme. *European Journal of Inorganic Chemistry*. 1894;27(3):2985-93.
105. Tripathi, Anushree, and Krishna Misra. "Molecular Docking: A Structure-Based Drug Designing Approach. *JSM Chem*. 2017;5(2): 1042.
106. Agarwal S, Mehrotra R. An overview of Molecular Docking. *JSM Chem*. 2016; 4:1024.

107. Lorber DM, Shoichet BK. Flexible ligand docking using conformational ensembles. *Protein Science*. 1998;7(4):938-50.
108. Huang SY, Zou X. Ensemble docking of multiple protein structures: considering protein structural variations in molecular docking. *Proteins: Structure, Function, and Bioinformatics*. 2007;66(2):399-421.
109. Ferreira LG, dos Santos RN, Oliva G, Andricopulo AD. Molecular docking and structure-based drug design strategies. *Molecules*. 2015;22;20(7):13384-421
110. Streicher H, Busse H. Building a successful structural motif into sialylmimetics—cyclohexenephosphonate monoesters as pseudo-sialosides with promising inhibitory properties. *Bioorganic & medicinal chemistry*. 2006; 14(4):1047-57.
111. Neres J, Bonnet P, Edwards PN, Kotian PL, Buschiazzo A, Alzari PM, Bryce RA, Douglas KT. Benzoic acid and pyridine derivatives as inhibitors of *Trypanosoma cruzi trans-sialidase*. *Bioorganic & medicinal chemistry*. 2007; 15(5):2106-19.
112. Neres J, Brewer ML, Ratier L, Botti H, Buschiazzo A, Edwards PN, Mortenson PN, Charlton MH, Alzari PM, Frasch AC, Bryce RA. Discovery of novel inhibitors of *Trypanosoma cruzi trans-sialidase* from in silico screening. *Bioorganic & medicinal chemistry letters*. 2009; 19(3):589-96.
113. McConkey BJ, Sobolev V, Edelman M. The performance of current methods in ligand-protein docking. *CURRENT SCIENCE-BANGALORE-*. 2002; 83(7):845-56.
114. Arioka S, Sakagami M, Uematsu R, Yamaguchi H, Togame H, Takemoto H, Hinou H, Nishimura SI. Potent inhibitor scaffold against *Trypanosoma cruzi trans-sialidase*. *Bioorganic & medicinal chemistry*. 2010; 18(4):1633-40.
115. Kim JH, Ryu HW, Shim JH, Park KH, Withers SG. Development of New and Selective *Trypanosoma cruzi trans-Sialidase* Inhibitors from Sulfonamide Chalcones and Their Derivatives. *ChemBioChem*. 2009; 10(15):2475-9.

116. da Silva EN, de Melo IM, Diogo EB, Costa VA, de Souza Filho JD, Valenca WO, Camara CA, de Oliveira RN, de Araujo AS, Emery FS, dos Santos MR. On the search for potential anti-*Trypanosoma cruzi* drugs: Synthesis and biological evaluation of 2-hydroxy-3-methylamino and 1, 2, 3-triazolic naphthoquinoidal compounds obtained by click chemistry reactions. *European journal of medicinal chemistry*. 2012; 52:304-12.
117. Morris, G.M.; Goodsell, D.S.; Halliday, R.S.; Huey, R.; Hart, W.E.; Belew, R.K.; Olson, A.J. Automated docking using a Lamarckian genetic algorithm and an empirical binding free energy function. *J. Comput. Chem*. 1998;19:1639–1662.
118. Pettersen EF, Goddard TD, Huang CC, Couch GS, Greenblatt DM, Meng EC, Ferrin TE. UCSF Chimera--a visualization system for exploratory research and analysis. *J Comput Chem*. 2004;25(13):1605-12.
119. Trott, O.; Olson, A.J. AutoDock Vina: Improving the speed and accuracy of docking with a new scoring function, efficient optimization, and multithreading. *J. Comput. Chem*. 2010;31:455–461.
120. Dassault Systèmes BIOVIA, [*Discovery studio client*], [*client R 2*], San Diego: Dassault Systèmes, 2017.
121. LigPlot+ software (v.1.4, European Bioinformatics Institute (EMBL-EBI), Hinxton, Cambridge, UK).
122. DeLano WL. The PyMOL molecular graphics system. <http://pymol.org>. 2002 and 2009.
123. A. Buschiazzo, M.F. Amaya, M.L. Cremona, A.C. Frasch, P.M. Alzari, The crystal structure and mode of action of trans-sialidase, a key enzyme in *Trypanosoma cruzi* pathogenesis, *Mol. Cell*. 2002;10:757-768.

124. Kashif M, Moreno-Herrera A, Lara-Ramirez EE, Ramírez-Moreno E, Bocanegra-García V, Ashfaq M, Rivera G. Recent developments in trans-sialidase inhibitors of *Trypanosoma cruzi*. *Journal of drug targeting*. 2017;25(6):485-98.
125. Marvin n.n.n (17.28), 201n (2017), ChemAxon (<http://www.chemaxon.com>).
126. Lebedev AV, Lebedeva AB, Sheludyakov VD, Kovaleva EA, Ustinova OL, Kozhevnikov IB. Competitive formation of  $\beta$ -amino acids, propenoic, and ylidenemalonic acids by the rodionov reaction from malonic acid, aldehydes, and ammonium acetate in alcoholic medium. *Russian journal of general chemistry*. 2005; 75(7):1113-24.
127. Ashfaq, Muhammad. "Synthesis of novel bioactive phthalimido-4-methyl pentanoateorganotin (IV) esters with spectroscopic investigation." *Journal of organometallic chemistry* .2006; 691: 1803-1808.
128. Bayoumi WA, Elsayed MA. Synthesis of new phenylcarbamoylbenzoic acid derivatives and evaluation of their in vitro antioxidant activity. *Medicinal Chemistry Research*. 2012;21(8):1633-40.
129. Sülsen VP, Cazorla SI, Frank FM, Redko FC, Anesini CA, Coussio JD, Malchiodi EL, Martino VS, Muschietti LV. Trypanocidal and leishmanicidal activities of flavonoids from Argentine medicinal plants. *The American journal of tropical medicine and hygiene*. 2007;77(4):654-9.
130. Díaz-Chiguer DL, Márquez-Navarro A, Noguera-Torres B, de la Luz León-Ávila G, Pérez-Villanueva J, Hernández-Campos A, Castillo R, Ambrosio JR, Nieto-Meneses R, Yépez-Mulia L, Hernández-Luis F. In vitro and in vivo trypanocidal activity of some benzimidazole derivatives against two strains of *Trypanosoma cruzi*. *Acta tropica*. 2012 ;122(1):108-12.

131. Villalobos-Rocha JC, Sánchez-Torres L, Nogueta-Torres B, Segura-Cabrera A, García-Pérez CA, Bocanegra-García V, Palos I, Monge A, Rivera G. Anti-Trypanosoma cruzi and anti-leishmanial activity by quinoxaline-7-carboxylate 1, 4-di-N-oxide derivatives. *Parasitology research*. 2014;113(6):2027-35.
132. Wong-Baeza C, Nogueta-Torres B, Serna M, Meza-Toledo S, Baeza I, Wong C. Trypanocidal effect of the benzyl ester of N-propyl oxamate: a bi-potential prodrug for the treatment of experimental Chagas disease. *BMC Pharmacology and Toxicology*. 2015;16(1):10.
133. Mendoza-Martínez C, Correa-Basurto J, Nieto-Meneses R, Márquez-Navarro A, Aguilar-Suárez R, Montero-Cortes MD, Nogueta-Torres B, Suárez-Contreras E, Galindo-Sevilla N, Rojas-Rojas Á, Rodríguez-Lezama A. Design, synthesis and biological evaluation of quinazoline derivatives as anti-trypanosomatid and anti-plasmodial agents. *European journal of medicinal chemistry*. 2015;96:296-307.
134. Cuevas-Hernández RI, Correa-Basurto J, Flores-Sandoval CA, Padilla-Martínez II, Nogueta-Torres B, de Lourdes Villa-Tanaca M, Tamay-Cach F, Nolasco-Fidencio JJ, Trujillo-Ferrara JG. Fluorine-containing benzothiazole as a novel trypanocidal agent: design, in silico study, synthesis and activity evaluation. *Medicinal Chemistry Research*. 2016;25(2):211-24.
135. Elizondo-Jimenez S, Moreno-Herrera A, Reyes-Olivares R, Dorantes-Gonzalez E, Nogueta-Torres B, A Gamosa de Oliveira E, C Romeiro N, M Lima L, Palos I, Rivera G. Synthesis, Biological Evaluation and Molecular Docking of New Benzenesulfonylhydrazone as Potential anti-Trypanosoma cruzi Agents. *Medicinal Chemistry*. 2017;13(2):149-58.



136. Brener Z. Therapeutic activity and criterion of cure on mice experimentally infected with *Trypanosoma cruzi*. *Revista do Instituto de Medicina Tropical de São Paulo*. 1962; 4(6):389-96.
137. Buschiazzo A, Frasch AC, Campetella O. Medium scale production and purification to homogeneity of a recombinant trans-sialidase from *Trypanosoma cruzi*. *Cellular and molecular biology (Noisy-le-Grand, France)*. 1996; 42(5):703-10.
138. Cano ME, Agusti R, Cagnoni AJ, Tesoriero MF, Kovensky J, Uhrig ML, de Lederkremer RM. Synthesis of divalent ligands of  $\beta$ -thio- and  $\beta$ -N-galactopyranosides and related lactosides and their evaluation as substrates and inhibitors of *Trypanosoma cruzi* trans-sialidase. *Beilstein journal of organic chemistry*. 2014; 10:3073.
139. Daina A, Michielin O, Zoete V. SwissADME: a free web tool to evaluate pharmacokinetics, drug-likeness and medicinal chemistry friendliness of small molecules. *Scientific reports*. 2017; 7:42717.
140. Henrique PM, Marques T, da Silva MV, Nascentes GA, de Oliveira CF, Rodrigues V, Gómez-Hernández C, Norris KA, Ramirez LE, Meira WS. Correlation between the virulence of *T. cruzi* strains, complement regulatory protein expression levels, and the ability to elicit lytic antibody production. *Experimental parasitology*. 2016; 170:66-72.
141. Junqueira, G.G.; Carvalho, M.R.; Andrade, P.D.; Lopes, C.D.; Carneiro, Z.A.; Sesti-Costa, R.; Silva, J.S.; Carvalho, I. Synthesis and in vitro Evaluation of Novel Galactosyl-triazolo-benzene sulfonamides Against *Trypanosoma cruzi*. *J. Braz. Chem. Soc.* 2014; 25, 1872–1884.
142. Ferrero García, M.A.; Sánchez, D.O.; Frasch, A.C.; Parodi, A.J. The effect of pyridoxal 5 phosphate and related compounds on *Trypanosoma cruzi* trans-sialidase. *An. Asoc. Quim. Argent.* 1993;8:127–132.



